MAREES TERRESTRES

BULLETIN D'INFORMATIONS

N° 89

15 AVRIL 1983

Association Internationale de Geodesie

Commission Permanente des Marees Terrestres

Editeur Prof. Paul MELCHIOR
Observatoire royal de Belgique
Avenue Circulaire 3
1180 Bruxelles

TABLE DES MATIERES

A Gravity Tidal Profile along the "Blue Road Geotraverse" - aims of research and present state of the project

by

Gerhard Jentzsch

Institut für Geophysikalische Wissenschaften
Freie Universität Berlin

1. Introduction

This paper serves as an introduction to the two following research articles. Here an overview of the tidal gravity project will be given to inform about the framework in which the work of Asch (1983) and Plag & Jahr (1983) is being carried out.

2. Aims of research

The Blue Road Geotraverse runs from the Norwegian coast near the polar circle about 35° SE through Norway, Sweden and Finland, right over the area of maximum land uplift. The aims of the tidal gravity profile along this Geotraverse can be summed up shortly:

1) Determination of realistic tidal parameters for the correction of precise gravity surveys along this line in addition to the tidal gravity measurements already carried out in Fennoscandia (Ducarme and Kääriäinen, 1980);
2) Study of the interaction of ocean tidal loading and structure of the lithosphere in that area;
3) Development of an ocean tidal model of the shelf esp. for the constituent M2 in order to augment the respective global model of Schwiderski (1979).

During the experimental realization of the profile using five gravimeters for at least a one year record at seven sites (three in Norway, two in Sweden, and two in Finland; see map, fig. 1), a fourth research aim had to be developed.

4) Experimental realization of long-term records with regard to stability of recording conditions, data treatment, and pre-processing.

This topic is described in detail by G. Asch.

Furthermore the treatment of the data collected in Berlin (calibration records) and along the Geotraverse gave rise to the study of several problems, such as interpolation of gaps, correction of steps, and analysis. This led to a detailed study described by H.-P. Plag and Th. Jahr.

3. Present state of the Project

After calibration records in Berlin (Tidal Observatory, international no. 0750) the measurements started in April 1980 (recording periods see legend to fig. 1). Now the records of three stations are finished, and four instruments are recording in parallel.

Data preparation and analysis is now being carried out, as well as preparations for the final interpretation with regard to ocean tidal models and earth structure.

The recordings will be finished in summer 1983, and a second calibration record will be added in Berlin. First results have been already published by Asch et al. (1981b) and Jentzsch (1981). The connections to other geophysical research aims in that area are given by Asch et al. (1981a). The results of the analysis of ocean tidal data from the Norwegian coast were published by Plag (1982).

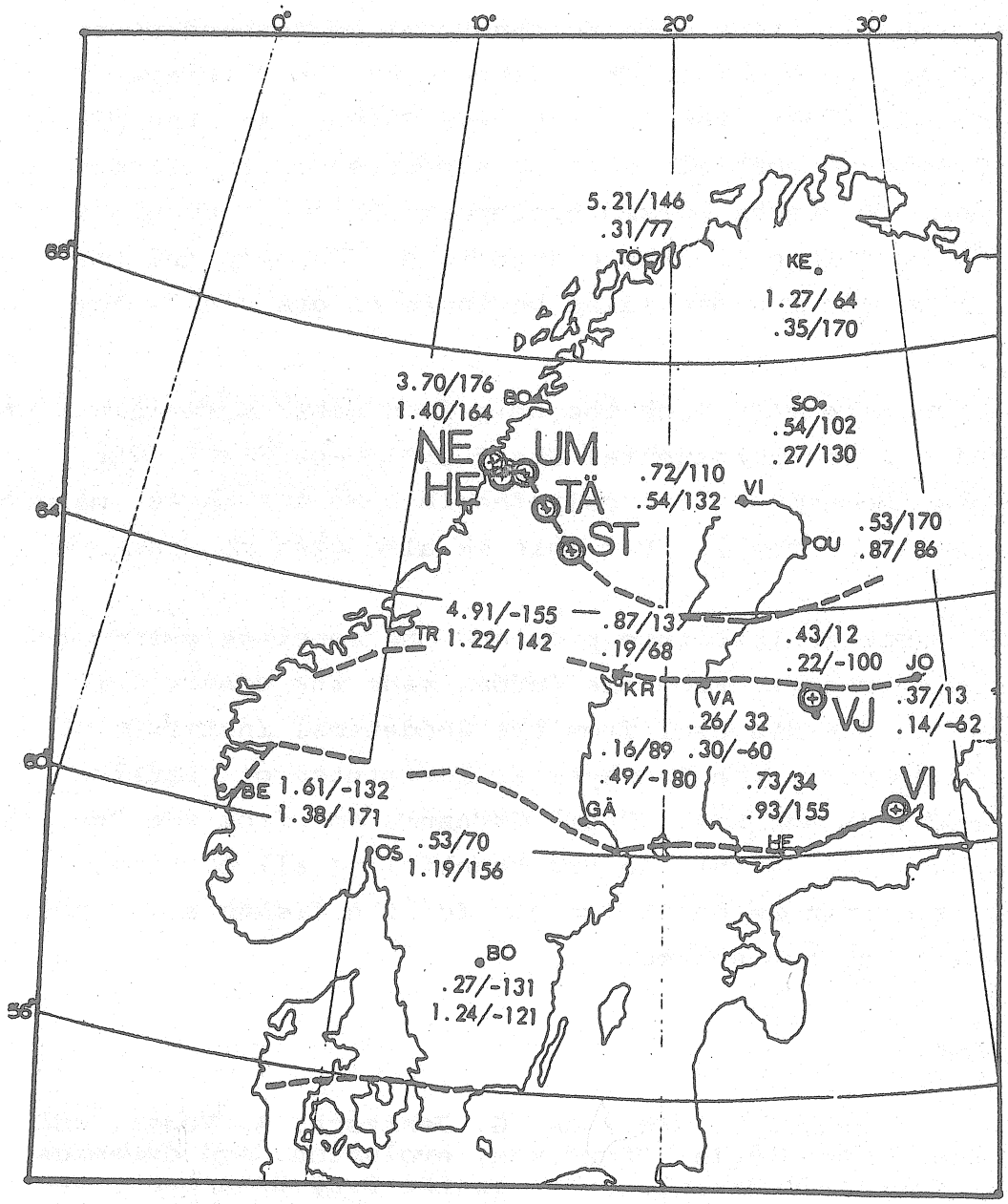

Fig. 1: Tidal residuals already obtained in Fennoscandia in microgal and degrees for M2 (upper) and O1 (lower), from Ducarme and Kääriäinen (1980); the dashed lines show the 'land-uplift-lines' for repeated precise gravity surveys; the circles denote the tidal gravity stations along the Blue Road: NE - Nesna, HE - Hemnesberget, UM - Umbukta, TÄ - Tärnaby, ST - Storuman, VJ - Vaajakoski, VI-Virojoki. NE recorded from April 1980 to March 1981; UM recorded from April 1980 to August 1981; VJ recorded from April 1981 to July 1982; TÄ, ST started in August 1981; HE started in August 1982.

4. Acknowledgements

The author and his group like to thank our Fennoscandian partners for their cooperation: The interest of the Norwegian GeographicalSurvey (NGO), the Swedish Land Survey, and the Finish Geodetic Institute enabled us to be supported by the German Research Soc. (Deutsche Forschungsgemeinschaft). They provided rooms and maintenance for the gravimeters. The help and the cooperation of our Fennoscandina partners is gratefully acknowledged.

We also appreciate very much the help from other Norwegian institutions such as the Continental Shelf Institute (IKU). The measurements themselves were only feasible by the carful maintenance of the local people. For this we also wish to thank very much.
The Finish Geodetic Institute provided one complete gravimeter unit for this project. From the German side the gravimeters were placed at our disposal from the Geodetical Institute of Bonn (Prof. Bonatz), the Geophysical Institutes of Clausthal (Prof. Rosenbach) and Kiel (Prof. Zschau), and from the Observatory Schiltach (Dr. Zürn). We are thankful to all of them.
We thank the German Research Society for the financial support of great parts of the project.

5. References

Asch, G., L. Gorling, R. Greiling, G. Jentzsch, A. Vogel, and K.v. Zadelhoff, 1981a: Structure, evolution, and dynamics of the Norwegian-Greenland Sea in the Blue Road Geotraverse area. - Geologische Rundschau, 70 (1), 282-295 (Proc. of the Int. A. Wegener Symp., Berlin 1980)

Asch, G., T. Jahr, G. Jentzsch, H.-P. Plag, and H. Scholz, 1981b: A gravity tidal profile along the'Blue Road Geotraverse' - experimental realization and first results. - Proc. 9th Int. Symp. Earth Tides, New York, 17.-22. Aug. 1981

Asch, G., 1983: Digital data acquisition and preprocessing of tidal data. - BIM, same issue

Ducarme, B. and J. Kääriäinen, 1980: The Finnish tidal gravity registrations in Fennoscandia. - Publ. of the Finnish Geodetic Institute, 90

Jentzsch, G., 1981: Ocean loading in Fennoscandia. - Proc. 9th Int. Symp. Earth Tides, New York, 17.-22. Aug. 1981

Plag, H.-P., 1982: Analysis of tidal data from the Norwegian coast. - IKU-Report p-203/1/82, Trondheim

Plag, H.-P. and T. Jahr, 1983: On processing of earth tidal data. - BIM, same issue

Schwiderski, E.W., 1979: Global ocean tides part II. - NSWC/DL 79-414

Digital Data Acquisition and Preprocessing of Tidal Data

by

Günter Asch

Institut für Geophysikalische Wissenschaften
Freie Universität Berlin

Abstract

The type of recording system of the ASKANIA gravimeters used along the "Blue Road Geotraverse" is discussed with respect to analog and digital recording. The digital recording system allows an increase of the dynamic of factor two. Problems introduced by digital data acquisition are discussed, and solutions on the basis of a micro-computer controlled system are given.

1. Introduction

In cooperation with NGO (Norges Geografiske Oppmåling) Norway, Statens Lantmeteriet, Sweden, and the Finnish Geodetic Institute, Finland, earthtide gravity measurements are carried out along the "Blue Road Geotraverse" (Jentzsch, s.i.).

The experimental problems in recording longterm time series (~ 1 year) under field conditions caused the author to study the used recording systems more deeply.

The use of longperiodic measuring instruments is very exacting on the requirements of the sensor and the reliability of the recording system and the power unit. Today longterm time series recorded under field conditions with justifiable expences can only be analysed by using sophisticated methods of data processing (Plag & Jahr, s.i.). Therefore the quality of these time series was only judged by the statistical errors calculated by the analysis methods. The amplitude- und phase errors caused by the recording systems were not taken into account adequately.

To make this clear we will first describe and investigate the recording systems used by us. Then an outlook on an improved recording system will be given.

2. The data acquisition system now in use

2.1 Configuration of the system

The gravimeter shown in the middle of fig. 2.1 is equipped with a capacitive bridgemeter which reads out the position of the gravimeter beam and transforms it into a voltage-output.

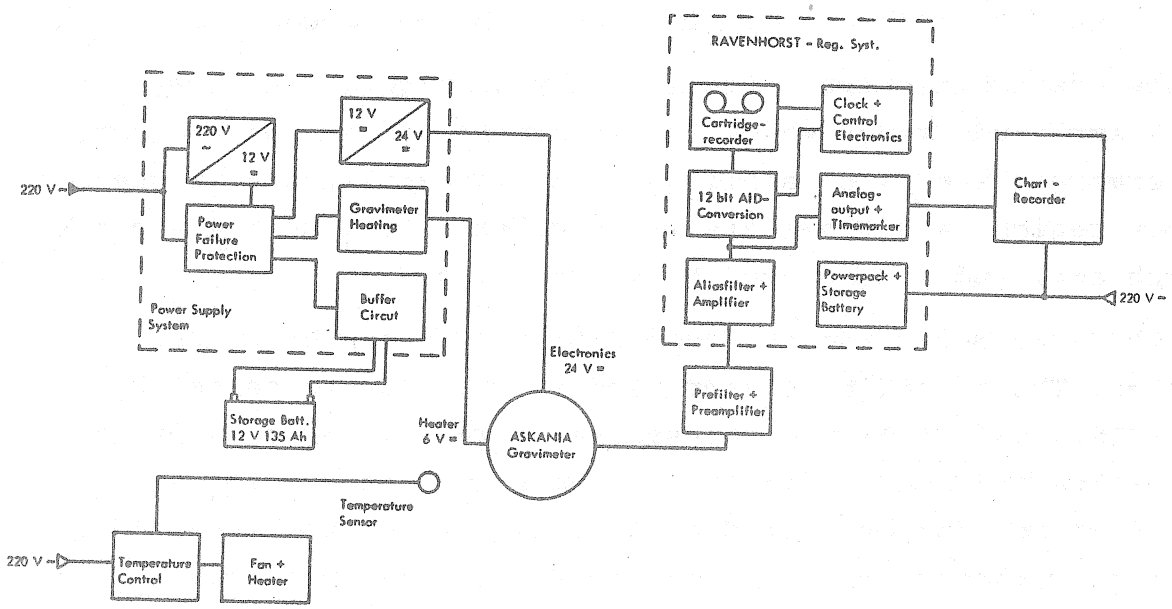

Fig. 2.1.: Station components of the tidal gravimeter station

Using this type of read-out system supply voltage and signal voltage cannot have common ground. Therefore and because of the very low signal voltage the problem of shielding and of ground loops has to be specially considered. Both of the supply voltages (electronic read out 24 V.d.c., heating 6 V d.c./2A) are regulated and d.c.-decoupled from each other. They are supplied from a common 12 V d.c. source. This allows an uncritical buffering with a 12 V lead-acid-cell, which is recharged by the power supply unit.

Attached directly to the output of the gravimeter is a circuit which performs two functions: Pre-filtering and adjustment of impedance to recording equipment. To avoid offset problems the used operational amplifier (type ICL 7650) works in chopper mode

(200 Hz). It provides a high common mode rejection ratio (120 dB) and an active clamp protection, which is especially important in this application. The input section of the circuit consists of a gain of one differential amplifier to convert the symmetrical gravimeter output to system ground. The amplitudes of the microseismic noise can be big enough to cause saturation of the front-end of the recording system; therefore good overload recovery is required. Then the signal is prefiltered with an active low-pass filter (10 sec) and coupled out with low impedance.

The now available output signal of the gravimeter is always in the amplitude range which the recording system can process. Furthermore there is no aliasing from high amplitudes in the cut-off region, and there are no simulated long period signals of high amplitudes generated by overdriving.

Thus the gravimeter and the recording system can be rather detached. The recording system used is produced in series by RAVENHORST, and it had to be used as it was. After a suitable alias-filtering and amplification the signal is sampled with a rate of 30 sec and converted into 12 bit values to be stored on a tape cassette. In front of the sample and hold unit (S & H) an additional circuit was installed to buffer a monitor output and to provide an hourly time mark. The monitor output is connected to a chart writer which enables the operator to estimate the drift and to perform necessary resets.

The timing of the A/D-conversion and storage is controlled by a free-running quartz oscillator which also provides the time-base for the clock of the recording system as well as the hourly time marks.

On the lower left of fig. 2.1 the room heating system is shown. An electronic sensor controls a convection element to keep the room temperature constant near 30° C.

2.2 Investigations of the transfer properties of the recording system

The correct interpretation of the record requires the knowledge of the transfer function of the whole data acquisition system,

i.e. from the gravimeter output till the storage device. To investigate this transfer function, measurements were carried out in the time domain using sine voltages of periods from 0.1 to 1000 sec. These time consuming measurements, the generation of the test signals and the processing of the response were carried out with a microcomputer system. The results are given in figs. 2.2 and 2.3.

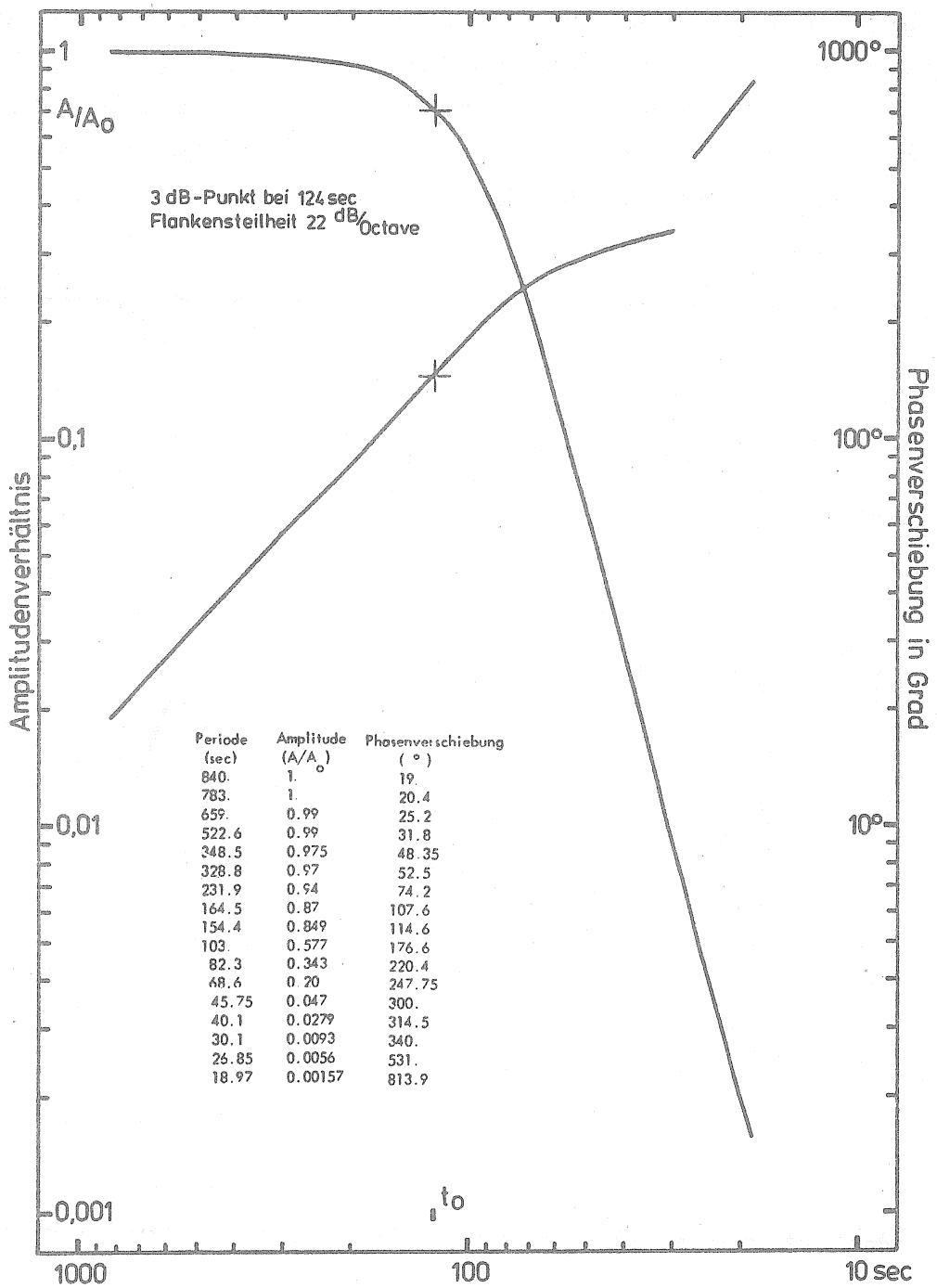

Periode (sec)	Amplitude (A/A_o)	Phasenverschiebung (°)
840.	1.	19.
783.	1.	20.4
659.	0.99	25.2
522.6	0.99	31.8
348.5	0.975	48.35
328.8	0.97	52.5
231.9	0.94	74.2
164.5	0.87	107.6
154.4	0.849	114.6
103.	0.577	176.6
82.3	0.343	220.4
68.6	0.20	247.75
45.75	0.047	300.
40.1	0.0279	314.5
30.1	0.0093	340.
26.85	0.0056	531.
18.97	0.00157	813.9

Fig. 2.2.: Amplitude-phase-diagram of the recording system

Fig. 2.2 shows the transfer-function in front of the S & H. Below the cut-off period (124 sec) the gain decreases without overshooting in the beginning with 22 dB/Oct. This corresponds fairly to the characteristic features of a 4-pole Bessel-filter at the beginning of the cut-off region. The sample rate of 30 sec is a little less than 1/4 of the cut-off period, and for a 4-pole filter this is just on the safe side.

Since the group travel-time for an ideal low-pass filter is constant, the phase is proportional to the frequency (Best, 1982). This holds true for periods above the cut-off period. Here the group travel-time turns out to be ~ 40 sec, which for M2 results in a phase shift of about 0.1% (see fig. 2.3).

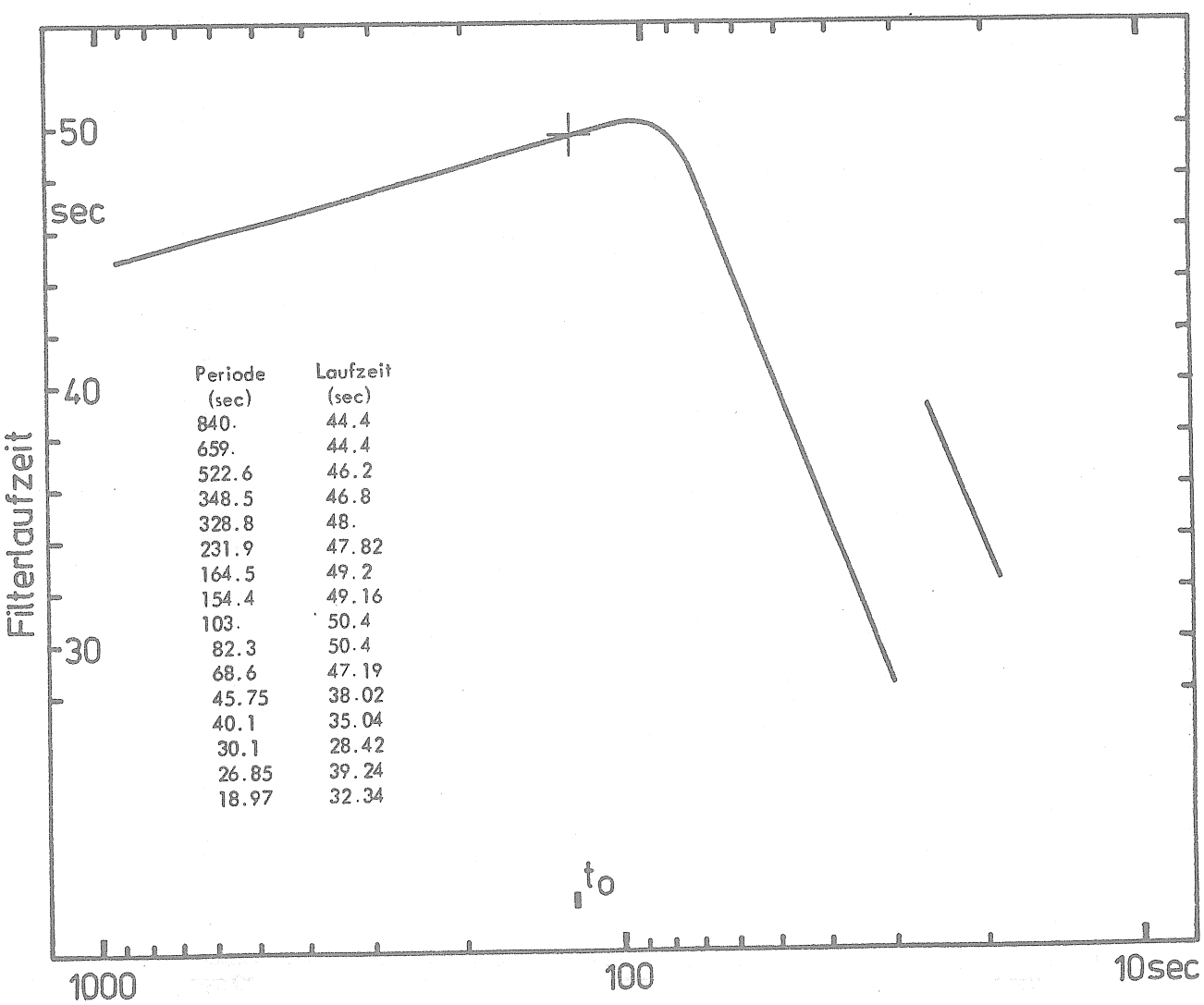

Fig. 2.3.: Group-travel time of the recording system

Below the cut-off period the signal periods are in the range of the filter travel time. From here on the alias filter is no longer linear. This is best demonstrated by the response of the filter to signals from strong shallow earthquakes (see fig. 2.4).

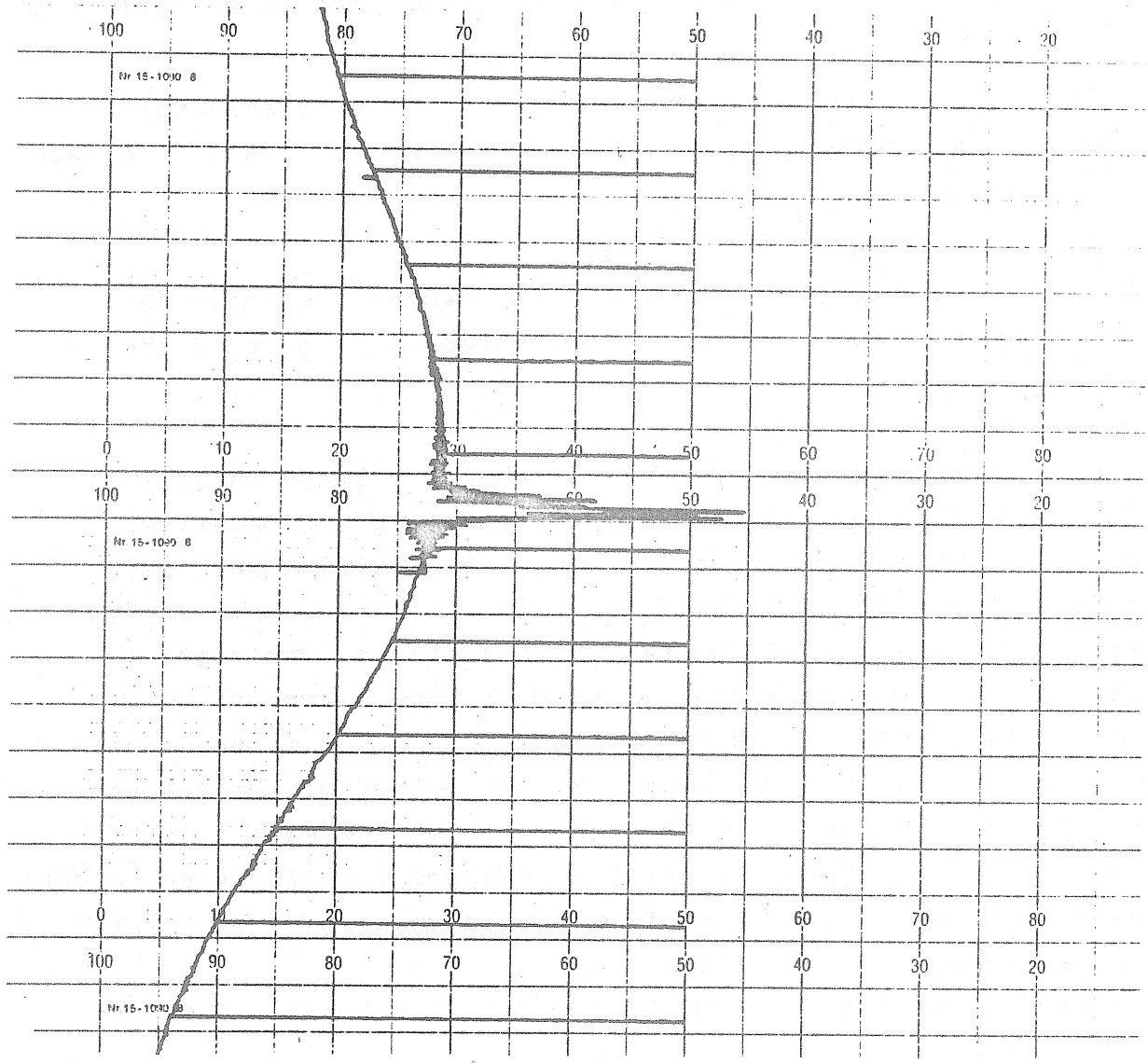

Fig. 2.4.: Analog record of the GS 15/206 (Berlin) showing the response of the filter to an earthquake (21.3.82. Hokkaido, M_S 6.7)

The gain of the whole recording system was determined with a high precision reference voltage. The measured errors in linearity are below the resolution of the 12 bit A/D-converter.

2.3 Description of the digital components

The digital part of the recording system consists of a DATEL-data logger type LPS-16 and the control mother board type RAVEN-HORST, which controls the timing, provides the necessary voltages, and displays time and binary values. The system is equipped with a buffer battery.

The LPS-16 data logging system consists of a standard digital recorder, four pluggable logic cards, and a mother board/card cage interconnecting them.

- Multiplexer/sample and hold card:
  This card contains the selection and sequencing logic for choosing one of 16 analog inputs and connecting it to the A/D-converter.
- Analog to digital converter card:
  This card changes the multiplexed analog voltage input into 12 bit parallel binary numbers representing the magnitude of the voltage input. The A/D converter utilizes successive approximation conversion techniques. It continuously approximates the analog input voltage by a factor 2. The complete conversion requires 12 steps. At each step a comparison is made that decides whether to put a "1" or a "0" in that position of the "output register". If the output of the D/A section of the converter is less than the analog signal, then the "0" is set. When this process reaches the 12th step, a conversion has been completed to within a resolution of 1/2 the least significant bit (LSB).

This card, together with the Multiplexer/S & H card, provides the data acquisition section of the system.

- Formatter card:
  This card accepts the 12 bit output word from the A/D converter, plus the 4 bit channel number, and converts the resultant 16 bit word into a serial data sequence for recording on the tape cassette. This card also generates motor clocking

signals and the gaps between words and files.

- Write/Step card:
  This card accepts data and clock inputs and drives the stepping motor and recording head to record data on tape.

Data are recorded serially as a flux change on two tracks on the tape cassette. A flux change on track 1 represents a logic ONE and a flux change on track 2 represents a logic ZERO. Data words are grouped with 16 bits per word, and are separated by a 3 step gap in which no flux changes occur on either track (DATEL, 1980).

The frequency resolution of the system is limited by the acquisition time of the S & H as well as the 12 bit resolution of the A/D-converter. Let the instantaneous input value be

$$U_e = A \cdot \sin \omega t$$

then the rate of change of U_e is

$$\frac{dU_e}{dt} = A\omega \cos \omega t$$

with its maximum at $\cos \omega t = 1$.

Then

$$\left(\frac{dU_e}{dt}\right)_{max} = A \cdot \omega$$

and

$$f_{max} = \frac{U_e}{t \cdot A \cdot 2} \quad \text{with} \quad U_e = \frac{2 \cdot A}{2^{12}} = 2.44 \text{ mV}$$

For $A = 5$ V and $t = 150$ µsec f_{max} is 0.5 Hz. Therefore the time error of the recording system is neglegible.

2.4 Disadvantages of this system: data security and time base

The data are recorded incremental; therefore according to the applied sampling rate every 30 sec the cassette tape is started, the data word is written, and the tape is stopped. At the beginning of every data block the number of the day of the year and the time (hours and minutes) are recorded. Incremental recording itself implies the possibility of errors because the tape is not moved with constant tape tension which causes data loss at the begin of the cassette. A second problem is caused by the movable head system: After insertion of the cassette the writing head

is moved into the cassette to writing position, which means, that the head position is variable with respect to the tape.

Both properties of the tape deck lead to a concept of digital data collection which may introduce gaps into the record because of unreadable tape sections. Therefore the analyses of some selected examples show, that the dynamic resolution of the gappy data may fall below that of the analog data. To approach the normal value of the dynamic resolution of the digital data often great efforts have to be applied for data restauration. This implies the application of sophisticated software, and the use of much computer time (see Plag & Jahr, s.i.).

The data security in the sense of readability of the data is not satisfying with the system presently used by us. Therefore the question arose, if there is a basically different solution for a digital data logging system, which provides the desired advantage of a higher dynamic range without the now necessary additional software application.

The disadvantages of our recording system mentioned above are crucial; but we should not forget, that they only become important in a dynamic range not achieved by conventional analog recording systems. For the analog record of about 15 cm double tidal amplitude digitized with a resolution of ~ 0.2 mm the dynamic is ~ 57.5 dB. In the case of our digital recording system the same amplitude is read out with a resolution of 66 dB, which is the 2.7-fold of the dynamic. The resolution is limited by the noise of the sensor, but an increased dynamic range would allow for a greater drift of the sensor such decreasing the number of necessary resets implying less disturbances for the sensor.

In addition to the resolutions of the amplitudes the respective resolutions of the phases have to be compared. The paper feed of the analog record of usually 2.5 cm/h provides a resolution of about 30 sec using again the already mentioned 0.2 mm as digitization error. This leads to a cut-off period in the minutes range. Applied to the period of M2 this gives a phase resolution of 0.1 %. In the case of the described digital recording system the same order of magnitude is found, but here the phase resolution is dependent on the time-base and the phase charac-

teristics of the alias-filter. The results of the filter test do not allow for the determination of phase errors for long-period signals less than 10 sec. The error of the time-base is also of this order of magnitude; thus 30 sec is a realistic estimate. Accordingly it is obvious that the digital recording system only improves the resolution of the amplitude, but not that of the phase. To achieve an improvement also here two steps are necessary: a higher sampling rate, which enables the application of alias-filters not effecting the interesting periods, and a more stable time-base.

Unfortunately the time-shift of the recording system has not the properties of a constant offset with respect to frequency. Without careful checks of the clock the accuracy of the quartz-time-base is not sufficient (Wenzel, 1976). We observed continuous drift of up to 5 sec within three months, and occasional discontinuities of up to 10 sec. For nearly all systems it was necessary to check the clock against an external time-base to obtain the time errors. Because of the lack of better models these errors have to be corrected by linear approximation (see Plag & Jahr, s.i.). These bad properties from the beginning motivated us to look for a more stable time-base; the achieved solution is described below in chap. 3.1.

3. The concept of an improved digital recording system

Recently there are several approaches to improved digital recording systems based on micro-computer control, which allow for higher sampling rates and preprocessing of the data (Harrison et al., 1981; Lambas et al., 1981; Poitevin et al., 1981). In the following the system is described, which is being developed on the basis of the experiences gained by the above described system.

3.1 Time-base

To solve the problem of a stable time-base there are several possibilities which mainly differ in their respective ratio of cost-to-results obtained.

The cheapest and most simple variant was successfully used for

more than one year in our observatory in Berlin: It consists of a network-clocked counter which works at its front end with a monoflop as noise-pulse trap, and it provides hourly signals as an output. Here the frequency of the mains serves as a time-base, but it only has a long-term stability. This system cannot be used to derive short time-marks. But for the hourly time-mark of an analog writer this system is sufficient. In our observatory we observed a difference of only about 1 sec over half a year. Since it is basing on the mains it is necessary to adjust the clock after main's break downs. This prevents this system from using it under field conditions.

Another system is recently offered by several companies: a satellite-synchonized clock as i.e. constructed by TRUE TIME DIVISION, KINEMETRICS. This instrument reads, decodes and displays the time of year information transmitted by the 'National Oceanic and Athmospheric Administrations' geostationary satellites known as GEOS. The receiver itself will select whichever satellite it is able to receive. From power on and satellite lock the time information is present after about 15 min with an accuracy $\pm$ 1 msec. Outputs providing 1 Hz and 1 kHz and an optional output for parallel BCD data are available. For our applications this system is too expensive (~ 3700 $), but it is also out of question with regard to the poor receiving conditions in Europe. This is because the three degree elevation limit cuts through eastern France.

The "Observatoire Cantonal", Neuchâtel, offers a time signal receiver under the trade marks OMEGAREC and OMEGAFACE, which use the transmitting pattern of the world-wide OMEGA navigation system. As time-base a frequency pattern between 12 and 13 kHz is used depending on the transmitter, which is repeated every 10 sec. The clock is initially set manually to the actual time ($\pm$ 5 sec), and it synchronizes in steps of 0.5 msec. The accuracy is given with $\pm$ 0.01 sec. The whole system is supplied with a serial BCD output, with different time-markers (minute, hour, day), and a display. For power-supply a lithium battery with a ten-years life time is used. The total price is about 1000 SFr. We intend to compare this system to the system used now described

in the following paragraph.

The "Physikalisch-Technische Bundesanstalt", Braunschweig, provides a transmitting station for time-signal and standard frequency (DCF 77). The relativ error of the standard frequency and the derived time information is $\pm 10^{-13}$. Within a minute the complete time information is transmitted. The time information is coded serially. Today a clock based on the DCF-information can be realized for less than 500,-- DM. Therefore this system is now used by us. The clock consists of two parts: a quartz-stable receiver (77,5 kHz) and a single-board computer. Both can be purchased as kits (ELECTOR, 1981). Second pulses are provided at the output of the receiver. Their leading edge determins the begin of a second. The pulse duration is 0.1 sec or 0.2 sec, depending on the weight of the single bits of the serial time information. These bits are interpreted by the microprocessor, and the time information is displayed. Furthermore the time information is provided at a parallel port at the begin of each second. From this port a recording system can be selected to receive the time information. The software originally supplied was only adopted for the receiving and displaying parts. The remaining part of the program memory (EPROM) was used to implement a driver program for different time markers. This program supplies second marks of constant length, minute marks with prolonged hourly and additionally prolonged day marks, as well as hourly marks with prolonged day marks. With these signals a chart writer can be supplied directly. The coded change of day simplifies the inter pretation to a great extent. The output of individually coded time marks is easily done by changing of the EPROM.
In case of weak field-strength or high noise level (daily variation of receiving conditions) the clock is controlled by the quartz-stable system clock of the microprocessor, and it is synchronized when the signal-to-noise ratio becomes high enough again.

Up to now this clock has been built by us twice. One is used as master clock in the seismic observatory in Berlin. Here only a small ferrite antenna is necessary. The other one is used in Tärnaby in northern Sweden, as station clock of our tidal gra-

vity station. Despite of the long distance of ~ 1800 km between transmitter and receiver a frame antenna (1 m^2) being installed in the attic is sufficient.

Compared to the previously used quartz oscillator this clock has some crucial advantages: It reduces the varying time error from 10 sec to 0.005 sec, and there is no drift; furthermore the clock starts itself after power-fails, and it introduces leap seconds and leap days correctly. Considering the accuracy of the time signal the transmission and receiving conditions in the VLF band have to be taken into account. Here the limited band-width and the noise level play a major role. The signal-to-noise ratio can be improved by the use of a narrow band antenna with a directional diagram and a selective receiver. The steepness of the transmitted pulses is a measure for the accuracy with which the leading or trailing edges can be determined; it is restricted by the limited band width of the transmitting antenna. For the OMEGA time information the achievable accuracy is 10 msec, and for the higher frequent DCF signal 5 msec are a good estimation for the accuracy. Because of the time used by the interrupt routine there is a time difference between input and output of the time information. For our DCF-clock this time error is below 0.1 msec, and therefore it is neglegible.

3.2 Sampling rate and data channels

With the DCF clock as time base only the alias filter is important for the phase error of the recording system. The time-base allows to increase the sample rate to introduce cut-off frequencies for the alias filter which are high enough to exclude any filter effects on our long-period signals. Furthermore today there are switched filter-ICs available which realize a 7-pole Bessel-filter with linear phase on a single IC without any external components. These ICs are nearly ideal alias filters with cut-off periods down to seconds.

Increasing sample rate has the disadvantage of increasing the number of data values. With the presently used system we record about 90.000 words of 16 bits each per month. The storage ca-

pacity of a data cassette is of about 120.000 words. Applying a sample rate of 1 sec the amount of data would be 2.6 Mio words; an amount of data which would be difficult to organize and to store. Introducing more intelligent recording devices which are capable of filtering numerically the incoming data down to 10 min samples, these problems can be solved. With a symmetrical transversal filter operator a low-pass filter without phase-shift can easily be realized. With this operator the data can be filtered requiring only little computing time provided enough memory is available. Referring to the given example this numerical filtering reduces the amount of data to about 5.000 words per month including date and time. For M2 the error in phase would be about 1 sec, and the phase error could be reduced from 0.1 % to 0.002 %, thus being neglegible. In this way the quality of the tidal information is improved considerably simultaneously reducing the amount of data.

The high sample rate and the large dynamic range of the system make it possible to record in frequency ranges which are out of the capability of former recording systems, e.g. free oscillations. A free oscillation channel can be realized by integral evaluating the d.c. offset of the digitized tidal channel and substracting the d.c. offset from the analog signal (Dumortier, 1979). After this high-pass filtering signal is amplified 20-fold and is available as free-oscillation channel. In case of an event the data of this channel are filtered to 10 sec samples and stored. For an event of 10 days 90.000 words of mass storage are necessary. The detection of events could be done by the use of a FFT-processor, which performs a frequency analysis of the converted free oscillation channel independent of the main processor, thus supplying frequency and amplitude criteria for triggering (Ferrell, 1980; Rabiner & Gold, 1975).

Another aspect for the equipment of the recording system with additional data channels lies in the influences of station conditions on the gravimeters, such as temperature, air pressure, etc. Up to now we are confined to the data provided by local meteorological observations which are not always close enough to our station. Furthermore our experiences in Fennoscandia

showed that it is necessary to record some properties of the station like heating current of the gravimeter, battery voltage, temperature of the gravimeter box, etc. in order to enable a remote error diagnosis in case of problems. Therefore a small "meteorological station" was built up converting air pressure, air temperatur and humidity electronically (ELEKTOR 1981, Franzis Verlag Sonderheft 40, Valvo: Techn.Inf. 790423). These data as well as the data describing the station properties are read out by a small subsystem every second, they are converted by a 12-bit dual-slope converter and are temporarily stored. This subsystem carries out necessary data handling and pre-filtering, e.g. the determination of average heating power of the gravimeter (Franzis Verlag Sonderheft 1982). The values are read out by the recording system at pre-selected (programmed) intervals, and they are stored on mass storage. On the other hand it is possible to use critical parameters to control the recording system itself: thus in case of power fail a dump of buffer values is possible.

3.3 State of realization of the system

The described system is still under construction, but several hardware and software modules are already completed. Fig. 3.1 gives a block diagram of the components of the system. The time base and the subsystem for the recording of station conditions are already working. Using new developments in electronics, the realization of the whole system will be possible soon. For the analog part the already mentioned alias-filters are available as well as the operational amplifier ICL 7652, which is nearly ideal for the frequency range under consideration. For the digital part powerful 16-bit processors are now on the market, which allow for the control of time-critical processes using sophisticated interrupt techniques. Already implemented routines like multiplication and division reduce the necessary user software as well as the computing time considerably. The microprocessor under consideration, the processor 68 000 from MOTOROLA, carries out a 32-bit multiplication within 11 µsec. Of special

importance is the fact, that there are now small and cheap development systems available which meet the requirements for building up individual systems.

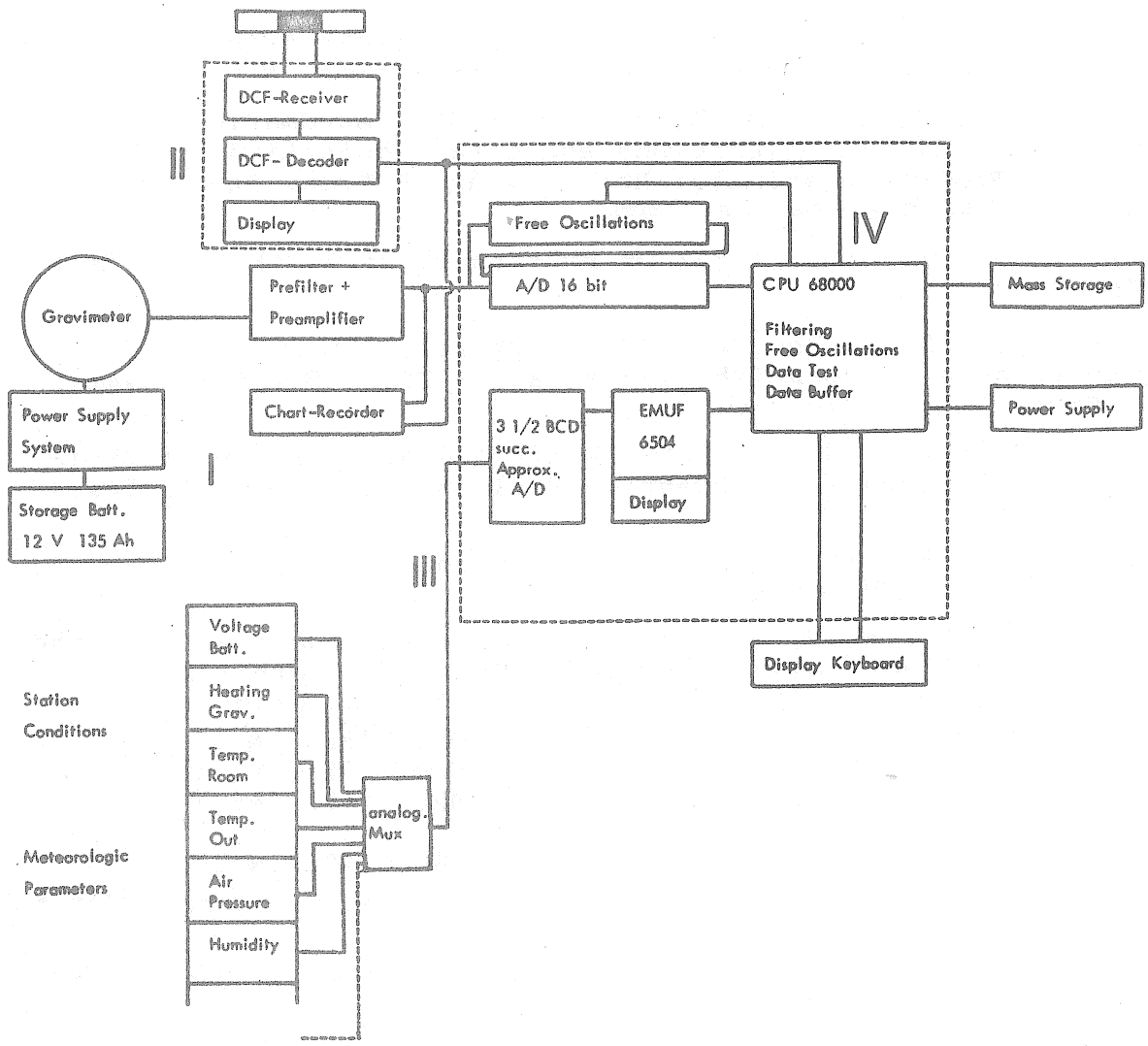

Fig. 3.1.: Block diagram of the recording system under construction: Part I is described in fig. 2.1; parts II and III are already working, and part IV is still under construction.

4. References

Best, R., 1982: Handbuch der analogen und digitalen Filterungstechnik, AT-Verlag Aarau

Dumortier, D., 1979: Digital/Analog and Analog/Digital Conversion Handbook, Motorola Inc.

Harrison, J.C., J. Levine, and C. Meertens, 1981: A deep borehole tiltmeter. Proc. 9th Int. Symp on Earth Tides, New York

Lambas, F., R., Vierva, and E. Giminez, 1981: Automatic control module of tilts, calibrations and data acquisition for La-Coste & Romberg Gravimeter Models G and D Proc. 9th Int. Symp on Earth Tides, New York

Plag, H.-p. and T. Jahr, 1983: On processing of earth tidal data. - BIM, same issue

Poitevin C. and M. de Becker, 1981: High rate sampling of tidal gravity data in Mogadishu (Somalia). - Proc. 9th Int. Symp. on Earth Tides, New York

Rabiner, L.R. and B. Gold, 1975: Theory and Application of Digital Signal Processing. Prentice-Hall-Inc. Englewood-Cliffs, N. Jersey

Ferrell, T.J., 1980: Introduction to digital filters. The Macmillan Press LTD. London

In addition to the above mentioned articles and books we used the electronical journals "Elektronik" and "MC", both Franzis-Verlag, Munic, and "Elektor", Elektor-Verlag, Gangelt.

Normalzeitempfänger für DCF, Elektor Okt. 1980, Nr.118
DCF-Computerschaltuhr, Elektor Sept.1981, Nr.129
DCF-Computerschaltuhr ohne DCF, Elektor,März 1982, Nr.135

Digitalbarometer, Elektor, Sept.1981,Nr.129

Sonderheft Nr. 40, 1982: Ungewöhnliche Bauelemente, Franzis Verlag München

Sonderheft Nr. 80, 1982: Das EMUF-Sonderheft, Franzis Verlag, München

OMEGAREC, OMEGAFACE (Data Sheet), Oberservatoire Cantonal, Neuchâtel, 1982

KINEMETRICS (Data Sheet), Satellite Synchronized Clock 468-DC, Santa Rosa, CA. 1978

DATEL-Intersil, Model LPS-16, Cassette Data Logger Instruction Manual-Document1658-12140-1, 1980

On Processing of Earth Tidal Data

by

Hans-Peter Plag & Thomas Jahr

Institut für Geophysikalische Wissenschaften
Freie Universität Berlin

Abstract

The program library used for the processing of gravity tidal data at the Free University Berlin is described. Some special steps (search for digitalization errors, removal of steps due to resets) in preprocessing the data are described in more detail and their effects upon the results of the final analysis are investigated. A method for interpolation of gaps is introduced. The effect of the interpolation on the results from a least squares analysis are investigated. As a result it cannot be recommended that gaps are interpolated, at all, prior to analyses with least squares methods in the time domain. The introduced interpolation method is found to be without any significant effect upon the results whenever the amount of interpolated data is less than 2% of the total data and individual gaps are not longer than 2...3 days. Thus this method can be used for necessary interpolation prior to analyses based on spectral methods.

1. Introduction

During the earth tidal gravity measurements along the Blue Road Geotraverse an enormous amount of data has been and is still being collected. At most of the stations the data have been recorded both digitally and continuously. The analog data are not only used as monitoring record but are as well as the digital data processed to quantitize the increase in resolution and accuracy by recording digitally instead of continuously.

At the same time the input for the calculation of the ocean tidal loading, i.e. the ocean tidal model for the Norwegian shelf, had to be improved. To achieve this existing water level records had to be processed and in addition water level measurements were carried out.

To process the resulting different types of records effectively it became necessary to standardize the processing to some extent. This was achieved by creating a program library in which each program represents a clearly defined step in the flow charts describing the data processing. Existing programs had to be changed to fit into the library while other programs - especially those for preprocessing - had to be written new. The resulting library is capable of preprocessing and analysing the four different types of records given in fig. 1.1.

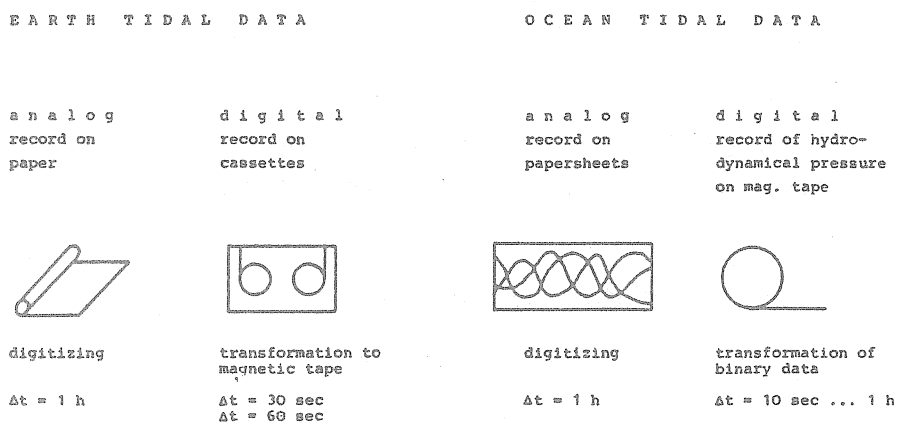

Fig. 1.1: The program library is capable of processing the four different types of time series given here. The drawings sketch the recording material. For each type the first step in processing is given as well as the sample rate

All programs were written in FORTRAN 77 or - when originally written in FORTRAN IV - changed to FORTRAN 77. The library is implemented on Cyber 700/835 of the Free University Berlin.

Here only the programs which apply to earth tidal data will be described. A description of the general procedure of processing both the digitally and continuously recorded data is given. The flow charts presented here are more sophisticated than those found in earlier works (e.g., Bachem and Wenzel, 1973; Ducarme, 1975), which is mainly due to better opportunities offered by increasing computer capacity. The high resolution required for the investigation of the geophysical problems (described in Jentzsch, 1983, same issue) can only be guaranteed by such treatment of the data.

Some of the algorithms developed for the preprocessing of the data are described in detail, and their influence on the results is investigated. Especially the effect of gaps in the records and the effect of interpolation of gaps on the results are examined.

2. Description of the general procedure

The preprocessing of the earth tidal data depends on whether the data were recorded digitally or continuously (fig. 2.1). In both cases the first step is the correction of errors due to the pro-

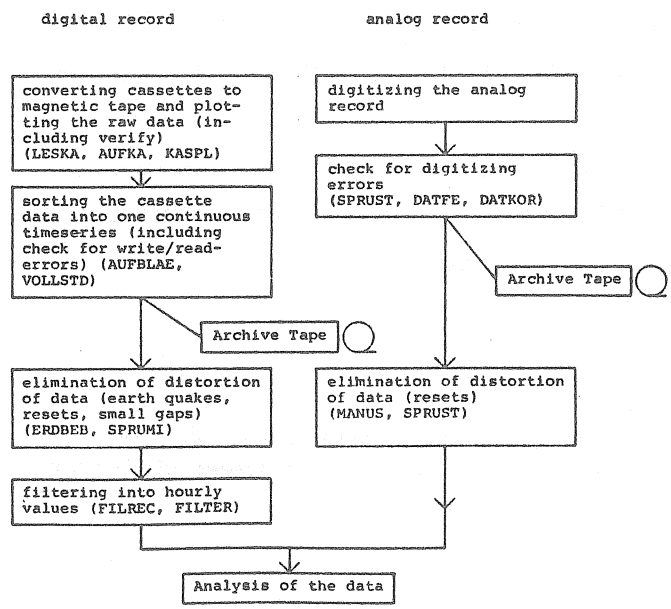

Fig. 2.1: General procedure of the treatment of earth tidal data (names in capital letters are program names)

cess of digitizing and storing the data in a computer compatible format. This results in a magnetic tape with the time series, containing no errors but all "real" distortions (such as earthquakes, steps, gaps) of the data.

Before the analyses take place these distortions are removed as far as possible and the digitally recorded data are filtered into hourly values.

The analyses are in general the same for digitally and continuously recorded data.

2.1 Preprocessing of the digitally recorded data

The digitally recorded earth tidal data are digitized and stored on cassettes with a CRS-recording system[1]. The data are written blockwise in incremental recording, i.e. each digitized value is written on the cassette immediately after digitizing, using a 16 bit data word for one value. Each block contains in its first 32 bits the station number, day, hour and minute of the first value in the block. The length of a block is fixed for one station but varies from station to station between 5 minutes and 60 minutes, while the sample rate can be 30 or 60 sec. At the end of each block an end-of-record mark is written. The 16 bit data word normally contains a 12 bit measured value in the 12 higher bits and a channel number in the 4 lower bits[2]. Only the recording system for the LaCOSTE ROMBERG gravimeter ET 18 uses the 14 lower bits for the value while the two highest bits are set zero.

The first step in treating these data is to read the cassettes and to store the data on a magnetic tape in computer compatible format. The reading of the cassettes is done with a "DATEL"-

1) Recording system type Ravenhorst with DATEL LPS 16

2) The channel number is used to distinguish between different gravimeters using the same recording system (reference station) or between different parameters (e.g. gravity and temperature)

cassette reader which is connected to a PET[1]. The PET is used as interface between the cassette reader and the IEC-bus of the HP 1000. On the PET the binary data are transformed into ASCII signs by combining four bits of information with a leading binary "0100" to an ASCII character. Two ASCII characters are stored in one 16 bit word. The transformation in ASCII characters is necessary to avoid the sending of control signs to the HP 1000 where it would cause driver problems.

The PET sends the data blockwise to the HP 1000. The HP 1000 writes the data on a magnetic tape, removing first the leading "0100". To avoid any problem with the storage of negative numbers in the 16 bit integer word of the HP 1000, 8 bits of the binary information are stored in the 8 lower bits of an integer word and written on the magnetic tape as a I3 number.

The file on the magnetic tape is also plotted on a HP 7221A plotter for a documentation of the raw digital data. The opportunity of plotting a cassette easily has proved to be useful especially in the remote detection of errors in our stations in Scandinavia, where a direct control of the stations by one of us is not possible.

The data sent to the HP 1000 are not without errors. The smaller part of the errors is due to write-errors or to drop-outs on the cassette-tape but they normally affect only one data word by one or more wrong bits. They turn out to be spikes that can easily be detected and corrected by linear interpolation from the neighbouring values. Most of the data errors are due to one or more bits, lost or added during the process of reading a cassette. These errors result in a shift of a part or the whole of the block in which the error occurs and by that affects up to 60 minutes (max. block length) of data.

[1] A COMMODORE CBM model 3032 computer

These errors occur in about 0.1...0.3% of the data words, depending on the cassette. This means that in about 1...5% of the blocks a read error is contained and data are changed. From our experience we know that these errors are in general not reproduceable. Therefore a verify of the data read is performed by reading each cassette twice. While reading a cassette the second time the data are checked for errors and whenever a read error occurs - i.e. a difference between the two data sets is found - the most plausible data are used. This procedure is quite time consuming (read time for one cassette, containing one month of data is 20...30 minutes), but because of the amount of data affected by the read errors we think this verify is necessary to avoid a large part of the data becoming artificial.

The further processing of the data is done on the CYBER 700/835 (CDC) of the Free University Berlin. Here the data are first checked for write/read errors that did pass the check on the HP 1000.

To remove errors due to shift of a whole data block the expected block identification (i.e. the first 32 bits in a data block) is calculated and checked against the actual block identification. To check for shift errors in the data the more significant bits of two succeeding values are compared and in addition the channel number is checked (in the ET18 data the two highest bits are checked for zero). The data are further checked for spikes, which are replaced by a value linearly interpolated from the neighbouring values.

These checks for shift errors were formerly done on the HP 1000 (Jentzsch, 1981), but because of the long processing time needed (the processing time for a cassette would take several hours) this is now done on CDC.

Comparing the two error checks at HP 1000 (verify by reading each cassette twice) and CDC (shift and spikes) it must be said, that both checks are necessary. Some of the shift errors are

reproduceable and pass the verify on the HP 1000, and all write errors are not detected in this verify. On the other hand, though most of the shift errors would be detected and could be corrected in the error search on CDC at least part of the restored data would have to be considered as being artificial. In order to keep the amount of artificially produced data as small as possible the verify is necessary.

The amount of data lost due to read errors is such reduced to somewhat between 0 and the maximum 7 blocks at the beginning of each cassette (the cassettes are changed about once a month).

After the error check on CDC the data of one station are sorted into one continuous time series, using a Random Access File (RAF)[1] in which the data are blocked in days and indexed by the day number. In this process any errors in time, due to errors of the time base in the recording system (CRS, up to 10 sec. per month have been noticed by us) (Asch, 1983, same issue) are corrected. At any stage of sorting the content of the RAF can be plotted and additional cassettes can be appended.

When a record of one station is finished and all cassettes are stored in the RAF the content of the RAF can be considered to be the measured time series and is as such written on a magnetic tape (in a packed format) which is stored in our archives. This tape contains the time series without any read or write errors but including all distortions, e.g. earth quakes, steps due to resets or high noise due to strong winds.

Before the data are filtered into hourly values especially the steps and the distortions due to earthquakes must be eliminated. The data strongly distorted by earthquakes are eliminated because they are not stationary (Asch, 1983, same issue). Thus the distortion cannot be smoothed out. The resulting gaps (normally less

1) In writing or reading the RAF, special system supplied routines (CDC) are used, but these routines only occur in special subroutines that can easily be changed for implementation of the programs on other computers

than one hour) are interpolated together with other gaps (up to one hour) with a polynomial of low degree in order to avoid a loss of data at such small gaps in the process of filtering.

One further remark concerning the write/read errors should be made: Most of the errors are clearly due to the incremental recording, which makes it impossible to verify the data while writing on a cassette. The use of more intelligent recording systems which could perform a preprocessing of the data (e.g. the filtering of the data into hourly values) and also a verify of the data stored on mass-storage devices would solve the problem of write/read errors in a most effective way. This would guarantee that no data would have to be created artificially (Asch, 1983, same issue). In addition the amount of preprocessing now necessary due to the huge amount of data could be considerably reduced.

2.3 Preprocessing the continuously recorded data

To process the continuously recorded data with a computer the analog record needs to be digitized first. This is done by reading out hourly values from the analog record. First in processing these data, the errors made while digitizing must be found. The result after correcting these errors will be a digital time series which can be considered to be the digital equivalent (DE) of the analog record.

It has proved to be useful first to check and correct the sequence of dates (DATUM). A data line normally is built up of 80 characters: Year, month, day and hour of the first value in the line - two characters each - and 12 values. For the further error search in the data two algorithms are used:

- the first and second numerical derivatives of the time series are investigated, and the variation of the first derivative is used to detect any steps (due to resets) in the record while the second derivative is used for detection of spikes (digitization errors) (SPRUST)
- a polynomial interpolation is used to calculate a test value

for a given time, and the digitized value is checked against this test value (DATFE)

The steps are corrected as detected by SPRUST before DATFE is applied to the data. Before correcting the errors found by DATFE, the smaller errors (less than 5 mm) are checked against the analog record. The larger errors need to be checked only when a group of errors is detected; this can be due to a shift of several values. The errors are always corrected in the originally digitized data, i.e. the steps are only removed for the detection of errors.

The application of the two algorithms can be repeated until no further errors are found. The combination of the two algorithms produces a result which can be considered to be the DE of the analog record and is as such written on a magnetic tape and stored in our archives.

The detection of steps only works for steps larger than a given limit which depends on the amplitude of the tides in the record. Smaller steps must be noticed while digitizing the data and are corrected as found in the analog record (MANUS) while the larger steps are corrected as found by SPRUST (for a discussion of the error in calculation of steps see chap. 3).

2.3 Analysis of the data

The earth tidal records measured with gravimeters normally contain a large part of longperiod non-tidal or aperiodic variations (this also includes periods longer than the recording interval), called drift, which must be removed prior to the calculation of the tidal parameters (Bonatz, 1974).

In principle two methods can be used to eliminate the drift:

- subtracting analytical models of the drift
- smoothing

The first method is best illustrated by the following example:

The running in of the ASKANIA GS gravimeter (e.g. after the spring has been fixed for transport) produces an almost exponental curve

$$(2.1)\quad f(t) \simeq \begin{cases} 0, & t \geq 0 \\ Ae^{-(t/t_o)}, & t<0 \end{cases}$$

with t_o from 2...4 weeks and A several hundreds... thousands µgal. The Fourier-transform of (2.1) reveals that it contains energy at all frequencies, thus also in the tidal frequency bands. By mere filtering the time series with a high-, low- or bandpass filter it would be impossible to separate this energy from the tidal energy. But by determining the parameters in (2.1) by a least squares fit of (2.1) to the data and later subtracting the resulting function from the time series, the energy due to the deterministic physical process can be separated from the tidal energy.

Therefore whenever parts of the time series are neither random nor periodic with periods closed to the tidal periods it is worthwhile to investigate the process producing this signal and to try to model the process by analytical functions.

If the modelling of parts of the drift is possible, the parameters of the model are determined by a linearized iterative least squares fit of the model to the data (DRIFT, fig. 2.2). This is done prior to any filtering of the data. In combination with subsequent filtering this gives much better results (lower noise level in the tidal frequency bands) than mere filtering would (Plag, 1982a).

In addition, this "analysis of drift" offers possibilities for a better understanding of some of the physics concerning the instruments used in earth tidal measurements or for the investigation of other geophysical processes influencing these measurements.

Most longterm recordings of earth tides also include some smaller gaps due to failures in the recording system or to the instrumental drift. These gaps need not be interpolated before determining the

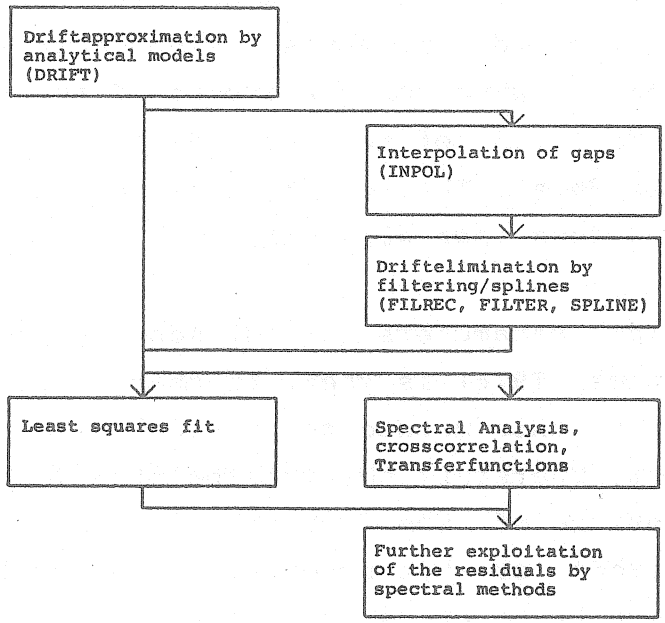

Fig. 2.2: Drift approximation and analysis of earth tidal data

parameters of a drift model. But in order to avoid a loss of data at each side of these gaps due to the unsymmetry of the convolution of the filter operator with the data, the gaps can be interpolated prior to any filtering. This is also true for smoothing the data with splines. Recent work with the use of splines for smoothing the data have been very promising and at the moment necessary tests are performed to evaluate the effect of spline-smoothing on the tidal parameters.

The interpolation of gaps is done by a least squares procedure: The amplitudes and phases of a set of the most important tidal constants (usually eight) are calculated together with the coefficients of a polynomial of variable degree from the data on both sides of the gaps by a least squares fit (INPOL). The polynomial is used to account for the longperiodic tidal and non-tidal variations in the record.

In interpolating gaps the main point is not to change significantly the information contained in the record. The used method of interpolation does not change the tidal parameters significantly - under certain restrictions - whenever the amount of the missing values is not more than 2...3% of the total data (depending on the quality of the recorded data). The length of an individual gap may not be more than 2...3 days (see also chap. 5).

For the calculation of the tidal parameters a least squares method (ET 6, Chojnicki, 1973 and Wenzel, 1976) is used. In chap. 5 it is shown that for an analysis using this method an interpolation of the gaps cannot be recommended. Therefore the interpolated data are only used whenever a smoothing of the data with long operators (transversal filters) is desired[1)] or when spectral methods will be used for the analyses. There is of course the possibility of using spectral methods in the presence of gaps (Sukhwani and Vieira, 1978), but this involves a convolution in the frequency domain which causes some difficulties. Especially for the calculation of power spectra or coherency analysis time series without gaps are required.

We use spectral analysis methods mainly for further exploitation of data, e.g. correlation of a record with other geophysical parameters such as temperature, airpressure or snow heights (in northern regions), and for the calculation of transfer functions of the recording systems for calibration purposes. The instruments used on the Blue Road Geotraverse are calibrated in two parallel recordings (before and after field work) with these instruments in our station in Berlin. These records are used for the calculation of the transfer functions by comparing the record of each instrument to the record of the ET 18 gravimeter by spectral methods. For the calibration, a calibration record of at least half a year is de-

1) The loss of data at gaps could also be reduced by the use of recursive filters which in general require by far shorter operators than transversal filters, but the design of stable recursive filters is more complicated than that of transversal filters (Best, 1982)

sired. For the instruments we use, the transfer function of the measuring system (gravimeter plus recording system) can be considered to be constant in time (the used gravimeters are static gravimeters or systems with feedback), and therefore a sensitivity check is not necessary during the recording period.

3. Correction of steps due to resets

Because of the instrumental drift or the change of meteorological parameters resets of most instruments are necessary to keep the pencil on the paper (in analog recordings). This holds also true for digital recording systems because in most of the systems presently used a 12 bit A/D converter is used, and to achieve the necessary resolution these 12 bits normally represent the same range as the paper-width.

Thus in most analog and digital records steps are present. In general, the treatment of steps in digitally and analogically recorded data is the same. But because of the higher sample rate in digital records (1 minute or 30 sec.) a reset affects several of the values while in a digitized analog record it can be assumed that a reset occurs between two of the hourly values. This must be taken into account in the calculation of the amount of steps in digitally recorded data.

Here a discussion of the algorithm used for the calculation of steps in hourly data will be given. Fig. 3.1 explains the equation

$$(3.1) \quad s = (\Delta y_1 + \Delta y_2)/2$$

which is used to calculate the step between two hourly values. Whenever s is greater than a given limit, a step is assumed and the following data are corrected by the accumulative amount of the steps. The limit depends on the amplitudes of the tides at a given station and on the gain of the recording system, and it must be found experimentally.

For a test of the accuracy of this correction three time series were used (tab. 3.1).

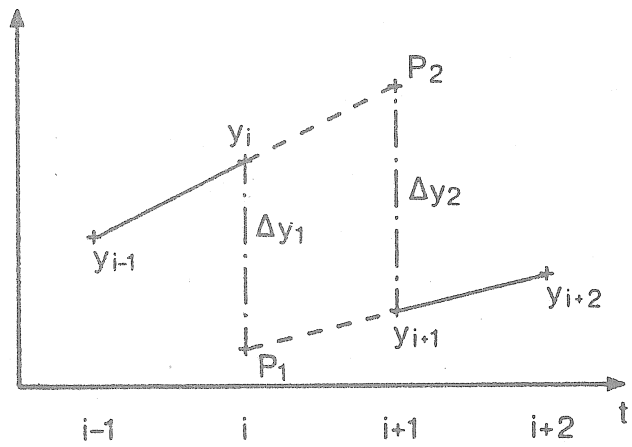

Fig. 3.1: Calculation of a step at $t=t_i$. The mean value of Δy_1 and Δy_2 is used for the calculation

The theoretical record contains no noise. The ET 18 record has a fairly low noise level compared to the noise level of the GS 15 record. The two measured time series were not calibrated prior to the test in order to facilitate a comparison of the result to the manual determination of steps.

Tab. 3.1: Time series used for the test of SPRUST

Instrument	Period	Number of steps built in
ASKANIA GS 15	12.11.78-06.02.80	172
LCR ET 18	24.05.78-15.02.80	254
Theoretical tides	01.01.78-31.12.78	175

In the time series, steps of known height were introduced and then SPRUST was used to remove these steps. Fig. 3.2 gives the errors in the calculation of the steps. The result for the ET 18 is slightly better than the result for the GS 15, which is due to the lower noise level in the ET 18 record. But in both cases 90% of the errors are less than 2 mm. For the ET 18 record only 2.0% of the errors are larger than 3 mm and for the GS 15 2.9% exceed 3 mm.

Taking into account the calibration factor for the ET 18 gravimeter (= 1.658 µgal/mm) this means that 90% of the residual steps are less than 3.3 µgal. For the GS 15 a calibration factor of about the same magnitude ($\sim$ 1.8 µgal/mm) can be used for comparison and here 90% of the errors are less than $\sim$ 3.6 µgal.

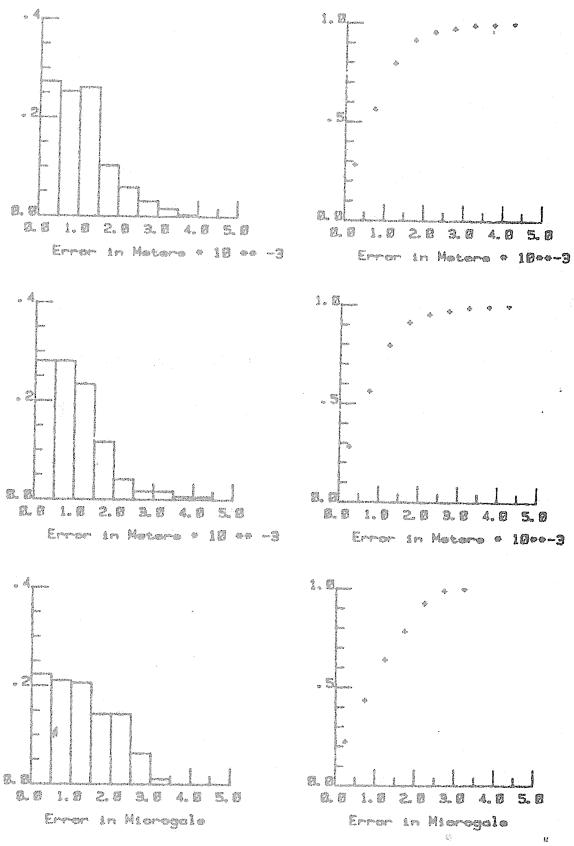

Fig. 3.2: Results of the test of SPRUST

The left diagrams give the relative frequency distribution and the right diagrams the relative cumulative frequency distribution of the errors.

a: The results for the ET 18 record

b: The results for the GS 15 record

c: The results for the theoretical tides

For comparison the results of the measured records can be multiplied by a factor of ~ 1.7 µgal/mm

The result for the theoretical tides show that, when no noise is present, about 90% of the errors are less than 2.5 µgal. Consequently it can be said that the influence of noise on the calculation of the steps is not as big as one might expect, and the errors are mainly due to small non-linear variations of the first derivative of the tidal curve that are not taken into account in the calculation of the steps.

It should be mentioned here that the calculation of the steps by using polynomials of higher degree for the approximation of the derivative gives worse results than the linear approximation used.

Comparing these results with the graphic determination of steps from the analog record, which always involves the graphical extrapolation of up to one hour of the record, it can be said that the numerical determination is at least as accurate as the graphic methods and it does not depend on graphic extrapolation which would be rather subjective.

In order to evaluate the effect of the residual step function left in the data by the step correction, 20 steps were built into each of two records of 100 days (ET 18 record and theoretical tides) and afterwards corrected with SPRUST. The amplitudes and phases of four main tidal constituents as calculated from the data without steps and with the residual step function are given in tab. 3.2 (calculated with ET6, using the Pertsev filter). Except for the theoretical M2 amplitude all parameters were not significantly changed. But considering the amount of change in the theoretical M2 amplitude ($\sim$ 0.03 µgal) even this cannot be considered to be significant concerning real measurements. In addition the number of steps built in is much higher than necessary in actual recording.

Tab. 3.2: Results from a least squares analysis for main tidal constituents from 100 days theoretical tides and 100 days of the ET 18 record (tab. 3.1) without steps and with a residual step function. Amplitudes are in µgal and phases in degrees

	100 days theoretical tides				100 days of ET-18 record			
	no steps		with residual steps		no steps		with residual steps	
	A	K	A	K	A	K	A	K
O1	29.9859 .0039	-0.7341 .0074	29.9674 .0081	-0.7115 .0345	34.8084 .0701	.1688 .1154	34.7668 .0746	.2164 .1230
P1S1K1	42.1866 .0039	-0.7103 .0053	42.1717 .0181	-0.7229 .0245	48.7778 .0701	.3129 .0824	48.7576 .0746	.3028 .0877
M2	27.7876 .0021	-1.4370 .0043	27.7567 .0099	-1.4492 .0205	33.2916 .0676	1.4239 .1164	33.2459 .0690	1.4076 .1189
S2K2	12.9215 .0021	-1.3906 .0093	12.9153 .0099	-1.3628 .0440	15.5467 .0676	.7679 .2493	15.5261 .0690	.8058 .2546
m_o	0.026		.160		.667		.712	

At gaps, two polynomials are calculated from the data in front of and behind a gap. The difference of the values of the polynomials in the middle of a gap is used for the calculation of step height in a gap. As there is no information present in gaps, only the smoothness of the drift function can be used as criterion for the

presence or absence of steps in a gap. The resulting drift function is smoothest, when the polynomial is of degree one. Thus we use linear regression polynomials.

4. Detection of digitalization errors

In the course of digitizing the analog record, i.e. of reading out hourly values from the analog record, errors are inevitable. Therefore the digital data need to be checked for such errors.

These errors normally disturb the smooth earth tidal curve and therefore a polynomial interpolation can be used for testing. To test a value x_i with DATFE a test value x'_i is calculated by fitting a polynomial of degree k=2l or k=2l-1 to the 2l values

$$x_j,\ j=i-l,\ldots,i-1,i+1,\ldots,i+l$$

and the difference

$$\Delta x_i = |x_i - x'_i| \tag{4.1}$$

is used as criterion Whenever Δx_i is greater than a user specified value s a data error is assumed and a message is printed. An option can be selected to replace x_i by x'_i if x_i did not pass the test. Of course, in the neighbourhood of a large data error x_i, a number of Δx_j, j=i-h,...,i-1,i,i+1,...,i+h, with h depending on the degree of the polynomial and on Δx_j, will be larger than s. But for all single data errors x_i, it was

$$\Delta x_i = \max_{j \in [i-h,i+h]} \Delta x_j \tag{4.2}$$

Therefore the replacement is done for the index i, for which (4.2) is true.

For all single errors the Δx_j, j=i-h,...i+h, decrease monotonously with distance to the data error. If two or more relative maxima are found in the Δx_j, j=i-h,...i+h, two or more data errors can be assumed in the interval i-h,i+h . In such cases a check against the analog record will always be necessary and no replacement is done by DATFE. This is also true when h is greater 1.

Instrument	Period	Number of data errors
ASKANIA GS 15	12.11.78-06.02.80	196
LCR ET 18	24.05.78-15.02.80	270

Tab. 4.1: Time series used for the test of DATFE

To test the accuracy of this method a large number of errors was introduced in two recorded time series (tab. 4.1). First a test was performed to find the optimal degree of the polynomial. The mean value of the interpolation error, i.e. the difference between the calculated values and the true values, together with the standard deviation was calculated in dependence on the degree of the polynomial. Tab. 4.2 gives the results for the polynomials of a

Tab. 4.2: Mean value and standard deviation of the interpolation error in dependence on the degree of the polynomial. Mean value and standard deviation are in mm

Degree of polynomial	LCR ET 18		ASKANIA GS 15	
	mean value	st.dev.	mean value	st.dev.
1	1.82	1.29	1.68	1.26
2	.65	.47	.65	.52
3	.28	.24	.41	.49
4	.27	.26	.38	.37
5	.26	.24	.37	.33
6	.28	.26	.40	.39
7	.27	.25	.39	.38
8	.29	.27	.41	.42
9	.28	.27	.40	.40

degree from 1 to 9 for the two time series. For a degree of 5 a minimum is found in both time series for both the mean value and the standard deviation. Therefore a polynomial of degree 5 is used for the detection of digitalization errors.

Fig. 4.1 gives the results for the error search in the two time series. The relative frequency distribution of the interpolation error is calculated for the two records. For the ET 18 record 95% of the interpolation errors are less than .7 mm (~ 1.1 µgal) while for the GS 15 record the 95% border is found at 1.1 mm (~ 2 µgal). This difference is clearly due to the higher noise level of the GS 15 record.

5. Interpolation of gaps in earth tidal data

5.1 The problem

In the last ten years the increasing computer capacity offered an ever better opportunity of performing easily the vast amount of calculations involved in the analysis of long time series. Thus there has been an increasing interest in the recording and analysing of longterm earth tidal records. But because of the degree of sophistication required for the measurement of earth tidal phenomena it is still very difficult, if not impossible, to ensure longterm recordings without gaps. This is especially true for recordings under field conditions.

Therefore some interest focussed on the problem of gaps. Different points of view have been developed in the course of the discussion, depending on the methods used for the subsequent analysis. On the one hand, methods for analysing data containing gaps were developed (Venedikov, 1966; Chojnicki, 1973; Wenzel, 1976; Suhkawani and Vieira, 1978, and other authors) while on the other hand several interpolation methods were introduced (Longman, 1960; Schüller & Schulz, 1973; Massot, 1977; Nakai, 1981, and other authors).

The aim in interpolating gaps in earth tidal data is not to change significantly the information contained in the recorded data. Therefore the interpolation methods were always tested by interpolating artificially introduced gaps in recorded or theoretical data and comparing the result of the analysis including the interpolated data to the result of the analysis without gaps.

Especially for spectral analysis methods this test is sufficient because it is obvious that the results of an analysis with the gaps included but not interpolated would be worst. But it was not investigated whether this holds true for least squares methods in the time domain. Here the necessity of interpolation is not clear at all.

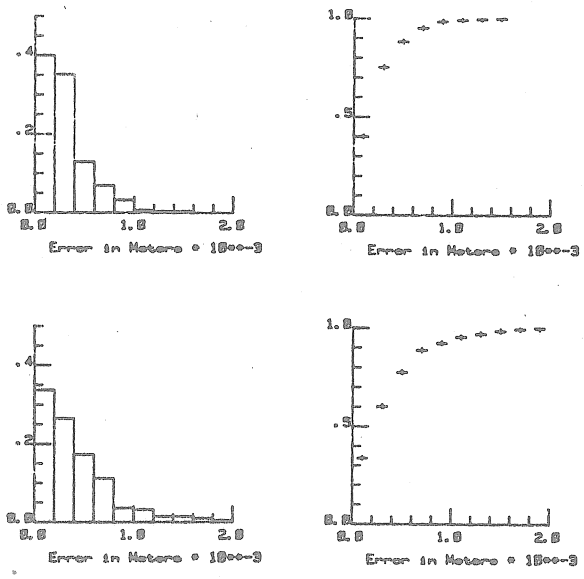

Fig. 4.1: Relative frequency distribution (left) and relative cumulative frequency distribution of the interpolation error in two time series (tab. 4.1). The interpolation error is the difference between the true value and the interpolated value (polynomial of degree 5)

While the largest interpolation errors found in the ET 18 record are 1.5 mm, the largest errors found in the GS 15 record are 1.9 mm. These two values also represent a limit for errors that can be detected by DATFE: all errors less than these values need to be checked against the analog record before being corrected.

The method of detecting data errors by polynomial interpolation only works if the curve is smooth enough, i.e. there are no large constituents with periods much less than the time interval used for the polynomial interpolation (in our case 6 hours). This is true for most earth tidal records. But when the same method was used for coastal ocean tidal records the results were much worse. This is especially true for stations with large shallow water constituents. Here other methods of detecting data errors are more useful and less computer time consuming (Plag, 1982b).

The problem of gaps in least squares fits in the time domain is quite difficult to attack theoretically, and therefore we decided to investigate this by performing a series of tests. The necessity of performing three analyses, i.e.

- analysis of the original record without any gaps
- analysis of the record including the artificially introduced (but not interpolated) gaps
- analysis of the record after the gaps have been interpolated,

was pointed out by Baker, 1982. Whether or not the gaps need to be interpolated can be judged by comparing the results of the first two analyses while the quality of the interpolation method can be determined by comparing the results of the two later analyses.

5.2 The interpolation method

For the interpolation of gaps with INPOL a fairly variable model function is used. This function is built up of a variable set of tidal constituents and a polynomial of low degree, i.e.

$$M(t) = \sum_{i=1}^{n} A_i \cos(w_i t - \varphi_i) + \sum_{i=0}^{k} a_i t^k \qquad (5.1)$$

In INPOL the degree of the polynomial must be lower than or equal to five while the number of constituents is restricted to a maximum of ten. Normally only the main diurnal and semidiurnal constituents are used for the interpolation while the polynomial is used to represent the longperiodic or aperiodic variations.

The parameters of the function (i.e. the amplitudes and phases of the selected constituents plus the coefficients of the polynomial) are calculated by a least squares fit of the model function to the data at both sides of a gap. The amount of data used in this calculation must be chosen as to ensure the numerical stability in the solution of the resulting normal equations. The presence of satellites to each of the constituents is not taken into account in the calculation of the normal equations and the apparent amplitudes, and phases are used for the interpolation without any

correction for the satellites. Including some corrections in the program would probably slightly reduce the effect of the interpolation but would also considerably increase the computer time needed for the interpolation.

5.3 The test results

For the test two time series were used (tab. 5.1). In tab. 5.2 the gaps introduced in the two records are given. Each of the six versions of the two records was analysed with the least squares program ET6 under three different conditions:

- The record without any interpolation of gaps was analysed. The Pertsev filter with 51 coefficients was used, thus enlarging each gap by two days.
- The gaps were interpolated prior to the analysis with INPOL, using 480 hours at both sides of the gaps for the calculation of the parameters. The model function included Q_1, O_1, K_1, N_2, M_2, L_2, S_2 and a polynomial of degree 3. The Pertsev filter was used.
- To avoid the loss of data at both sides of the gaps due to the filtering, the gaps were interpolated and the data were filtered with a 501 hours filter operator (combination of diurnal and semidiurnal bandpass; Jentzsch, 1978). Then the interpolated data were removed prior to the analysis in order to reduce the effect of the interpolation on the results as much as possible.

Record	Period	Length of record in days
ELR ET-18	1978.11.22-1979.03.01	100
Theoretical tides	1978.11.22-1979.03.01	100

Tab. 5.1: The records used for the test of INPOL

Fig. 5.1 gives the results for the theoretical tides and fig. 5.2 for the recorded data. Each single diagram displays the amplitude or phase of a constituent as calculated from the six versions under one of the three conditions. Only the results for the four largest

Total amount of gaps	gap 1	gap 2	gap 3
0	0	0	0
1	.5	0	.5
2	1	0	1
3	1	1	1
5	2	1	2
10	3	4	2

Tab. 5.2: The gaps introduced in the records given in tab. 5.1. Gap 1 was centered at day 16 from the beginning of the record, gap 2 at day 50 and gap 3 at day 84. All numbers are in days

constituents are given, for O_1 and the $P_1S_1K_1$-group in the diurnal band and for M_2 and S_2K_2-group in the semidiurnal band.

The results from the analyses under the first condition (no interpolation of gaps) are surprisingly stable (fig. 5.1a (5.2a) for the diurnal and fig. 5.1d (5.2d) for the semidiurnal theoretical (recorded) bands). There is almost no change of the parameters when small gaps are introduced and even up to 10% of the data can be eliminated without any significant effect on the calculated parameters.

The results for the second condition (gaps interpolated with INPOL) show a strong dependency of the parameters on the length of the interpolated gaps. The errors increase strongly with the amount of interpolated data (Fig. 5.1b (5.2b) for the diurnal and fig. 5.1e (5.2e) for the semidiurnal theoretical (recorded)band). The used method of interpolation gives satisfying results for gaps up to 2 days. Thus whenever spectral analysis methods are applied, INPOL can be used to remove small gaps of up to 2 days but not more than 2% of the total data should be interpolated.

Comparing the two results one realizes that the effect of the interpolation is much stronger than the effect of the gaps themselves. In fact, the effect of the gaps on the results in the least squares analysis is so small that an interpolation of gaps prior to an analysis with this method cannot be recommended.

The results for the third condition (interpolated data only used for filtering) depend only slightly on the amount of data inter-

polated (fig. 5.1c (5.2c) for the diurnal and fig. 5.1f (5.2f) for the semidiurnal theoretical (recorded) band). Though one finds significant changes in the parameters from the theoretical data there are not such changes in the presence of noise as is in the recorded data. Therefore this procedure is useable whenever the filtering with long filter operators is desired. This procedure might especially be valuable in analysing longperiod constituents, though this method should be used carefully.

The test results presented here are only a small part of the actually performed tests. For the smaller constituents it can be said, that in general the results are the same as for the large ones, i.e., taking into account the larger error bars for the smaller constituents, significant changes of the parameters only occur when such changes are found for the large constituents, too.

Considering all test results, including those for other gap functions than the symmetrical ones given in tab. 5.2, the following main points can be stated:

- For the analysis of earth tidal data with a least squares fit as done in ET6 an interpolation of gaps cannot be recommended.
- The effect of the non-interpolated gaps on the results does not depend systematically on the distribution of the gaps. For a given recorded data set there is of course a slight dependency because of the different noise in different parts of the record.
- The effect of the non-interpolated gaps depends mainly on the number of gaps. This can best be seen from the results from the recorded data (fig. 5.2): between two and three days of total gaps, the number of gaps increased from two to three. There is also a slight dependency on the size of the largest single gap.
- The method of interpolation used in INPOL is valid for the interpolation of gaps of up to two days, but the amount of interpolated data should not be more than 2% of the total record.

- For lowpass filtering - requiring long filter operators - even long gaps can be interpolated prior to the filtering, but the interpolated data must not be used in the subsequent analysis.

Fig. 5.1 (next page): Results of testing INPOL with theoretical tides (see text).

Fig. 5.2 (page behind next page): Results of testing INPOL with recorded tides (ET 18, see text).

References

Asch, G., 1983: Digital data acquisition and preprocessing of tidal data. - BIM, same issue

Bachem, H.C. and H.G. Wenzel, 1973: Zur Aufbereitung der Erdgezeitenregistrierungen für die Harmonische Analyse. - BIM, 67, 3718-3726

Baker, T.F., 1982: Private communication

Best, R., 1982: Handbuch der analogen und digitalen Filterungstechnik. - AT Verlag Aarau, Stuttgart

Bonatz, M., 1974: On the problem of non-eliminated drift effects in earth-tide data. - BIM, 68, 3755-3762

Chojnicki, T., 1973: Ein verfahren zur Erdgezeitenanalyse in Anlehnung an das Prinzip der kleinsten Quadrate. - Mitt. Inst. Theor. Geod. Bonn, 15

Ducarme, B., 1975: The computation procedures at the International Center for Earth Tides (I.C.E.T.). - BIM, 72, 4165-4181

Jentzsch, G., 1978: Improved tidal filters. - BIM, 77, 4523-4533

Jentzsch, G., 1983: A gravity tidal profil along the 'Blue Road Geotraverse' - aims of research and present state of the project. - BIM, same issue

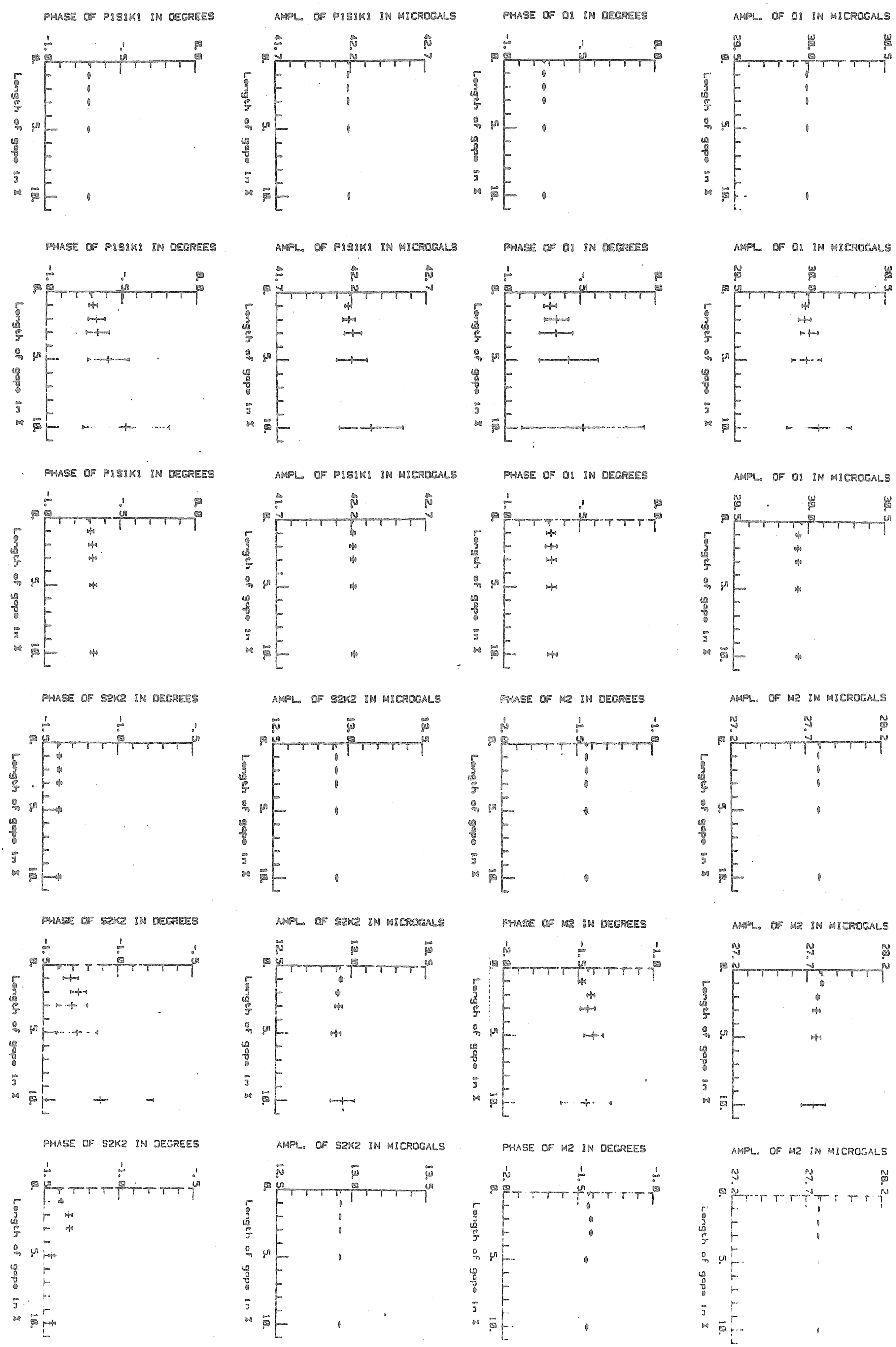
PHASE OF P1S1K1 IN DEGREES
AMPL. OF P1S1K1 IN MICROGALS
PHASE OF O1 IN DEGREES
AMPL. OF O1 IN MICROGALS
PHASE OF P1S1K1 IN DEGREES
AMPL. OF P1S1K1 IN MICROGALS
PHASE OF O1 IN DEGREES
AMPL. OF O1 IN MICROGALS
PHASE OF P1S1K1 IN DEGREES
AMPL. OF P1S1K1 IN MICROGALS
PHASE OF O1 IN DEGREES
AMPL. OF O1 IN MICROGALS
PHASE OF S2K2 IN DEGREES
AMPL. OF S2K2 IN MICROGALS
PHASE OF M2 IN DEGREES
AMPL. OF M2 IN MICROGALS
PHASE OF S2K2 IN DEGREES
AMPL. OF S2K2 IN MICROGALS
PHASE OF M2 IN DEGREES
AMPL. OF M2 IN MICROGALS
PHASE OF S2K2 IN DEGREES
AMPL. OF S2K2 IN MICROGALS
PHASE OF M2 IN DEGREES
AMPL. OF M2 IN MICROGALS

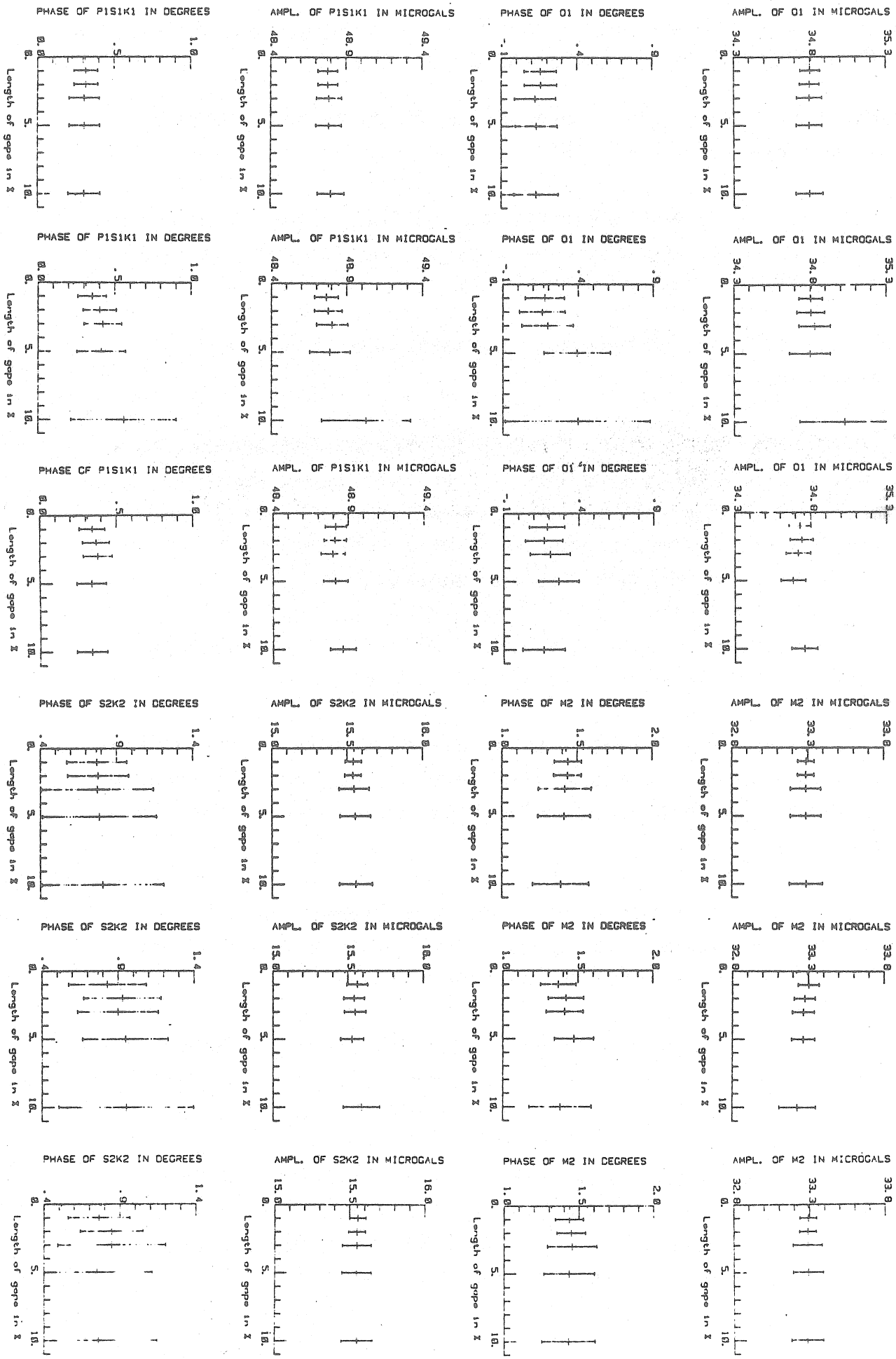
PHASE OF P1S1K1 IN DEGREES
AMPL. OF P1S1K1 IN MICROGALS
PHASE OF O1 IN DEGREES
AMPL. OF O1 IN MICROGALS
PHASE OF P1S1K1 IN DEGREES
AMPL. OF P1S1K1 IN MICROGALS
PHASE OF O1 IN DEGREES
AMPL. OF O1 IN MICROGALS
PHASE OF P1S1K1 IN DEGREES
AMPL. OF P1S1K1 IN MICROGALS
PHASE OF O1 IN DEGREES
AMPL. OF O1 IN MICROGALS
PHASE OF S2K2 IN DEGREES
AMPL. OF S2K2 IN MICROGALS
PHASE OF M2 IN DEGREES
AMPL. OF M2 IN MICROGALS
PHASE OF S2K2 IN DEGREES
AMPL. OF S2K2 IN MICROGALS
PHASE OF M2 IN DEGREES
AMPL. OF M2 IN MICROGALS
PHASE OF S2K2 IN DEGREES
AMPL. OF S2K2 IN MICROGALS
PHASE OF M2 IN DEGREES
AMPL. OF M2 IN MICROGALS
Length of gaps in %

Jentzsch, G., 1981: Automatic treatment and preprocessing of tidal data recorded at 1 min intervals. - BIM, 85, 5415-5424

Longman, I.M., 1960: The interpolation of earth-tide records. - J. Geophys. Res., 65, 3801

Massot, J.P., 1977: New interpolation method of Lacuna of earth tides records. Principle of Fourier coefficient's evolution. - Proc. 8th Int. Symp. Earth Tides, Bonn

Nakai, S., 1977: Pre-processing of tidal data. - BIM 75, 4334-4340

Plag, H.-P., 1982a: Analysen von Pegelstandsregistrierungen entlang der norwegischen Küste - Entwicklung und Anwendung eines Programmsystems sowie Ergänzungsmessungen im Bereich des Ranafjords. - Diploma thesis, Institut für Geophys. Wiss. der Freien Universität Berlin (unpublished)

Plag, H.-P., 1982b: Analysis of tidal data from the Norwegian Coast. - IKU-Rapport, P-203/1/82, Trondheim

Schüller, K. and B.S. Schulz, 1973: Die Anwendung der Prädiktion auf periodische Prozesse, eine Methode zur Überbrückung von Lücken in der Erdgezeitenregistrierung. - Mitt. Inst. Theor. Geod. Bonn, 14

Sukhwani, P. and R. Vieira, 1978: Three different methods for taking into account the gaps in spectral analysis of earth tides records. - BIM, 78, 4690-4698

Venedikov, A.P., 1966: Une méthode pour l'analyse des marées terrestres a partir d'enregistrements de longueur arbitraire. - Observatoire Royal de Belgique, Communications No. 250

Wenzel, H.G., 1976: Zur Genauigkeit von gravimetrischen Erdgezeitenbeobachtungen. - Wissenschaftliche Arbeiten der Lehrstühle für Geodäsie, Photogrammetrie und Karthographie an der Technischen Universität Hannover, Nr. 67

Traduction

ANALYSE NUMERIQUE DES OBSERVATIONS DE MAREES TERRESTRES

G.P. Pilnik, V.Ia. Galkin, E.D. Youkovskii, S.YOU Pliskin

Méthodes de calcul et Programmation - Publ. 37, Editions de l'Université de Moscou pp 134-146-1982

(N.B. L'introduction a été abrégée)

Nous nous limitons ici à l'étude des ondes de périodes de 9 à 32 jours (voir table 1). Les difficultés de l'étude des ondes de périodes plus longues sont signalées en [2] où on parle aussi du procédé de composition de la fonction aléatoire pour l'étude de ces ondes. Comme données de départ on s'est servi des écarts des observations astronomiques dans différents observatoires en fonction du système libre $u_* - u$ et des erreurs Δ purement instrumentales publiées dans les Bulletins "Temps étalon" [3].

Table 1.

Caractéristique de la fonction de marée

N°	Coefficient du sinus (en $0^s.0001$)	Argument	Période	Symbole
1	+ 3.2k	$2\mathbb{C}+\ell$	9.133	M_{tf}
2	+ 1.3k	$2\mathbb{C}+\ell-\Omega$	9.121	
3	+24.9k	$2\mathbb{C}$	13.661	M_f
4	+10.3k	$2\mathbb{C}-\Omega$	13.633	
5	+ 1.0k	$2\mathbb{C}-2\Omega$	13.606	
6	+ 1.1k	2ℓ	13.777	
7	+ 2.3k	$2\mathbb{C}-2\odot$	14.765	MS_f
8	+26.5k	ℓ	27.555	M_m
9	- 1.7k	$\ell+\Omega$	27.667	
10	- 1.7k	$\ell-\Omega$	27.443	
11	- 1.4k	$2\mathbb{C}-\ell$	27.093	
12	- 0.6k	$2\mathbb{C}-\ell-\Omega$	26.985	
13	+ 5.9k	$2\mathbb{C}-\ell-2\odot$	31.812	MS_m

Table 1 (Suite)

N°	Coefficient du sinus (en $0^s.0001$)	Argument	Période	Symbole
14	+ 6.1k	$2\odot+\ell'$	122	
15	+155.3k	$2\odot$	183	S_{sa}
16	- 3.8k	$2\odot-\Omega$	183	
17	+ 49.6k	ℓ'	365	S_a
18	- 2.3k	$2\odot-\ell'$	365	
19	+5198.0k	Ω	18.6	
20	- 27.0k	2Ω	9.3	

Notations: k est le nombre de Love, $\mathbb{C}$ est la longitude moyenne de la Lune, ℓ est l'anomalie moyenne de la Lune, Ω est la longitude moyenne du noeud lunaire, $\odot$ est la longitude moyenne du Soleil, ℓ' est l'anomalie moyenne du Soleil.

Les recherches théoriques de M.S. MOLODENSKII montrent que pour un modèle de Terre avec noyau liquide k = 0.3070 et pour un modèle avec un noyau liquide et graine solide k = 0.3015 [4,5], le procédé de déduction de k d'après les variations de marées du plus grand moment d'inertie de la Terre peut servir à une étude précise.

Table 2.

Résultats de la détermination du nombre de Love

N°	$k(M_f)E$	$k(M_m)E$	Auteur
1	0.331±0.061	0.265±0.068	Guinot [9]
2	0.334±0.005	0.295±0.011	Guinot [8]
3	0.315±0.012	0.285±0.006	Pilnik [10]
4	0.309±0.018	0.290±0.013	Pilnik [11]
5	0.300±0.005	0.282±0.007	Pilnik [2]
6	0.300±0.007	0.291±0.012	Pilnik [12]
7	0.301±0.005	0.281±0.005	Pilnik [13]
8	0.28 ±0.04	0.26 ±0.26	Lambeck,Cazenave [14]
9	0.352 -	0.195 -	Djurovic,Melchior [15]
10	0.349 -	0.261 -	Djurovic,Melchior [15]
11	0.396 -	0.262 -	Djurovic [16]
12	0.390 -	0.282 -	Djurovic [16]
13	0.343±0.030	0.301±0.044	Djurovic [17]

Ici, une limitation regrettable provient de la grande dispersion des erreurs dans la détermination du temps.

Nous donnons dans la table 2 les valeurs du nombre de Love k évaluées par les méthodes de l'analyse spectrale.
Nous y constatons que les valeurs obtenues pour les différentes ondes, divergent: k(Mf) > k(Mm). Il est donc extrêmement souhaitable d'obtenir ces valeurs par d'autres méthodes mathématiques. De fait, on introduit dans les observations astronomiques les corrections de nutation mais celles-ci doivent sans doute être précisées. Les coefficients de nutation ont été déduits dans l'hypothèse d'une Terre absolument rigide. Les marées et la nutation sont provoquées par une même cause et leurs ondes ont les mêmes périodes.

§ 1. Estimation récurrante du nombre de Love k

1° Le modèle mathématique de la déformation de marée de la Terre solide est décrit par l'équation

$$y(t) = k\,x(t) + v(t) \qquad (1)$$

où y(t) sont les résultats des observations astronomiques du service soviétique de l'heure pour la période de 1951 à 1974, x(t) est la fonction théorique de l'irrégularité de marée de la rotation de la Terre représentée par la formule

$$\begin{aligned} x(t) = 0^{s}.0001\,(&3.2\sin(1{,}39936474+0.68797022t) + \\ &+1.3\sin(1.52748374+0.68889437t)+ \\ &+24.9\sin(1.74459318+0.45994295t)+ \\ &+10.3\sin(1.87432582+0.46086728t)+ \\ &+2.0\sin(2.00244476+0.46179143t)+ \\ &+1.1\sin(5.59111476+0.45605436t)+ \\ &+2.3\sin(4.44957846+0.42553745t)+ \\ &+26.5\sin(5.93808851+0.22802709t)+ \\ &+1.7\sin(5.80822421+0.22710294t)- \\ &-1.7\sin(6.06607575+0.22895142t)- \\ &-1.4\sin(2.09143527+0.23191586t)- \\ &-0.6\sin(2.21942251+0.23284019t)+ \\ &+5.9\sin(4.79467515+0.19751036t), \end{aligned} \qquad (2)$$

qui correspond à la somme des 13 premières ondes de la table 1; v(t) sont les erreurs d'observations.

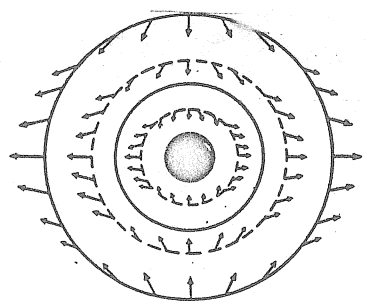

Fig.1

Nous noterons que les valeurs observées y(t), obtenues lorsque le paramètre t varie de 0 à 8762 avec un pas 1, sont le résultat de la moyenne de la série des mesures effectuées dans les jours donnés en différents observatoires. La quantité de mesures en des jours différents n'est pas constante et dépend de l'époque de l'année, des programmes scientifiques, des conditions climatiques etc... . Habituellement le nombre des observations varie dans les mois d'hiver de 0 à 10, au printemps de 5 à 15, en été de 10 à 20.

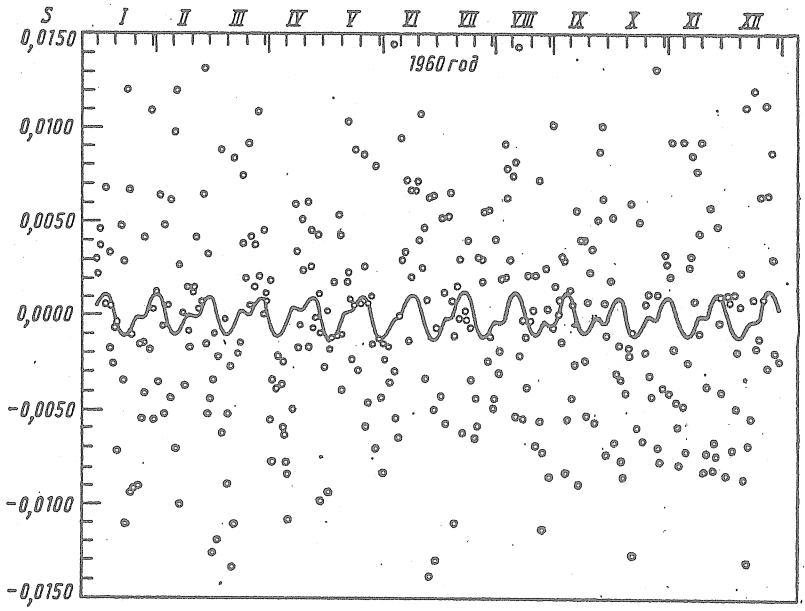

Figure 2

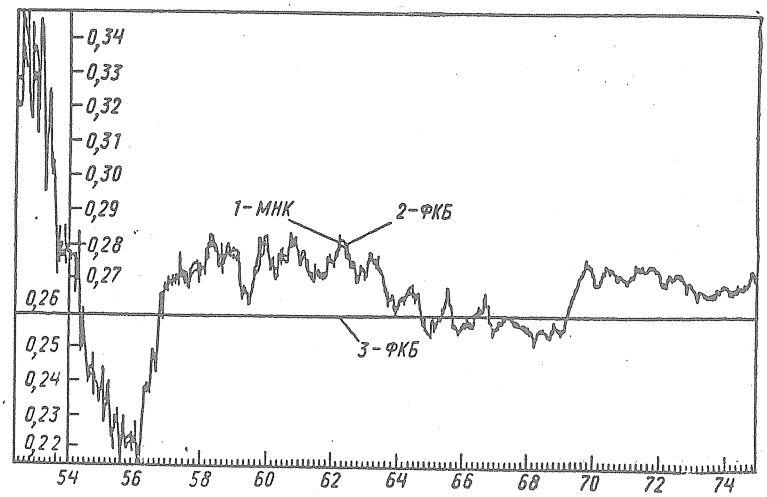

Figure 3

Les observations sont intensifiées lors des programmes géophysiques internationaux et croît de 50 à 70 observations, c'est pourquoi la valeur calculée du nombre de Love k pour cette époque est la plus sûre. Nous donnons sur la figure 2 les observations de l'année 1960 (petits cercles) et le signal de marée kx(t) pour k = 0,3. Cette figure montre clairement la complication du problème de l'évaluation des paramètres du modèle (1) et de son interprétation.

2° Dans l'hypothèse d'une répartition normale du bruit on applique la méthode des moindres carrés selon la formule

$$k_n = \frac{\sum_{i=0}^{n} (1/\sigma_i^2)\, x_i y_i}{\sum_{r=0}^{n} (1/\sigma_i^2)\, x_i^2}. \qquad (3)$$

Nous donnons dans la table 3 les résultats du calcul de k_n et de son écart quadratique moyen annuel. La figure 3 montre la variation de l'estimation du nombre de Love en fonction de l'augmentation du nombre d'observations. Elle montre que pour l'intervalle initial d'environ 3000 points et à cause des particularités de la fonction x(t) (2) dont nous effectuerons ensuite l'étude, le nombre de Love k présente une grande divergence et se stabilise ensuite jusqu'à être quasi constant avec une variation à la troisième décimale.

Table 3

Evaluation du nombre de Love par moindres carrés et par la méthode de Kalman

Epoque	Nombre de points	moindres carrés		Kalman-Buss	
		k	E	k	E
1951-1974	8763	0,270	±0,09	0,273	±0,03
1961-1974	5115	0,261	±0,13	0,266	±0,04
1956-1959	1461	0,304	±0,24	0,299	±0,06
1957	365	0,703	±0,40	0,621	±0,20
1957-1958	730	0,520	±0,30	0,462	±0,09
1957-1959	1095	0,400	±0,26	0,374	±0,08
1958	365	0,344	±0,36	0,299	±0,12
1958-1959	730	0,250	±0,29	0,254	±0,10
1959	365	0,165	±0,42	0,194	±0,15

3° A cause du bruit important dans le signal (fig.2) il nous a paru utile d'appliquer le filtre de Kalman-Buss [18-20] pour l'évaluation de k sous la forme

$$k_{i+1} = k_i + \left(\frac{\gamma_i x_{i+1}}{\sigma_i^2 + \gamma_i x_{i+1}^2} \right) (y_{i+1} - k_i x_{i+1}), \quad k_i|_{i=0} = k_0,$$
$$\gamma_{i+1} = \gamma_i - \frac{\gamma_i^2 x_{i+1}^2}{\sigma_i^2 + \gamma_i x_{i+1}^2}, \quad \gamma_i|_{i=0} = \gamma_0. \tag{4}$$

où k_i est l'estimation de l'espoir mathématique (de la première époque) du nombre de Love k et γ_i est l'estimation de sa dispersion d'après la longueur correspondante de la série temporelle. Les équations (4) conviennent non seulement par leur simplicité de calcul mais par le fait qu'elles permettent de tenir compte facilement de l'information a priori sur la solution cherchée. Elles donnent une forme récurrente de l'enregistrement de la méthode de régularisation de A.N. Tikkonov [20] et trouvent notamment l'extrémale minimisée de la fonctionnelle

$$T(k) = \sum_{i=0}^{8762} \left[\left(\frac{y_i - kx_i}{\sigma_i} \right)^2 + \left(\frac{k - k_0}{\gamma_i} \right)^2 \right]. \tag{5}$$

Ainsi à titre d'information à priori sur le nombre de Love on peut utiliser le fait que k est une constante et non une fonction ce qui est impossible dans les moindres carrés. Pour calculer cela il faut donner une approximation initiale pour k_o (nous avons pris k_o = 0,5) et diminuer fortement la dispersion a priori (γ_o = 0,00001). La courbe 3 (voir fig.3) est le résultat de cette procédure de régularisation. Lors de l'augmentation de γ_o (γ_o = 0.05) ce qui correspond à l'affaiblissement du régularisateur on obtient une courbe qui suit la courbe obtenue par la méthode des moindres carrés (voir la courbe 2 sur la fig.3).

4° Pour évaluer la valeur scalaire du nombre de Love on a appliqué également l'algorithme récurrent de la minimisation de la fonctionnelle entropique

$$H(k) = \sum_{i=0}^{8762} \left(\frac{y_i - kx_i}{\sigma_i} \right)^2 e^{-\left(\frac{y_i - kx_i}{\sigma_i} \right)^2} + \left(\frac{k - k^0}{\gamma^0} \right)^2 e^{-\left(\frac{k - k^0}{\gamma^0} \right)^2}, \tag{6}$$

qui représente la généralisation de la méthode régularisée des moindres carrés [2]. En effet, en décomposant l'exposant en série, nous obtiendrons dans le cas particulier aussi les moindres carrés. L'avantage de ce procédé d'estimation réside dans le fait que le facteur de poids

$$\exp\left\{-\frac{(y_i - kx_i)^2}{\sigma_i}\right\}$$

élimine automatiquement les observations "anormales" en leur attribuant un poids faible ce qui est important pour les problèmes dotés d'une mauvaise statistique.

Nous décrivons la tactique d'application de l'algorithme itératif [22] pour la minimisation des fonctionnelles du type:

$$H(k_1, \ldots, k_n) = \sum_{i=1}^{m}\left(\frac{y_i - \sum_{j=1}^{n} k_i x_{ij}}{\sigma_i}\right)^2 e^{-\left(\frac{y_i - \sum_{j=1}^{n} k_i x_{ij}}{\sigma_i}\right)^2} + \sum_{i=1}^{n}\left(\frac{k_i - k_i^0}{\gamma_i^0}\right)^2 e^{-\left(\frac{k_i - k_i^0}{\gamma_i^0}\right)^2}.$$

Dans le processus d'itération pour obtenir le minimum on procède de la façon suivante:

$$\begin{aligned} k^{s+1} &= k^s - \tau_s B_s q_{l_s}^T (q_{l_s} k^s - y_{l_s}), \\ B_{s+1} &= B_s - \tau_s B_s q_{l_s}^T q_{l_s} B_s. \end{aligned} \tag{7}$$

Ici τ_s est le paramètre numérique, q_{ℓ_s} - ℓ_s ième ligne de la matrice de dimension (m x n) composée des x_{ij}; B_s est la matrice carrée (n x n).

1. Choisissons les valeurs initiales des coefficients de poids

$$\omega_i^0 = \begin{cases} 1/\sigma_i^2, & 1 \leqslant i \leqslant m, \\ 1/\gamma_i^2, & m < i \leqslant m+n. \end{cases}$$

2. Les valeurs initiales k et B seront à priori:

$$k = k^\circ, \quad B_o = \gamma^\circ$$

3. Effectuons un pas d'après les formules (7) en choisissant

$$\ell_s = s + 1, \quad \tau_s = \omega_{\ell_s}^\circ / (1 + \omega_{\ell_s}^\circ p_s), \quad s = 0, 1, \ldots, m-1,$$

où $p_s = q_{\ell_s} B_s q_{\ell_s}^T$

4. Effectuons les pas ultérieurs du processus (7) en partant de

$$\ell_s: \max |\alpha_i^s - \omega_i^s|, \quad \tau_s = \mu_s / (1 + \mu_s p_s),$$

où $\mu_s = \alpha_{\ell_s}^s - \omega_{\ell_s}^s$;

$$\alpha_i^s = \begin{cases} 1/\sigma_i^2 \, e^{-\left(\sum_{j=1}^{n} k_j x_{ij} - y_i\right)^2/\sigma_i^2}, & 1 \leqslant i \leqslant m, \\ 1/\gamma_i^2 \, e^{-(k_i^s - k_i^0)^2/\gamma_i^2}, & m < i \leqslant m+n, \end{cases}$$

$$\omega_i^{s+1} = \omega_i^s - \mu_s \delta_{i l_s}, \quad i = 1, \ldots, m+n,$$

où δ_{il_s} est le symbole de Kronecker. Les itérations se prolongent jusqu'à ce que la valeur p_s ne devienne pas plus petite que celle donnée.

Dans notre cas concret les dimensions du problème sont les suivantes:
m = 8763, n = 1 c'est à dire que la matrice X a les dimensions (8763 x 1) et B_s se transforme en paramètre numérique. Pour les différentes valeurs σ_i^2 nous obtiendrons les estimations suivantes du nombre de Love k:

$$\sigma^2 = 10,\ \sigma^2 = 1,\ \sigma^2 = 0.1,\ \sigma^2 = 0.01,\ \sigma^2 = 0.001,$$

$$k = 0.276,\ k = 0.277,\ k = 0.278,\ k = 0.280,\ k = 0.288.$$

§ 2. Etude du modèle de marée en informatif

1° Par l'enregistrement analytique du modèle d'irrégularité de marée (2) il est facile de s'apercevoir qu'elle contient arbitrairement cinq intervalles localisés de fréquence ou cinq groupes des fonctions quasi périodiques. Dans le premier groupe entrent la 1ère et la 2ème ondes; dans le deuxième, la 3e et la 6e ondes; dans la troisième, la 7e onde; dans la quatrième, la 8e et la 12ème ondes et dans la cinquième la 13e onde. Cependant le modèle analytique et son analogue de forme matricielle d'approximation discrète peuvent différer fortement d'après leurs propriétés mathématiques. Ainsi par exemple, les ondes du deuxième groupe ont des périodes de 13.661; 13.633; 13.606 et 13.777 jours et sont différentes dans l'enregistrement analytique et par conséquent linéairement indépendantes. Cependant si on les examine sur le réseau discret dans la représentation vectorielle, à cause finalement de la représentation de catégorie de ces fonctions presque périodiques, elles peuvent être des vecteurs linéairement dépendants. Nous sommes amenés à cette déduction également par le comportement instable de l'estimation du nombre de Love k dans les premiers trois milles points (voir fig.3). Ce fait peut s'expliquer par le fait qu'à cause de la dépendance linéaire de certains groupes de vecteurs dans cette partie les successions autocorrélative et réciproquement corrélative ont la forme en delta, ce qui explique la conduite instable de leurs relations. Pour étudier ce fait le modèle (2) a été soumis au rangement (mise en ordre des

colonnes selon l'accroissement de leur dépendance linéaire) dans différents intervalles: dans les premiers 50 points (i = 1 jusqu'à 50 avec le pas 1; dans les premiers 80 points (i = 1 jusqu'à 80 avec le pas 1) etc... (voir table 4); comme on le constate dans la table 4, plus l'intervalle de temps examiné est grand, plus grande est l'indépendance linéaire pour les vecteurs correspondant à ces ondes ce qui est déterminé "par la divergence" naturelle des fonctions quasi-périodiques pour l'intervalle de temps toujours croissant.

D'après les données de la partie supérieure de la table 4 nous essayons de répondre à la question principale: quelles ondes dans les cinq groupes précédemment examinés sont interprétées comme "importantes" et par conséquent lesquels de ces cinq groupes existent?
Pour répondre à la question donnée nous construisons un graphique de poids arbitraire des harmoniques suivant le numéro de l'onde (fig.4) et d'après la partie supérieure de la table 4.

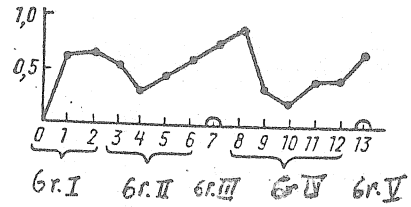

Fig. 4.

Comme on le constate sur la figure 4 les harmoniques 4ème dans le deuxième groupe, la 9e et la 10e dans le quatrième groupe "s'expriment presque linéairement" par les autres ondes et portent "faiblement" une information indépendante dans le modèle (2).
Les harmoniques 8e, 7e, 13e, 2e et 6e sont les ondes principales qui représentent cinq groupes.

2° L'analyse spectrale de la différence y(t) - kx(t) [10] montre la présence d'ondes "parasites" avec des périodes de 29,5 - 25,1 - 14,8 - 14,2 et 5,5 jours. Ces ondes sont provoquées non pas par les variations de marées du moment d'inertie et sont déterminées par d'autres causes. C'est pourquoi leur utilisation pour l'estimation du nombre de Love k est impossible. On peut préciser le modèle (1) après l'avoir représenté sous la forme

$$y(t) = kx(t) + p(t) + v(t) \qquad (6)$$

Table 4

Résultats de rangement du modèle (2)

i = 1 jusque 50	i = 1 jusque 80	i = 1 jusque 500 par 10	i = 1 jusque 800 par 10	i = 1 jusque 5000 par 100	i = 1 jusque 8000 par 100	Rangement des 50 premiers points (MHK)	Rangement selon tout intervalle (MHK)
8	8	8	8	8	8	3	8
3	1	2	7	5	13	10	4
2	5	7	6	1	12	2	1
7	7	5	2	7	3	13	7
13	13	13	5	11	6	7	13
6	11	6	12	13	2	1	6
11	3	12	13	6	7	6	12
1	2	1	3	2	9	11	2
5	6	3	1	4	1	5	5
12	9	9	9	9	10	9	11
9	12	11	11	12	11	4	9
4	4	4	10	3	4	8	10
10	10	10	4	10	5	12	3

Coefficients normalisés de la dépendance linéaire des colonnes du modèle

1.		1		1.		1		1	1	1		1	
0.998		0.999		0.999		0.999		1	0.999	0.993		1	
0.994		0.998		0.999		0.999		0.999	0.999	0.749		0.999	
0.885		0.864		0.997		0.999		0.999	0.999	0.209		0.999	
0.877		0.658		0.894		0.989		0.998	0.999	0.749	10^{-1}	0.998	
0.614	10^{-1}	0.143		0.830		0.985		0.993	0.998	0.724	10^{-4}	0.978	
0.603	10^{-1}	0.677	10^{-1}	0.599		0.931		0.958	0.990	0.264	10^{-4}	0.978	
0.219	10^{-1}	0.259	10^{-1}	0.131		0.507		0.958	0.980	0.260	10^{-4}	0.923	
0.2	10^{-2}	0.122	10^{-1}	0.120		0.248		0.944	0.986	0		0.557	
0.7	10^{-3}	0.219	10^{-2}	0.687	10^{-1}	0.227		0.903	0.985	0		0.528	
0.1	10^{-5}	0.264	10^{-4}	0.395	10^{-1}	0.948	10^{-1}	0.901	0.975	0		0.290	
0.4	10^{-7}	0.228	10^{-5}	0.132	10^{-2}	0.616	10^{-2}	0.719	0.964	0		0.280	
0.1	10^{-7}	0.150	10^{-6}	0.612	10^{-3}	0.328	10^{-2}	0.459	0.626	0		0.190	

où p(t) est la superposition des ondes "parasites" et on évalue la valeur des amplitudes et des phases de ces ondes. En [10] ces estimations ont déjà été obtenues par la méthode d'analyse spectrale. Nous avons évalué les paramètres des ondes parasites par moindres carrés et avons obtenu les valeurs suivantes (table 5).

Table 5

Valeurs des amplitudes des harmoniques évaluées ($0^s.0001$) par moindres carrés

Période / a priori, valeur k	$5^d.5$	$14^d.2$	$14^d.8$	$25^d.1$	$29^d.5$
0.26	1.0	7.9	1.7	2.7	3.2
0.35	1.0	8.0	1.7	2.7	3.3
0.40	0.9	8.1	1.7	2.5	3.2

L'étude a montré que l'évaluation de k dans le modèle (1) avec les ondes "parasites" ne change pas fortement l'évaluation. Ainsi, par exemple, le calcul de k par la méthode de Kalman avec les mêmes paramètres a donné k = 0,2735 (avec soustraction des ondes parasites; k = 0.2739 (sans soustraction de ces ondes.

3° Comme on l'a déjà dit, les marées et les nutations sont provoquées par une seule cause et leurs ondes ont les mêmes périodes (voir table 1). Les corrections à la nutation sont introduites dans les déterminations astronomiques du temps et si elles sont erronnées cela se fera sentir sur la détermination de k pour les différentes ondes. Il est extrêmement intéressant d'obtenir k à partir d'ondes séparées. Dans ce cas, le modèle (1) prend la forme

$$y(t)=\sum_{i=1}^{13} k_i x_i(t)+v(t), \qquad (7)$$

où k_i est le nombre de Love correspondant à la $i^{\text{ième}}$ composante de la fonction de marée théorique. Nous donnons dans la table 6 les résultats de l'évaluation du secteur $k = (k_1 \ldots k_{13})$ par moindres carrés avec soustraction des ondes "parasites" et sans soustraction (de façon analogue à la méthode de Kalman).

Les recherches faites permettent de tirer les conclusions suivantes:

Table 6

Evaluation du vecteur k

	Procédé	MHK(.B.)	MHK(C.B.)	ΦKB(.B.)	ΦKB(C.B.)
	Amplitude (en 0^s0001) Période (en jours)	E^k_k	E^k_k	E^k_k	E^k_k
1.	+3.2	0.338	0.387	0.397	0.363
	9.133	-	-	0.144	0.137
2	+1.3	0.779	0.781	0.557	0.605
	9.121	-	-	0.250	0.242
3	+24.9	0.233	0.233	0.230	0.224
	13.661	-	-	0.021	0.020
4	+110.3	0.331	0.338	0.335	0.337
	13.633	-	-	0.051	0.048
5	+1.0	0.002	0.049	0.208	0.269
	13.606	-	-	0.272	0.268
6	+1.1	0.855	0.809	0.540	0.492
	13.777	-	-	0.264	0.258
7	+2.3	-0.119	-0.261	-0.011	-0.113
	14.765	-	-	0.250	0.260
8	+26.5	0.293	0.293	0.303	0.295
	+27.555	-	-	0.020	0.018
9	-1.7	0.008	0.001	0.050	0.136
	27.667	-	-	0.222	0.215
10	-1.7	0.882	0.850	1.251	1.225
	27.443	-	-	0.250	0.245
11	-1.4	1.117	1.189	0.697	0.654
	27.093	-	-	0.243	0.236
12	0.6	0.082	0.118	0.380	0.330
	26.859	-	-	0.296	0.294
13	+5.9	0.324	0.314	0.294	0.313
	31.812	-	-	0.080	0.081
Moyenne pondérée de k		0.298	0.296	0.299	0.296
Moyenne pondérée de E		-	-	0.063	0.062

1. Les valeurs du nombre de Love k = 0.298; 0.296; 0.299; 0.296 (voir Table 6) obtenues par les différentes méthodes concordant bien avec sa valeur théorique pour le modèle de Terre avec un noyau liquide et une graine solide.

2. L'étude du problème doit être continuée par les méthodes d'analyse spectrale puisque il y a les écarts possibles des phases initiales des composantes harmoniques dans la représentation théorique de la fonction de marée.

Bibliographie.

1. WOOLARD E.
Inequalities in Mean Solar Time from Tidal Variation in the Rotation of the Earth.
Astron. J. 1959, v 64, N°4, p. 140-142.

2. PILNIK G.P.
Irrégularité de marée de la rotation de la Terre.
R.A. 1975 T.52, N°1 pp. 179 à 188.

3. Temps étalon.
M. Edit. de l'état. Bulletin de 1951 à 1974.

4. MOLODENSKII M.S.
Marées terrestres et nutation de la Terre.
M. Edit. Ac. des Sc. URSS, 1961.

5. PARIISKII N.N.
Marées terrestres et structure interne de la Terre.
Izv. Ac. des Sc. URSS,série géophys. 1963, N°2 pp 25 à 36.

6. MELCHIOR P.
Marées Terrestres. M. Mir. 1968.

7. BARSENKOV S.N.
Séparation des ondes à longue période provenant des variations de marées de la force de pesanteur.
Izv. Ac. des Sc.URSS, série Physique de la Terre,1972,N°6-pp.46 à 61.

8. GUINOT B.
A determination of the Love Number k from the Periodic Waves of UTI.
Astron. and Astrophys., 1974, v.36, N 1, p. 1-4.

9. GUINOT B.
Short-period Terms in Universal Time.
Astron. and Astrophys., 1970, v.8, N 1, p.26-28.

10. PILNIK G.P.
Analyse corrélative des marées terrestres et de la nutation.
A.J. 1970, T.47, N°6 - pp.1308 à 1323.

11. PILNIK G.P.
Analyse spectrale des marées terrestres à longue période.
Izv. Ac. des Sc. URSS,Série Physique de la Terre 1974,N°4 - pp 3 à 14.

12. PILNIK G.P.
De l'étude de la nutation forcée.
A.J. 1976, T.53, N°4, pp. 889 à 898.

13. PILNIK G.P.
Fonction accidentelle du temps universel.
A.J. 1979, T.56, N°3 - pp.664 à 671.

14. LAMBECK K., CASENAVE A.
The Earth's Rotation and Atmospheric Circulation.
The Continuum.-Geophys. J. Roy. Astron. Soc., 1974, V. 38, N 1, p.49-61.

15. DJUROVIC D., MELCHIOR P.
Recherche des Termes de Marée dans les Variations de la Rotation de la Terre.
Commun. Obs. Roy. de Belgique, Série B, 1972, N 79, p. 3-15.

16. DJUROVIC D.
Les Termes de Marée dans le Temps.
Universal. Bull. - Observation Marées Terrestres, 1975, v.4, f.3, p.3-16.

17. DJUROVIC D.
Détermination du nombre de Love K et du facteur affectant les Observations du Temps Universel.
Astron. and Astrophys., 1976, v.47, N 3, p. 325-333.

18. LIPTSER R.Ch. SCHIRAEV A.N.
Statistique des processus accidentels.
M. Naouka 1974.

19. JOUKOVSKII E.D., ZAIKIN R.N.
Sur les algorithmes statistiques numériques de découverte des systèmes algébriques linéaires.
J.V.M. et M.F. 1975 - T.15, N°3 pp 560 à 572.

20. JOUKOVSKII E.D.
Sur l'application des algorithmes statistiques régularisant à la solution de certains types des problèmes posés incorrectement.
Dans le livre, certaines questions de la réduction automatisée et de l'interprétation des expériences physiques.
M. Edit. M.Ï.Y. 1973, pp 133 à 170.

21. JOUKOVSKII E.D.
Méthode d'entropie maximum et régularisation des systèmes linéaires.
Dan. 1979, T.246, N°5, pp. 1041 à 1045.

22. BERSENEV S.M.
Sur le calcul des solutions généralisées des systèmes avec des matrices de lentilles.
Dans le livre - Méthodes de calcul de l'algèbre linéaire.
Novossohirsk. Edit. S.A. des Sc. URSS, 1978 pp.102 à 105.

Traduction

SUR LE CONTENU SPECTRAL DES VARIATIONS DE LA PESANTEUR D'APRES LES OBSERVATIONS A YALTA.

V.P. Schliakhovii, P.S. Korba

Rotation et déformations de marées de la Terre - vol.13 - pp.34-38 - 1981

Il est bien connu que les méthodes d'analyse harmonique (1) utilisées habituellement lors de la réduction des observations de marées terrestres, permettent de déterminer les amplitudes et les phases des ondes de marées dont les fréquences sont connues. Les paramètres des composantes ayant d'autres fréquences restent inconnus, ce qui est souvent insuffisant pour l'interprétation géophysique des observations.

Pour estimer par exemple le niveau du bruit de différentes sortes, dans la séparation des harmoniques qui ne sont pas d'origine de marée, il faut déterminer les amplitudes et les phases d'harmoniques de fréquences inconnues. L'analyse spectrale permet d'obtenir l'une et l'autre information nécessaire.

Le propre de l'analyse spectrale (2,3), à l'inverse de l' analyse harmonique, pose des exigences supplémentaires pour le matériau observé. Pour obtenir une haute séparation en fréquence la durée nécessaire des observations, déterminée par la relation $\Delta w \, L$ (Δw - séparation en fréquence) (L est la durée d'observation), doit être suffisamment grande. En outre pour simplifier les calculs il faut toujours avoir des observations ininterrompues. D'autre part, la durée de l'enregistrement est limitée par le volume de la mémoire de l'ordinateur. Toutefois,

l'analyse spectrale des marées terrestres présente un grand intérêt dans beaucoup de cas et ces derniers temps elle est largement appliquée (3,8).

Nous donnerons ci-après les résultats de l'analyse spectrale faite dans le domaine de fréquences de 2,49 à 4,49 cycle/jour (domaine des vitesses angulaires de 37,42 à 67,33 degré/heure) des observations de marées terrestres faites de 1966 à 1968 à Yalta, à l'aide d'un Gravimètre GS-11. Les ordonnées horaires obtenues à la suite d'une préparation préliminaire des données (4) ont servi de données de départ.

Tenant compte des exigences de l'analyse, on a choisi une partie de l'enregistrement d'une durée de 1,3 ans - du 03.03.1967 au 30.05.1968. Pour trouver les spectres de Fourier à partir de ces données on a formé cinq ensembles avec recouvrement d'une durée de six mois chacun. A l'aide de filtres numériques passe-bas on réalise préalablement l'élimination des composantes diurnes et semi-diurnes principales pour diminuer leur apport dans la partie étudiée du spectre.

L'analyse a été faite sur EC-1020 d'après les formules classiques des transformations de cosinus et de sinus de Fourier avec une fenêtre rectangulaire (programme composé par B.S. DOUBIK). L'échelle de sensibilité de l'enregistrement pour chaque ensemble de six mois a été prise constante et on a pris la moyenne de toutes les déterminations de l'ensemble.

Les résultats des calculs sont donnés sur les figures 1 à 3. La courbe supérieure est le spectre obtenu pour le premier ensemble de données, la courbe moyenne est le spectre trouvé d'après cinq ensembles successifs, la courbe inférieure est le spectre énergétique calculé pour les cinq ensembles.

Pour évaluer l'influence des variations lentes de la sensibilité sur le contenu spectral de l'enregistrement, le dernier ensemble (du 30.11.1967 au 30.05.1968) où l'on a observé une variation maximale de la sensibilité de l'enregistrement a été réduit aussi bien avec sensibilité constante que variable: la dérive de la sensibilité expérimentale y avait une allure décroissante linéaire atteignant environ 1,8% par mois.

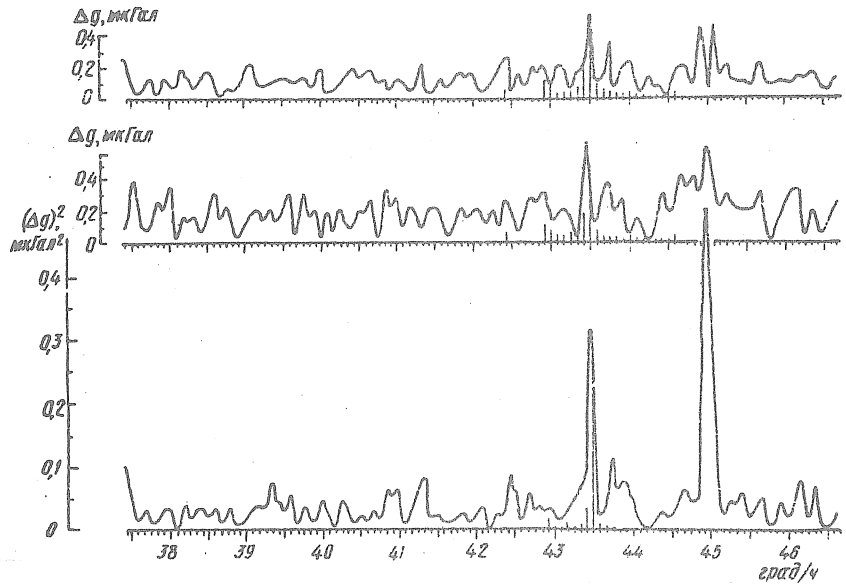

Fig.1: Vue générale des spectres des variations de la pesanteur dans la zone de 37,5 à 46,7 degrés/heure.

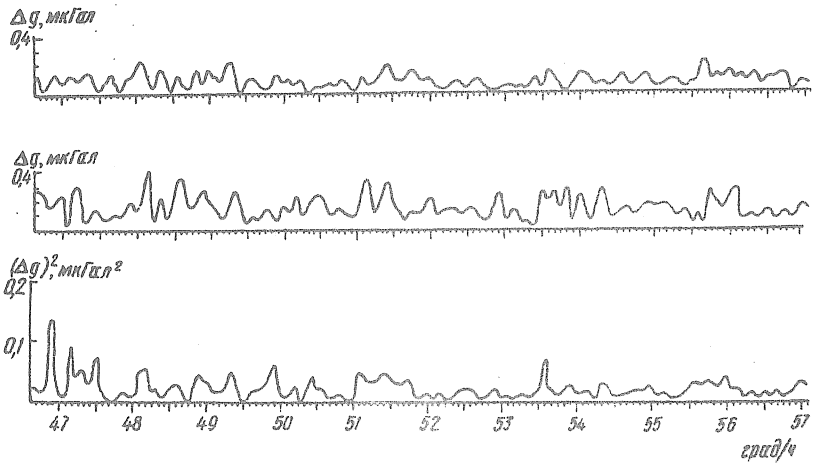

Fig.2: Vue générale des spectres des variations de la pesanteur dans la zone de 46,7 à 57,0 degrés/heure.

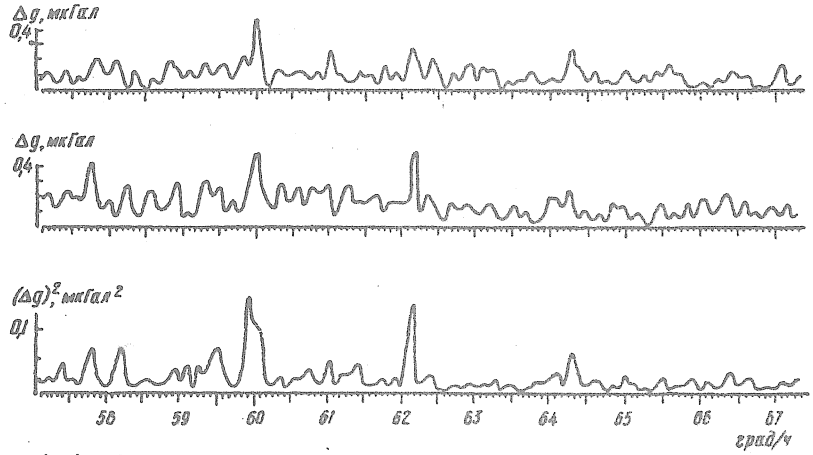

Fig.3: Vue générale des spectres des variations de la pesanteur dans la zone de 57,0 à 67,4 degrés/heure.

C'est pourquoi on a utilisé un modèle linéaire de variations de la sensibilité avec des coefficients trouvés d'après les données expérimentales. La comparaison des spectres obtenus pour deux variantes de la sensibilité de l'enregistrement a montré que l'influence de la dérive lente de la sensibilité du système gravimètre - galvanomètre n'est pas importante.

Le choix de l'échelle de l'enregistrement reflétant bien la réalité de ces variations est très complexe. Outre l'allure lente de la dérive de sensibilité au cours des mois il y a aussi des fluctuations à courte période. Il y a beaucoup de causes déterminant la dérive lente de la sensibilité du système (incandescence de l'ampoule, variation de pression, température et autres). La réalité de l'existence de grandes fluctuations à courte période de la sensibilité est douteuse.

De plus les recherches les plus récentes faites à Poltava (5) ont montré que cette divergence dépend très fort de la méthode choisie de la détermination de l'échelle d'enregistrement et n'apparaît pas lors de grands déplacements.

Pour contrôler la méthode de calcul on a calculé le spectre de la marée théorique (6) aussi bien avec une sensibilité constante qu'avec sensibilité variable comme ce qui a été fait pour un seul ensemble expérimental. On n'a pas décelé de différences importantes dans le spectre de la marée théorique ni des raies supplémentaires. C'est pourquoi on a conclu que la méthode utilisée convient tout à fait pour étudier la composition spectrale des enregistrements gravimétriques dans le domaine de fréquence envisagé.

La différence dans la constitution spectrale des cinq calculs que nous avons obtenus à partir des données d'observations, était sensible.

On peut en juger en comparant deux spectres expérimentaux présentés sur les figures.

La différence obtenue s'explique apparemment par des perturbations de différents genres: un bruit aléatoire, la séparation insuffisante de fréquences voisines et la structure fine dans le spectre du signal étudié. Cela amène à une certaine imprécision des résultats de l'analyse spectrale. Ainsi apparaît une importante indétermination dans les valeurs

des amplitudes et des fréquences des harmoniques dont l'origine n'est pas la marée, dans les environs des vitesses angulaires de 45 degré/heure. L'utilisation du spectre énergétique c'est à dire le spectre de puissance permet dans notre cas de juger plus sûrement de l'existence de tels signaux.

Le spectre de puissance a été trouvé par les spectres de Fourier calculés pour les cinq analyses par la moyenne des carrés de leurs amplitudes. Cette approche bien qu'elle ne soit pas assez rigoureuse peut s'appliquer à certaines hypothèses par rapport à la stationnarité et l'ergodicité du processus étudié (2).

Dans le spectre d'amplitude aussi bien que dans le spectre de puissance on a une série de pics se détachant sur le fond général. Cela témoigne de l'existence d'harmoniques ayant des amplitudes sensibles. Les vitesses angulaires de ces harmoniques sont respectivement égales à 43,5; 45,0; 46,9; 53,6; 57,8 et 60,0, 62,2 degrés/heure.

Comme il fallait s'y attendre un maximum brusque se détache près de la fréquence de l'onde M3 (43, 47 degrés/heure) dans les cinq calculs. La relation de l'amplitude observée à celle calculée théoriquement est donnée par le facteur gravimétrique $\delta(M3)$ qui d'après les calculs de M.S. MOLODENSKII (7) pour son modèle de structure interne de la Terre le plus proche de la réalité est de $\delta(M3) = 1,064$. D'après les données analysées ici $\delta(M3) = 1,169 \pm 0,105$.

On est étonné par l'existence du brusque maximum sur la fréquence de l'onde S3 (vitesse angulaire 45 degrés/heure) où comme on le sait manque une composante de marée terrestre quelque peu importante. La valeur de ce maximum dépasse même l'onde M3 existant réellement dans la marée terrestre. Les autres maxima sont sensiblement plus petits et ne se détachent manifestement que sur la courbe du spectre de puissance. La valeur absolue de ces pics aux vitesses angulaires de 53,6 et 60,0 degrés/heure dépasse de 3 à 4 fois le niveau du bruit de fond existant dans les environs de ces fréquences. Les causes ne sont pas bien connues. L'existence de l'onde S3 et des autres harmoniques de vitesse angulaire multiples de 15 degrés/heure, indique leur origine solaire ce qui peut être en liaison avec les influences directes ou indirectes des mesures de la température et également les variations de tension dans le réseau électrique.

La pression est encore une source de perturbations de l'enregistrement gravimétrique. Les gravimètres du type GS-11 ont une assez bonne étanchéité à la pression et une compensation barométrique.

Cependant comme l'a montré Varga (8), pour certains gravimètres il y a une corrélation sensible entre la pression et des variations qii ne sont pas dues aux marées.

Ainsi Varga explique par la pression certaines particularités du spectre qu'il obtient lors de l'analyse spectrale des variations de la pesanteur dans la gamme des fréquences qui ne sont pas de marées. Dans le travail (8) le pic sur la vitesse angulaire de 45 degrés/heure ne se détache pas et d'après les données de notre travail le maximum à cette fréquence se détache avec une grande sûreté. D'autre part, le pic sur la vitesse angulaire de 56,5 degrés/heure séparé dans le travail (8) d'après les observations à Yalta n'apparaît pas malgré que pour l'analyse on a pris une série d'observations d'une durée deux fois plus grande.

Il y a encore une série d'hypothèses sur les causes possibles des anomalies dans le spectre obtenu. Cependant, à présent il n'y a pas de données expérimentales qui témoignent en faveur de l'une ou l'autre conception.

Bibliographie

1. MELCHIOR M.
Marées Terrestres
M. Mir. 1968, p. 482.

2. SEREKENNIKOV M.G., PIERVOSVANSKII A.A.
Apparitions de périodicités cachées.
M. NAOUKA, 1965, p. 243.

3. BARSENKOV S.A.
Calcul des marées du troisième ordre par les observations gravimétriques.
Isvestia Ac. des Sc. URSS, Série Physique de la Terre, 1967,N°5, pp.28-32.

4. KORBA P.S., KORBA S.N.
Variations de marées de la force de pesanteur à Yalta de 1966 à 1968.
Rotation et déformations de marées de la Terre., 1970 public.2. pp.18-34.

5. BALENKO V.G., BOULATSEN V.G., SCHLIAKOVII V.P. et autres.
Variations de marées de la force de pesanteur à Poltava de 1973 à 1976.
Rotation et déformations de marées de la Terre 1978. Publ.10, pp 3-14.

6. KRAMER M.V.
Tables des variations de marées de la force de pesanteur provenant de la Lune et du Soleil pour la Terre absolument rigide en 1962.
M. VINITI 1962 - p.50.

7. MOLODENSKII N.S., KRAMER M.V.
Marées terrestres et nutation de la Terre..
M. Edit. Ac. des Sc. URSS 1961, p.40.

8. VARGA P.
Investigation of gravimetric records at non-tidal frequencies.
Stud. Geophys. et geod., 1977, N 2, c. 195-199.

Traduction

DETERMINATION DE L'ONDE DE NUTATION SEMI-MENSUELLE DANS LES VARIATIONS DE LA LATITUDE DE POLTAVA.

R.I. Popova, N.I. Panchenko.

Rotation et déformations de marées de la Terre - vol.13, pp.94-96, 1981.

Les travaux de nombreux auteurs (1 à 5) sont consacrés au problème de la détermination des corrections des termes à courte période de la nutation d'après les données d'observations.

On utilise très souvent pour cela les résultats des observations régulières de la latitude dans les stations du Service International du Mouvement du Pôle à cause de la longueur et de la continuité de ces observations mêmes.

Nous donnons ici quelques résultats. E.P. Fédorov a obtenu par l'analyse des observations des deux stations du S.I.L., Carloforte et Ukiah pour 1900 à 1934 l'expression suivante de l'onde de nutation semi-mensuelle (7):

$$\Delta\phi = \underset{\pm 7}{0{,}0106''}\sin(2L-\alpha-\underset{\pm 4°}{7°}),$$

où L est la longitude de la Lune; α est l'ascension droite d'une paire d'étoiles de latitude. La valeur théorique du coefficient pour sin (2L-α) est égale à 0,085". V.K. Taradii et A.A. Korsoun en se servant des résultats des observations de trois stations du SIL - Mizusawa, Carloforte et Ukiah pour 1935 à 1955, ont trouvé dans les variations de la latitude une onde de nutation de la forme suivante (9):

$$\Delta\phi = -0{,}0085''\sin(\alpha-2L-10^\circ)$$
$$\pm \quad 17 \qquad\quad \pm 13^\circ$$

D'après les données (10) l'onde de nutation semi-mensuelle a une amplitude de 0,01" dans les observations à la lunette zénithale photographique:

$$\Delta\phi = -0{,}010''\sin(\alpha-2L-7^\circ)$$
$$\pm \quad 2 \qquad\quad \pm 11^\circ$$

Dans les observations de latitude de Poltava, l'onde semi-mensuelle a été déterminée par N.A. Popov qui a analysé les observations des étoiles zénithales brillantes au télescope zénithal de Zeiss, de 1939 à 1949 et il a trouvé une onde nettement exprimée avec une période semi-mensuelle. La cause de l'apparition de cette onde, d'après son avis, réside dans l'imprécision du coefficient du terme semi-mensuel de nutation (3) pris pour le calcul des déclinaisons d'étoiles.

En analysant les observations d'après le programme par groupes au télescope zénithal de Zeiss pour les six premières années des observations (de 1949 à 1955) E.P. Fédorov a trouvé l'onde suivante avec pour argument $(2L-\alpha)$ (2):

$$\Delta\phi = 0{,}0090''\sin(2L-\alpha+21^\circ)$$
$$\pm \quad 30 \qquad\quad \pm 19^\circ$$

P.S. Matveyev (4) et Filippov A.E. (5) ont également obtenu les ondes semi-mensuelles par de plus courtes séries d'observations à Poltava.

Nous avons utilisé pour la détermination de l'onde de nutation semi-mensuelle les observations des variations de la latitude à Poltava, réalisées avec un télescope zénithal de Zeiss de 1940 à 1967 avec un programme par groupes. Pour l'analyse on a pris les latitudes seulement d'après deux groupes principaux A et C dont les ascensions droites sont respectivement 6^h et 18^h.

Lors de la réduction de cette série, on a tenu compte de la nouvelle valeur de la constante d'aberration (k = 20,496") et de la réduction de précession et de nutation sur la base des décompositions plus précises de E. Woolard (8).

Pour calculer les latitudes on a tenu compte des corrections des mouvements de l'axe de rotation de la Terre sous l'effet de la Lune et du Soleil (nutation diurne forcée de Poisson). Pour cela on a calculé les termes principaux de la décomposition en tenant compte de l'élasticité de la Terre:

$$-\Delta\phi = -0{,}0066''\sin S + 0{,}0047''(S-2L) + 0{,}0022''(S-2),$$

On a introduit également la correction due à la déviation de la verticale sous l'effet de l'attraction luni-solaire. La valeur de la projection de l'inclinaison de la verticale sur le méridien due à cette action perturbatrice a été déterminée par la formule (6)

$$\Delta\varphi_C = \lambda \frac{3}{2} \frac{M_C}{M_\odot} \left(\frac{R}{R_C}\right)^3 \sin 2z_C \cos A_C.$$

par laquelle on a tenu compte de l'influence de la plus grande onde de marée M2. Pour l'analyse successive on a pris les écarts $\Delta\phi$ égaux à la valeur moyenne de la nuit pour un groupe donné(ϕ_N) moins ϕ_{SG} relevé sur la courbe adoucie pour cette même date: $\Delta\phi = \phi_N - \phi_{SG}$.

Les valeurs $\Delta\phi$ obtenues pour chaque groupe ont été réparties d'après les phases de la double longitude de la Lune, dont les valeurs ont été prises dans un annuaire astronomique et on les a interpolées pour le moment de l'observation du centre de chaque groupe.

On a obtenu enfin 12 valeurs moyennes $\Delta\phi$, rapportées à l'argument de la double longitude de la Lune. Ces valeurs sont données dans la table (n: quantité d'observations).

Valeurs $\Delta\phi$, 0,001"

2L	Groupe A		Groupe C	
	$\Delta\phi_A$	n	$\Delta\phi_C$	n
0°	+ 4	64	- 1	110
30	-11	74	+ 8	122
60	+ 7	77	+ 1	115
90	+ 8	67	+ 3	114
120	- 3	62	- 6	112
150	- 3	67	+ 2	124
180	+ 9	59	-10	115
210	+ 7	61	- 8	125
240	+ 6	59	- 1	113
270	+10	57	-13	123
300	-11	48	+ 6	116
330	-14	64	+18	111

L'influence du terme de nutation semi-mensuelle sur les déclinaisons des étoiles, conformément aux coefficients de décomposition de la nutation pris dans l'annuaire astronomique, peut être représentée par la façon suivante:

$$-0{,}081''\sin 2L \cos\alpha - 0{,}0884''\cos 2l \sin\alpha. \qquad (1)$$

Puisque la valeur moyenne de l'ascension droite des étoiles pour les groupes A et C est respectivement égale à 6^h et 18^h le premier terme de l'expression (1) est égal à zéro. Si le coefficient du terme de la nutation à courte période pour $\cos^2 L$ n'est pas tout à fait exact, on peut s'attendre à l'apparition d'une onde ayant cet argument.

On a calculé les valeurs des amplitudes et des phases initiales des ondes semi-mensuelles (période de 13,66 jours) d'après les valeurs $\Delta\phi_A$ et $\Delta\phi_C$ données dans la table par la méthode des moindres carrés.

Nous donnerons ci-après les résultats obtenus pour les groupes A et C.

$$\Delta\phi_A = \underset{\pm\ 32}{0{,}0062''}\cos(2L+\underset{\pm 31^\circ}{184^\circ}),$$

$$\Delta\phi_C = \underset{\pm\ 28}{0{,}0075''}\cos(2L-\underset{\pm 21^\circ}{20^\circ}).$$

Comme on le constate par l'expression (1) la phase des ondes de nutation dépend des ascensions droites des étoiles du programme d'observations. Pour les groupes A et C pour lesquels la différence des ascensions droites est égale à 180°, les phases initiales des ondes de nutation doivent différer de 180°.

Ainsi, nous pouvons considérer le fait que dans les expressions que nous avons obtenues des ondes semi-mensuelles d'après les deux groupes la différence des phases initiales est voisine de 180° comme la confirmation que ce sont des ondes qui trouvent leur origine dans la nutation, étant provoquées par l'imprécision du coefficient pris pour cos 2L dans l'expression (1).

La valeur moyenne de la correction du coefficient pour cos 2L d'après deux groupes (A et C) sera d'après nos déterminations:

$$\underset{\pm\ 2}{-0{,}007''}\cos 2L.$$

Bibliographie.

1. ORLOV A.Ia.
   Termes périodiques lunaires et autres dans les observations de Cassiopée à Poulkovo.
   Trav. 3eme T. Kiev: Ac. des Sc. d'Ukraine 1961, T_1 pp. 38-45.

2. FEDOROV E.P.
   Nutation et mouvement forcé des pôles de la Terre d'après les données des observations de latitude.
   Kiev., Edit. Ac. des Sc. Ukraine - 1958, p. 143.

3. POPOV N.A.
   Sur les termes à courte période de la nutation dans les observations des étoiles zénithales brillantes à Poltava.
   Trav. de l'Observatoire Gravimétrique de Poltava, 1951, 4, pp.103-137.

4. MATVEYEV P.S.
   Variations de nutation semi-mensuelles de la latitude d'après les observations de 1949 à 1953 à Poltava.
   Circulaire Astronom., 1953 N°143 , pp. 17-18.

5. PHILLIPOV A.E.
   Essai de détermination de l'onde d'atténuation lunaire dans les variations de la latitude d'après les résultats des observations sur deux téléscopes zénithaux à Poltava de 1948.8 à 1954.8
   Circulaire Astronomique 1956, n°168, pp. 14-16.

6. SCHTERNBERG P.K.
   Latitude de l'observatoire de Moscou en liaison avec le mouvement des pôles.
   Typogr. Univers. 1903, p.357.

7. FEDOROV E.P., EVTOUCHENKO E.I.
   Variations lunaires semi-mensuelles de la latitude d'après les observations à Carloforte et Ukiah de 1899 à 1934.
   Revue astronom. 1952. Publ.4. pp 731-733.

8. WOOLARD E.
   Théorie de la rotation de la Terre autour du centre de masses.
   Phys. Math., 1963 - p.140.

9. KORSUN A.A., TARADIJ A.A.
   Fortnightly nutation from the ILS data.-In/Nutation and the Earth's Rotation.
   Reidel Publishing Company, 1980 p.41-46.

10. O'HORA N.P.J.
    Fortnightly terms in PZT observations. Astron.J.,1973,78,n°10,pp.1115-1117

Tidal Gravity Computations Based on Recommendations of the Standard Earth Tide Committee

Rapp R.H.

Introduction

At the 1979 General Assembly of the International Association of Geodesy Resolution Number 11 was adopted that (in part) recommended that "a uniform model for theoretical earth tide computation should be adopted on the recommendation of the Earth Tides Commission." In August 1981, Dr. John T. Kuo, president of the Permanent Commission on Earth Tides, appointed the Standard Earth Tide Model Committee. Members of the committee were Professors Baker, Groten, Melchior, Moritz, Wahr, Zschau, and Rapp (chairman). This committee was charged with making recommendations that could be used to satisfy the pertinent part of Resolution 11.

It was clear, however, that this group could not be concerned only with Resolution 11 but must also consider the implications of Resolution 15. This resolution recommended "that the tidal effect be removed completely from all geodetic observations, without restoring the permanent deformation...".

In December 1981 a draft document was prepared by the committee chairman which was submitted to the members of the committee and other interested parties for comment. Comments were received and a discussion was held with most members of the committee in May 1982 in Tokyo at the General Meeting of the International Association of Geodesy. On the basis of the comments and discussion a revised document outlining the various possibilities was prepared. On this basis of the discussion in Tokyo a specific agreement was reached on the recommendations and proceedings to be followed for making tidal corrections. This paper documents these recommendations.

The Rigid Earth Theory

If we assume that the earth is a rigid body the net gravitational attraction of the moon and the sun can be calculated given the latitude and longitude of the computation point, the time of the observation and the location

of the sun and moon. A number of papers have described such computations.

For the purposes of the Standard Earth Tide Model (of a rigid earth) we recommend the development described by Cartwright and Tayler (1971) and Cartwright and Edden (1973) with supplemental terms. The total number of waves in the recommended model is 505 as defined by the Cartwright-Tayler-Edden model with additional terms defined by the International Center for Earth Tides. It should be noted that the Cartwright-Tayler-Edden model is based on the 1964 constants adopted by the International Astronomical Union. No significant change is expected if more recent constants are used.

The amplitude of the tidal potential, in meters, can be represented in series form as follows:

$$\frac{W_T(P)}{\gamma} = \sum_{\ell,m,f} H_{\ell,m,f} \qquad (1)$$

where $H_{\ell,m,f}$ are the tidal amplitudes given by the Cartwright-Tayler-Edden model. γ is an average value of gravity taken as $9.798529\,m\,s^{-2}$ (Wahr, 1981).

The tidal correction to be subtracted from observed gravity would (in a radial direction) be:

$$g(P) = \frac{-dW_T(P)}{\partial r} = -\frac{2}{r} W_T(P) \qquad (2)$$

The tidal potential will contain a constant part that can be found from the Cartwright-Tayler-Edden model. We have:

$$W_C(r_0) = -1.944\ P_2(\sin\psi)\ m^2s^{-2} \qquad (3)$$

or

$$W_C(r_0) = 1.458\ (\cos 2\psi - \tfrac{1}{3})\ m^2s^{-2} \qquad (4)$$

where r_0 is an average earth radius (6371 km) and ψ is the geocentric latitude. The W_C value implies a constant (in time) tidal amplitude which is found by dividing (4) by γ :

$$\Delta N_C = 0.149\ (\cos 2\psi - \tfrac{1}{3})\ \text{meters} \qquad (5)$$

The Elastic Earth Theory

In the past a number of developments describing the elastic earth have been published with usual starting references to the work of Love (1909). Today the most comprehensive analysis, for an ellipsoid, rotating, elastic earth, has been described by Wahr (1981). We represent the Wahr tidal gravity correction for the elastic (E) earth in the following form (ℓ indicates degree; m, order; and f indicates the frequencies at a given degree and order):

$$g_E(P) = \sum_{\ell,m,f} \delta f_{\ell,m,f} \qquad (6)$$

where

$$\delta f_{\ell,m,f} = -\frac{2}{r_0} H^m_{\ell,f} \times 10^2 \; g_a \; Y^m_\ell \; G^m_{\ell,f} \qquad (7)$$

where $r_0 = 6371\,\text{km}$, $g_a = 9.798529\,\text{m s}^{-2}$, $H^m_{\ell,f}$ are the amplitude coefficients (in meters) given by the Cartwright-Tayler-Edden model. Y^m_ℓ are the spherical harmonics (Wahr, 1981, eq. 2.4):

$$Y^m(\theta,\lambda) = (-1)^m \left[\frac{2\ell+1}{4\pi} \frac{(\ell-m)!}{(\ell+m)!}\right]^{\frac{1}{2}} P^m_\ell(\cos\theta) \exp(im\lambda) \qquad (8)$$

where $\theta = 90° - \psi$, λ is longitude, and $P^m_\ell(\cos\theta)$ are the associate Legendre functions. The $G^m_{\ell,f}$ functions are components of an apparent gravimetric factor:

$$G^m_{\ell,f} = [G_0 + G_+ \; Y^m_{\ell+2} / Y^m_\ell + G_- \; Y^m_{\ell-2} / Y^m_\ell \;]_f \qquad (9)$$

where G_0, G_+ and G_- are frequency dependent coefficients given by Wahr (1981, p.695). These coefficients are dependent on the earth model being used. We recommend that the earth model to be used for the tidal gravity corrections is the neutrally stratified variant of the Gilbert and Dziewonski (1975) model. Although more current earth models exist, for example, the Preliminary Standard Earth Model (Dziewonski and Anderson, 1981) it is unlikely that any substantial changes would be found in the gravimetric factor coefficients. There is also some evidence (Melchior and De Becker, 1982) that the Wahr theory may not fit the observed data completely. However it is sufficiently accurate to serve for reference purposes.

A part of $g_E(P)$ is constant in time. This constant part is the long period term at $\ell = 2$, $m = 0$ and can be written as:

$$\delta f_c = - \frac{2}{r_0} H_2^0 \times 10^2 \, g_a \, Y_2^0 \, G_2^0 \tag{10}$$

In writing this equation it is assumed that the permanent deformation of the earth is elastic. Such an assumption is not warranted as pointed out by Groten (1980). (If we were dealing with the spherical earth and Love numbers, our assumption would be that the elastic and secular Love numbers are the same.) In order to avoid this assumption we recommend that the direct part of the tidal attraction be included in $g_E(P)$ but that the indirect effect due to the permanent yielding of the earth not be removed due to the fact that we do not know the appropriate factors. This procedure will yield an external gravitational potential which is a harmonic function. The recommended correction would then be:

$$\bar{g}_E(P) = g_E(P) - \overline{\delta f}_c \tag{11}$$

where

$$\overline{\delta f}_c = - \frac{2}{r_0} H_2^0 \times 10^2 \, g_a \, Y_2^0 \, G_2^0 - \delta f_d \tag{12}$$

with δf_d (the constant effect for a rotating, elliptical, rigid earth) given by (Wahr, 1982, private communication)

$$\delta f_d = - \frac{2}{r_0} H_2^0 \times 10^2 \, g_a \frac{1}{2} [3\cos^2\theta - 1 + \varepsilon (-9\cos^4\theta + 6\cos^2\theta + \tfrac{1}{3})] \tag{13}$$

with ε the flattening. Using the numerical coefficients from Wahr we have:

$$\overline{\delta f}_c = -4.83 + 15.73 \sin^2\psi - 1.59 \sin^4\psi \ \mu\text{gals} \tag{14}$$

Zero and Mean Geoids

We will define the zero geoid as the equipotential surface that would exist without the direct influence of the sun and moon but including the indirect effect due to the permanent yielding of the earth which can not be determined without assumption. If gravity anomalies, that have been formed from gravity measurements from which the modified tidal correction (equation 11) has been removed, are used in the Stokes equation, the corresponding undulations would refer to the zero geoid.

The mean geoid would be that equipotential surface that would exist with the sun and moon present. Such a surface would correspond to that observed (after averaging) by tidal gauges if we neglect oceanographic effects. The undulations of the mean geoid can be obtained by adding the results of equation (5) to the undulation of the zero geoid:

$$N_m = N_z + 0.149(\cos 2\psi - \frac{1}{3}) \text{ meters} \qquad (15)$$

Recommendations

The following recommendations are made by the Standard Earth Tide Model Committee.

1. The rigid earth tidal model known as the Cartwright-Tayler-Eden model should be adopted with additional waves specified by the International Center for Earth Tides to yield a total of 505 tidal constituents.

2. The calculations of Wahr using the 1066A earth model should be adopted for the determination of the apparent gravimetric factor.

3. The direct constant part of the tidal effect should be removed from the observed gravity but the indirect part due to the permanant yielding of the earth should not be. Therefore the tidal correction to be subtracted from observed gravity is

$$\bar{g}_E(P) = g_E(P) - \overline{\delta f}_c$$

where $g_E(P)$ is the tidal correction from the Wahr theory for the 1066A Earth Model and $\overline{\delta f}_c$ is given by equation (13).

4. For a more precise tidal reduction the ocean loading effects must be calculated assuming an oceanic tidal model. We recommend that the tidal maps and data produced by Schwiderski serve as the "working standards" for the ocean loading calculation.

5. For other observations, needing precise tidal reductions, such as satellite altimeter data, laser tracking data, VLBI measurements, leveling, etc, we recommend that analogous procedures be adopted using the Wahr equations with the 1066A earth model.

References

Cartwright, D.E. and R.J. Tayler, New Computations of the Tide-generating Potential, Geophys, J.R. astr. Soc, 23,45-74, 1971.

Cartwright, D.E. and A.C. Edden, Corrected Tables of Tidal Harmonics, Geophys. J.R. astr. Soc. 33, 253-264, 1973.

Dziewonski, A., and D. Anderson, Preliminary Reference Earth model, Physics of the Earth and Planetary Interiors, 25, 297-356, 1981.

Gilbert, F. and A.M. Dziewonski, An Application of Normal Mode Theory to the Retrieval of Structural Parameters and Source Mechanism from Seismic Spectra, Phil. Trans. R. Soc., 278A, 197-269, 1975.

Groten, E., A Remark on M. Heikkinen's Paper "On the Honkasalo Term in Tidal Corrections To Gravimetric Observations", Bulletin Geodesique, 54, 221-223, 1980.

Love, A.E.H., The Yielding of the Earth to Disturbing Forces, Proc. R. Soc., 82A, 73-88, 1909.

Melchior , P., and M. De Becker, A Discussion of World-wide Measurements of Tidal Gravity with Respect to Oceanic Interactions, Lithosphere Heterogeneities, Earth's Flattening and Inertial Forces, Physics of the Earth and Planetary Interiors, in press, 1982

Comments on Gravimetric Tidal Corrections and the Permanent Deformation of the Earth, Prepared for the Standard Earth Committee, R.H. Rapp, Chairman, May 1982.

R. H. Rapp
January 28, 1983

A PREDICTION OF TIDAL OCEANIC LOADING AND ATTRACTION EFFECTS ON GRAVITY MEASUREMENTS IN CONTINENTS

B. Ducarme and P. Melchior

Observatoire Royal de Belgique

At the request of the International Gravity Commission we have calculated the loading and attraction effects due to the oceanic tides on the intensity of gravity all accross the continents.

The program of computation is based upon Green functions according to the Farrell procedure. Results have been compared with those obtained by Clyde Goad (1980) with a different and independent procedure and give a fair agreement.

The oceanic cotidal maps are those of E. Schwiderski (1978) which are the best working standards presently existing. Moreover such computations give in general an excellent agreement with tidal gravity measurements as recently demonstrated by Melchior and De Becker (1983).

For each large continent we have drawned equal amplitude lines (co-range lines) which indicate the *peak to peak* amplitude for the main semi-diurnal wave M_2, that is the *maximum difference* to be expected if one considers this wave only. The effects of other semi-diurnal waves (N_2, S_2 principally) are more or less in phase with M_2 so that it seems sufficient to give only the M_2 maps. These maps clearly indicate the

areas where the oceanic effects are minimized (amphidromic loading areas). They are not necessarily in the center of the continent:

North of Mexico in North America
North of Argentina in South America
Mauritania in Africa
Lanzhou area in Asia

On the other hand it is to be pointed out that in Europe where the loading effects are not negligeable they are however well under control because the oceanic cotidal maps are quite precise in this area. Thus absolute measurements of gravity made anywhere in continental Europe can be properly corrected for oceanic tidal effects to better than one microgal.

This is not true in Asia where residues of some microgals are still unexplained (see Melchior and De Becker, 1983).

Bibliographie

1. GOAD C., 1980.
The computation of tidal loading effects with integrated Green's functions.
NAD Symposium 1980, 587-601, Ottawa

2. MELCHIOR P. and DE BECKER M. 1983.
A discussion of world-wide measurements of tidal gravity with respect to oceanic interactions, lithosphere heterogeneities, Earth's flattening and inertial forces.
Physics of the Earth and Planetary Interiors, 31, pp. 27-53.

3. SCHWIDERSKI E.W., 1978.
Global Ocean Tides.
A detailed hydrodynamical interpolation model.
Naval Surface Weapons Center, Dahlgreen, Virginia.


Tidal gravity loading and attraction
M2 Component
Peak to peak amplitude in microgals
EUROPE
1.0
1.2
1.6
2.2
2.8
3.8

Tidal Gravity loading and attraction
- M_2 component
Peak to peak amplitudes in microgals
Northern Asia

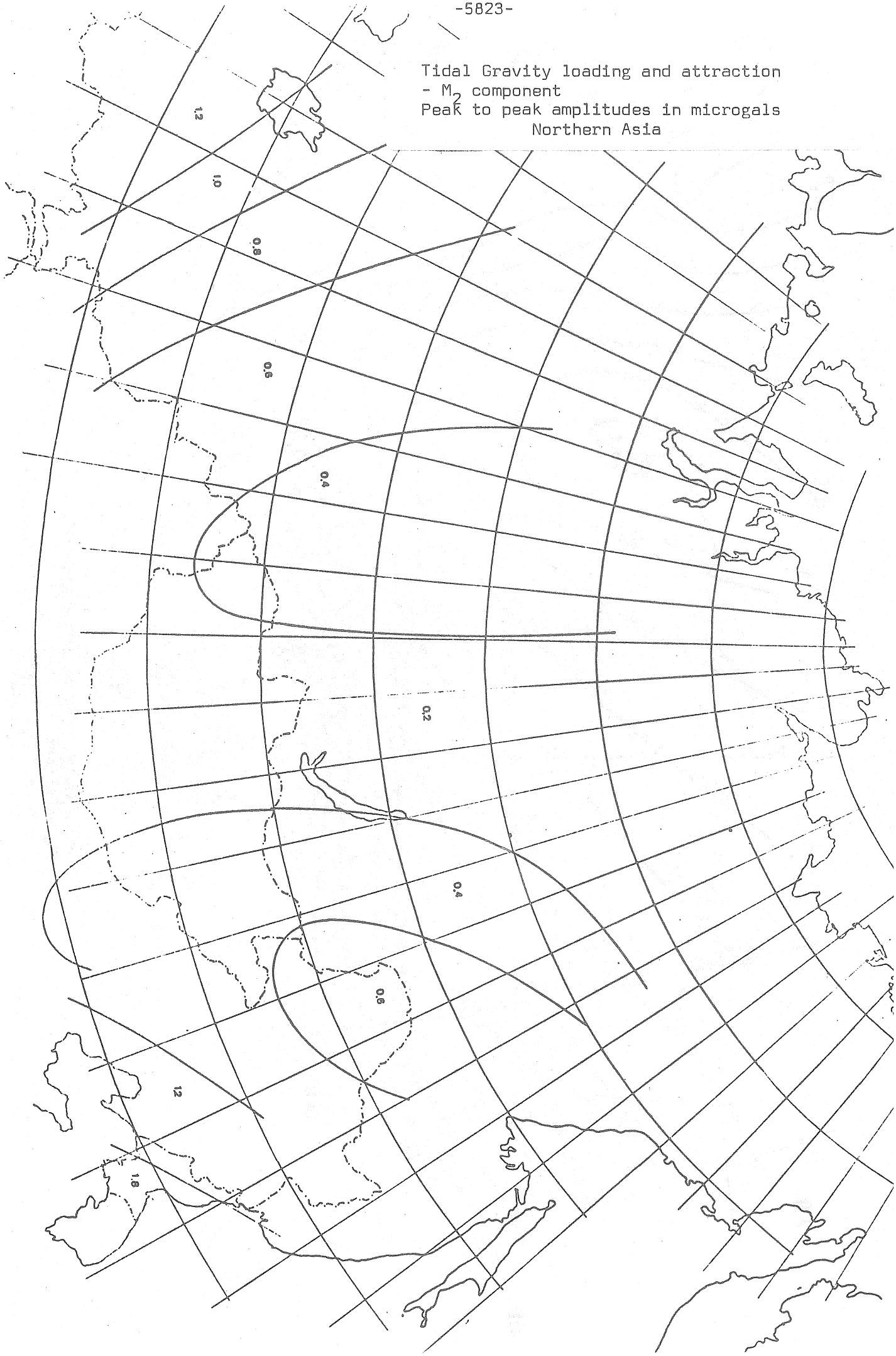

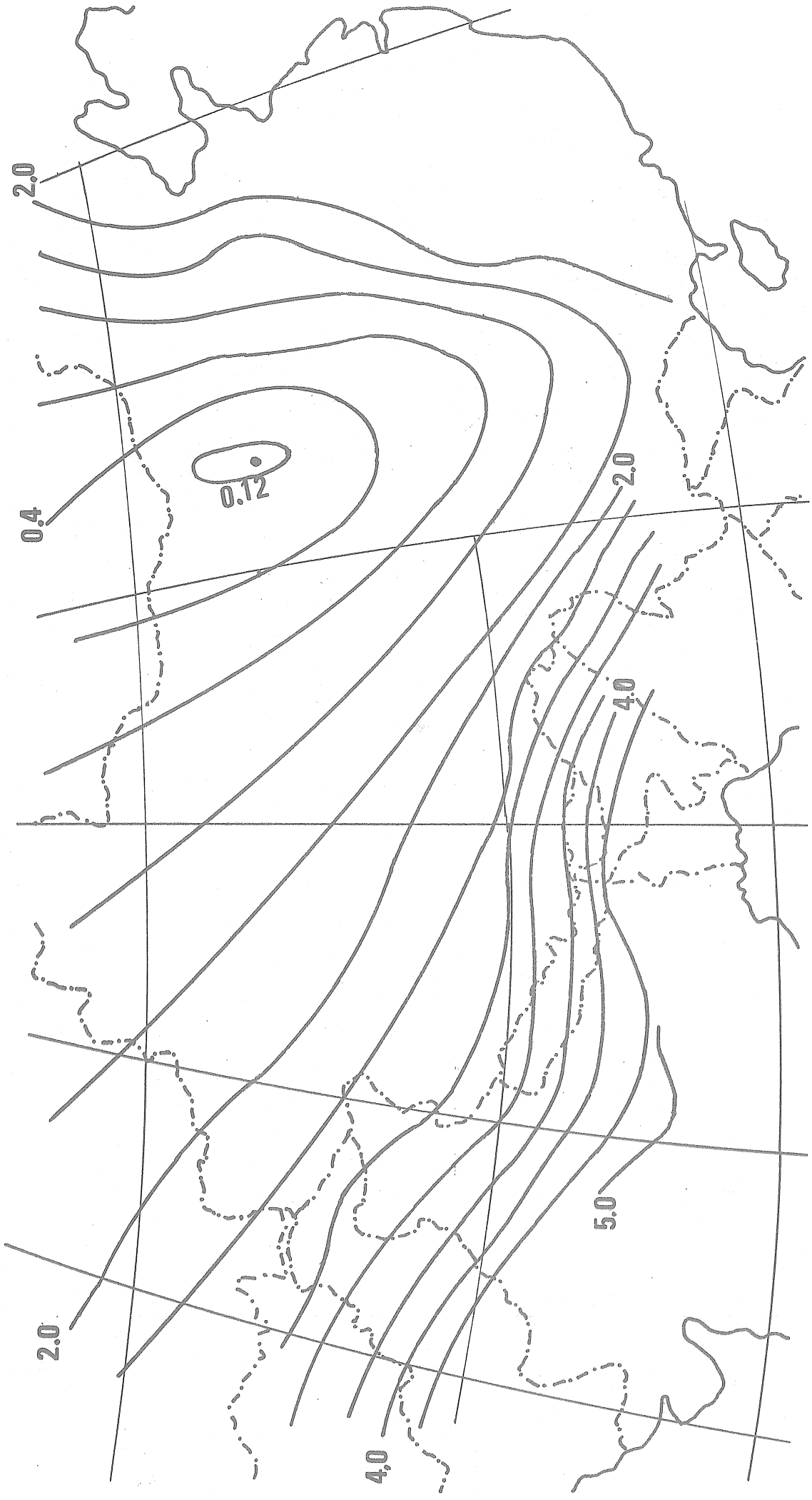

Tidal Gravity loading and attraction
- M_2 component
Peak to peak amplitudes in microgals
Eastern Asia

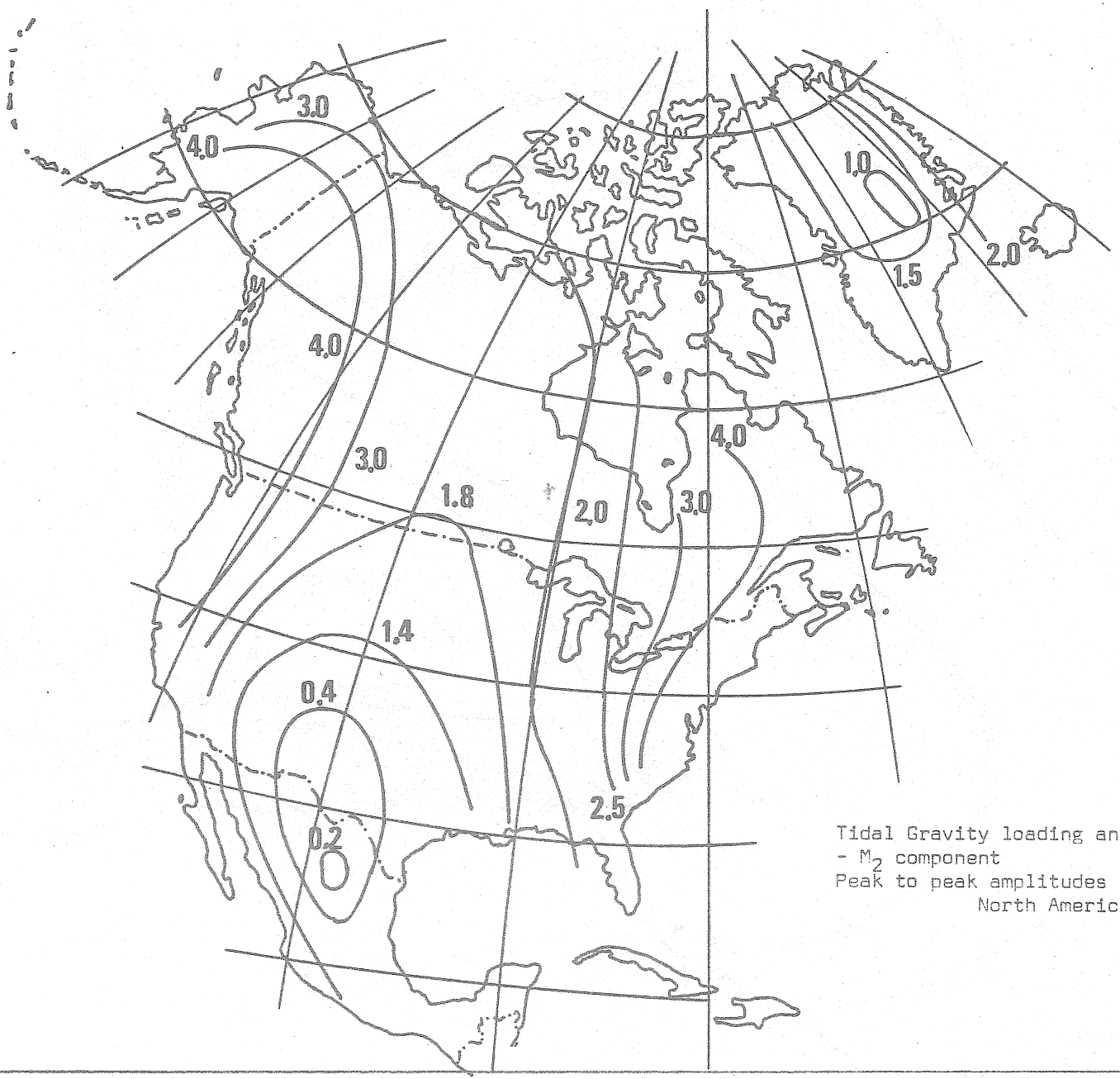

Tidal Gravity loading and attraction
- M_2 component
Peak to peak amplitudes in microgals
North America

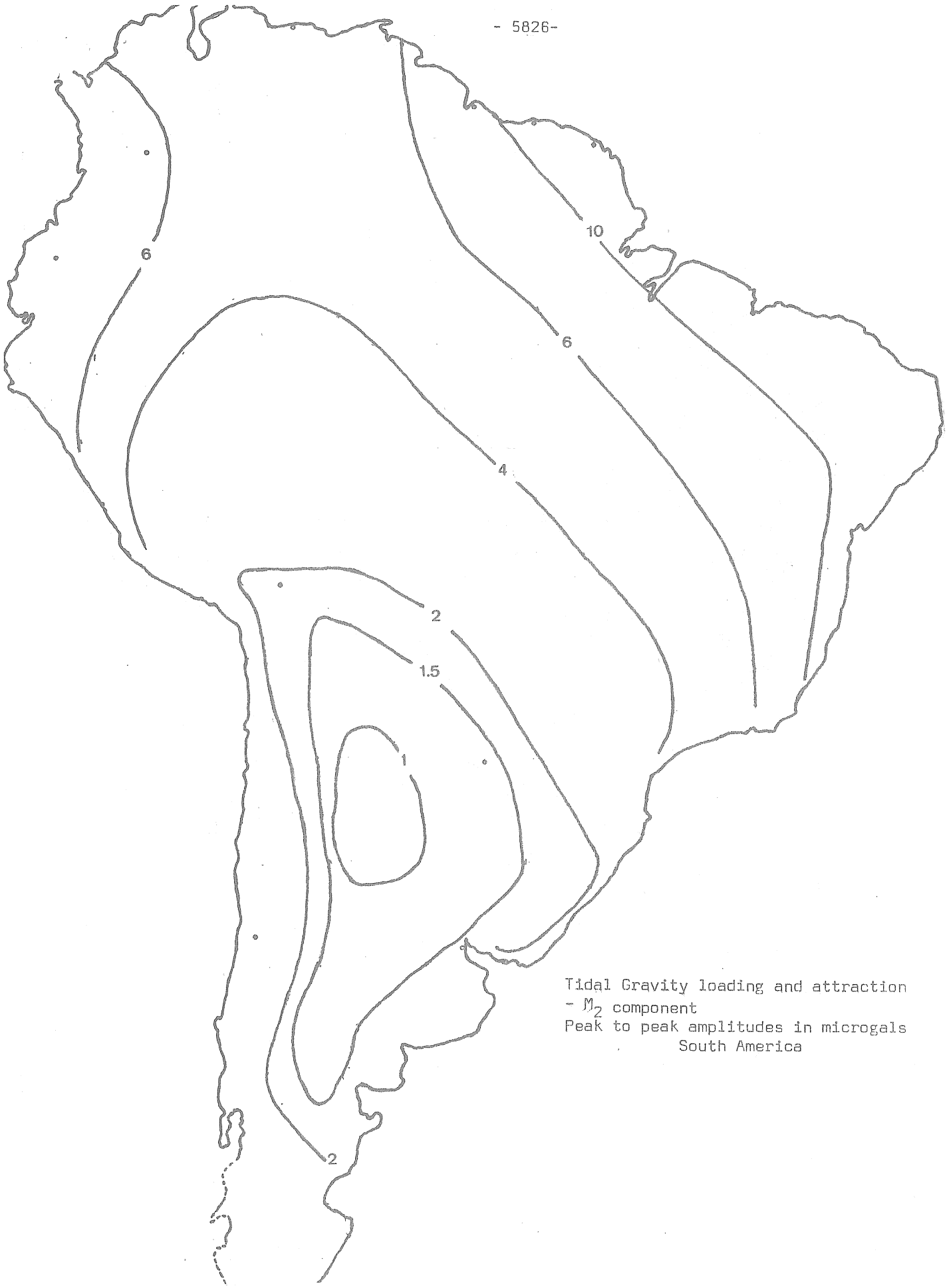

Tidal Gravity loading and attraction
- M_2 component
Peak to peak amplitudes in microgals
South America

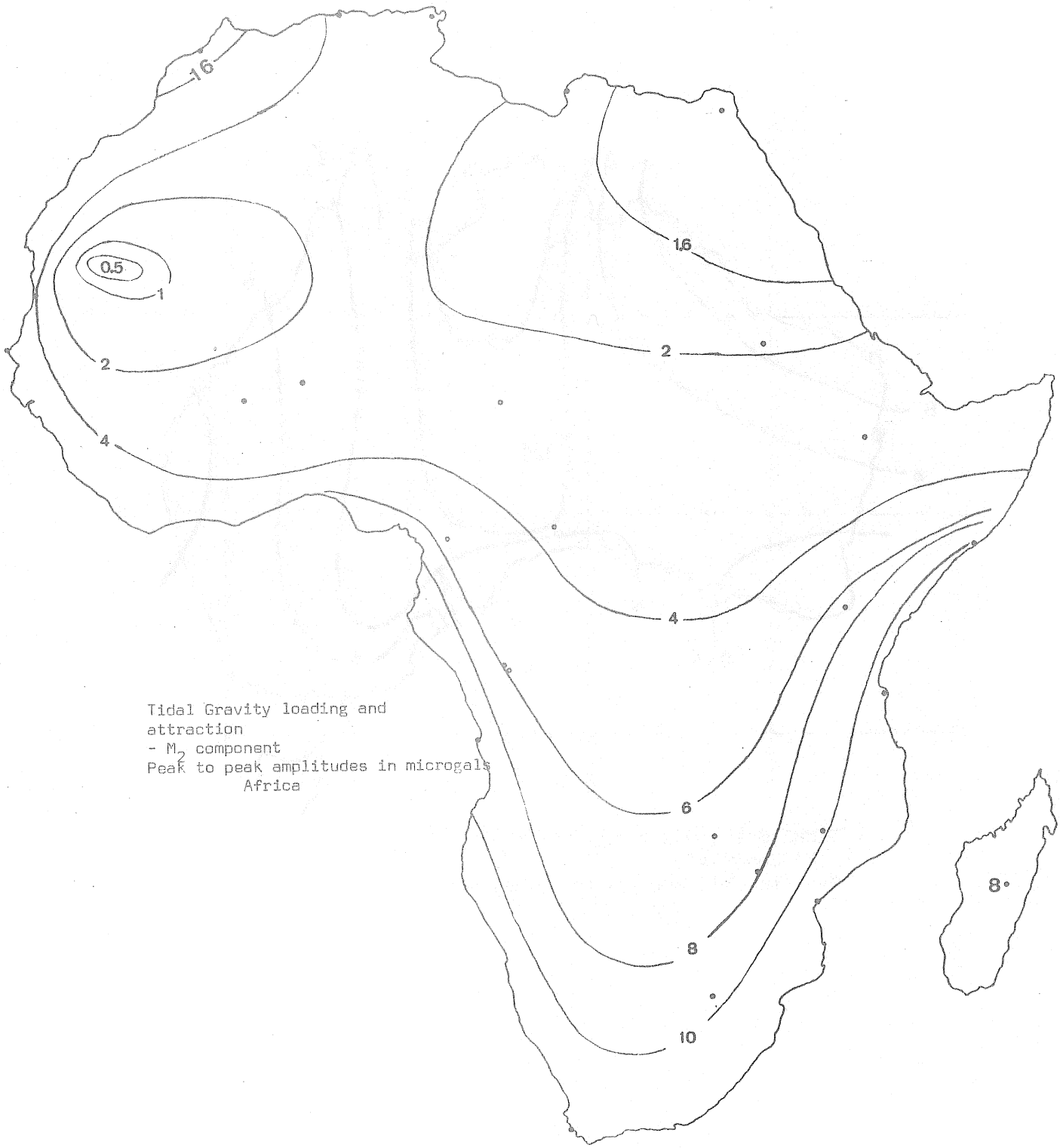

Tidal Gravity loading and attraction
- M_2 component
Peak to peak amplitudes in microgals
Africa

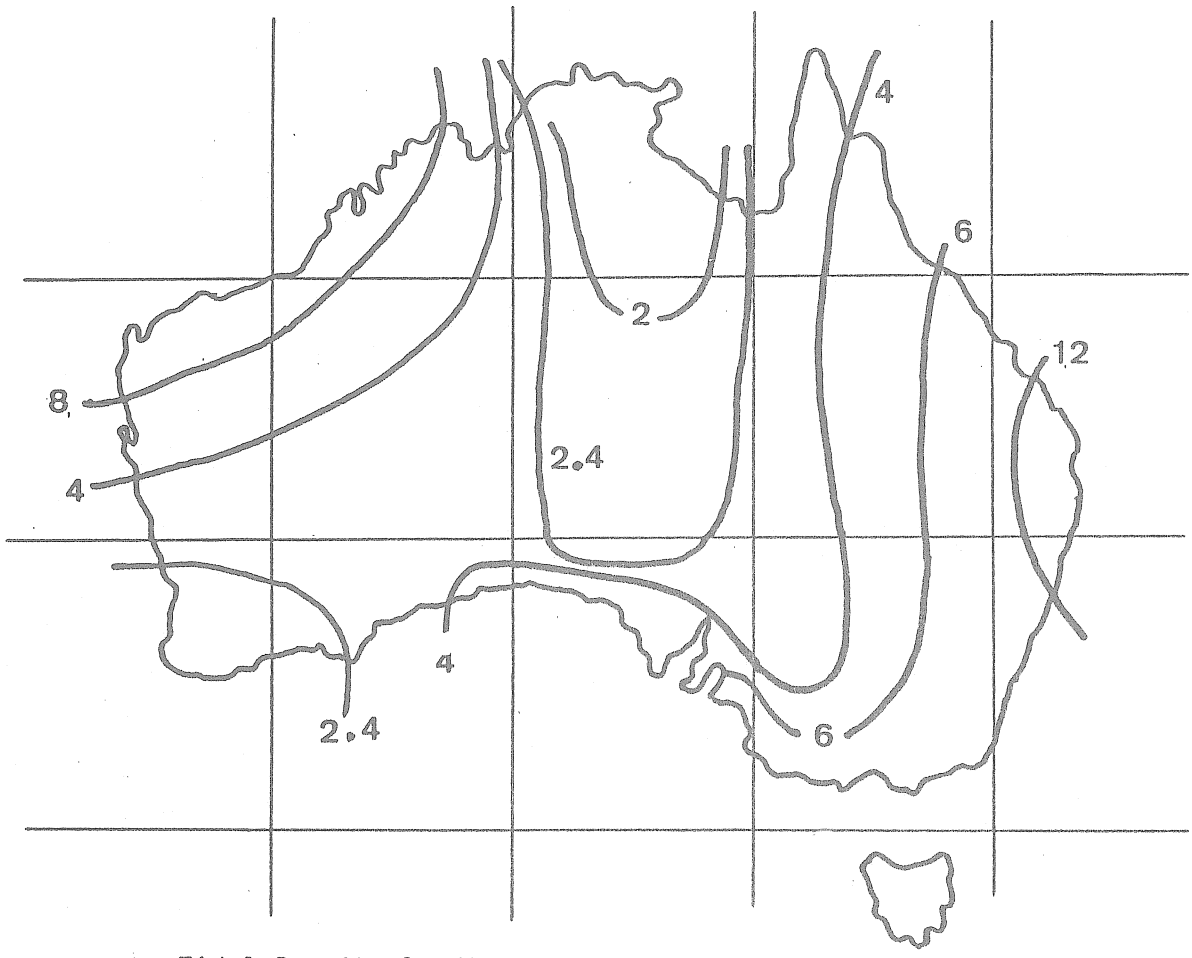

Tidal Gravity loading and attraction
- M_2 component
Peak to peak amplitudes in microgals
Australia

PARAMETRISATION OF FORCES IN PLANE CAPACITIVE TRANSDUCERS

J.L. Aseglio - Université Catholique de Louvain, Belgium

Geophysical researches very often call for performing devices that are able to measure very weak physical phenomena. The instrumentation presently used by geophysicians often reach the borders of the present technical possibilities.

Let's quote, for example, the rate of importance of observable parameter variations for the devices that are set up in the Underground Geodynamics Laboratory at Walferdange, in the Great Duchy of Luxembourg. This information has been conveyed by M. Van Ruymbeke.

- gravity : resolution of 10^{-10} of 9
- force : resolution of 10^{-10} for 100 grams
- displacement : resolution of 10^{-9} m
- temperature : resolution of 10^{-5} °C
- capacity : resolution of 10^{-17} F

At the Royal Observatory of Belgium, one uses gravimeters extensometers and horizontal pendulums, fitted out with capacitive transducers for measuring the variations of the gravity vector. Those captors are made up by one capacitor whose capacity changes with the moving of the arm of the gravimeter or the horizontal pendulum, and a adjusted electronics.

One of the models worked out by M. Van Ruymbeke (1979) can be described as follows :

It is made up with 3 external brass sheets encompassing an aluminium movable sheet. The whole makes up a capacitive bridge. The external sheets of the transducer are submitted to a difference of changing potential, allowing to measure the shifts of the central sheet, and consequently, the changes of the gravity vector.

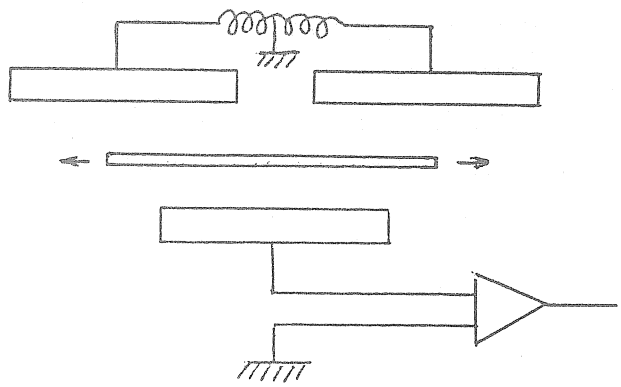

The excitation of the transducer by oscillating electrical signals may give birth to various kinds of forces that add themselves up to the geophysical forces that we want to measure. That's why we (1982) have made a survey of the physical phenomena that can influence the transducer. We have also examined their importance in the geophysical measuring, taking the quoted resolutions into account.

The first purpose of our study has been to mould the transducer into a capacitor that is made up with 2 parallel sheets of the same size under the influence of a constant electric field. Since we know the force in a capacitor, we work out (starting from conformal mapping) the correction that is to be given to this result, when we take the side effect into account. We obtain the same manifestion of the electrostatic force. The side effect alters in no way the measuring that has been done. A similar calculation enables us to show that the expression of the force is left unchanged, when we take the thickness of the sheet into account.

The more intricate outline of the capacitive transducer prompts us to improve this model, having in mind a non-conducting medium in the framework - the transducer stands indeed in the open air -. The feeding of the captor under alternating tension nevertheless allows the suppression of the heath increase that occurs when charging a capacitor, and the electrostriction phenomena too.

In order to get closer to the real transducer, the study proceeds by replacing one of the firm framework sections of the captor by an isolated metal sheet that is moving within an oscillating electric field. The latter considerations invite us to debate - on the one hand the existence of a convection current in the movable sheet (we show it can be disregarded) - and on the other hand, the appearance of a magnetic field $\vec{B}$. induced by the oscillating electric field.
According to the Lorentz law : $\vec{F} = q\ (\vec{v} \wedge \vec{B})$, this induction field can introduce an additional force on the movable metallic sheet, providing that the latter has some electric charges. Our study demonstrates that the force obtained in this way is not to be taken into account ($\simeq 10^{-18}$ N), if we take for granted that there is a lack of balance in the charges reaching a factor of 10,000 between the sheets.

An improvement is made to our study, taking the paramagnetisme of aluminium into consideration ; the force that is obtained remains undetectable by the transducer.

In accordance with that has just been dealt with, the possible lack of balance between the framework sections should be known ; that is why the study aimed at describing the physical phenomena that can bring or pull back charges of a metallic sheet in the open air.
One by one, we enter upon the adsorption and oxidation phenomena, the photoelectrical and thermoelectronical effects. In their way, we will discover that these phenomena - when they are not neglectable - are inclined to neutralise possible charges that would be on the movable sheet ; which is a good thing in the transducer. Though, an asymmetry between materials making up the framework shows an oxidation asymmetry that comes off by a difference of contact potentiel. This difference adds itself to the one applying to the captor. There we can detect possible trouble that can be done awaywith when building the transducers.

A rapid estimation enables us afterwards to ascertain that the magnetic field of the earth is not the source of a detectable force in the captor.

Finally, in order to round up the physical phenomena that can induce parasitic forces in the transducer, we look upon it as an aerial able to pick up the electromagnetic waves that intercept it, and we compute the quantity of energy it absorbs.

This study which is very encouraging by its results enables us to foresee a future full of promises for the capacitive transducers of the Royal Observatory of Belgium, and this, within a widening field of uses.

Litterature

ASEGLIO J.-L. 1982. Paramétrisation des forces existant dans les capteurs capacitifs plans.
Mémoire de licence - UCL -
VAN RUYMBEKE M. (1979) Capteurs capacitifs de très haute résolution adaptés aux clinomètres et extensomètres.
Dissertation doctorale - UCL -

TIDAL CURVATURES AND TRIGGERING OF EARTHQUAKES

Martin Ekman

National Land Survey of Sweden
S-801 12 Gävle, Sweden

and

University of Uppsala
Department of Geodesy
Hällby
S-755 90 Uppsala, Sweden

ABSTRACT

Gaussian curvatures and mean curvatures of earth tides are used in an investigation of tidal triggering of earthquakes. It is shown that a major earthquake can be triggered by the combined semi-diurnal and diurnal earth tide in such a way that the earthquake is more likely to occur when the tidal curvature is increasing than when it is decreasing, provided the curvature is great enough.

1. Introduction. Gaussian and mean tidal curvature formulae.

In a previous report (Ekman, 1981) the theory of Gaussian and mean tidal curvatures was treated. It was also stated there that this could be used in an investigation of tidal triggering of earthquakes, the result of which would be published later. This task is now fulfilled. The present report presents the investigation and its result.

Before going into the investigation we will briefly give the basic curvature formulae for the rotational tide, i.e. the combined semi-diurnal and diurnal tide (a list of symbols can be found at the end of the paper):

The Gaussian tidal curvature is given by

$$
\begin{aligned}
K = \sum_{i=\mathbb{C}}^{\odot} \sum_{j=\mathbb{C}}^{\odot} h_2^2 \left(\frac{3GM_i}{2\gamma r_i^3}\right)\left(\frac{3GM_j}{2\gamma r_j^3}\right) \Big[& \cos^2\delta_i \cos^2\delta_j \\
& \Big(\cos 2\varphi\ (1 + \cos^2\varphi) \cos 2t_i \cos 2t_j \\
& - \sin^2\varphi \sin 2t_i \sin 2t_j\Big) + \cos^2\delta_i \sin 2\delta_j \\
& \sin 2\varphi \Big((1 + 4\cos^2\varphi) \cos 2t_i \cos t_j \\
& + \sin 2t_i \sin t_j\Big) \\
& + \sin 2\delta_i \sin 2\delta_j \Big(2 \sin^2 2\varphi \cos t_i \cos t_j \\
& - \cos^2\varphi \sin t_i \sin t_j\Big)\Big]
\end{aligned}
\qquad (1)
$$

The mean tidal curvature is

$$H = - \sum_{i=\mathbb{C}}^{\odot} h_2 \frac{9GM_i}{4\gamma r_i^3} \left[\cos^2\delta_i \cos^2\varphi \cos 2t_i + \sin 2\delta_i \sin 2\varphi \cos t_i\right] = - \frac{3}{R^2} u \qquad (2)$$

We also have the following relations between tidal curvatures and tidal strain tensor components:

$$K = \frac{h_2^2}{l_2^2} \frac{1}{R^2} \left(e_{\varphi\varphi} e_{\lambda\lambda} - \frac{1}{4} e_{\varphi\lambda}^2 - \frac{h_2(h_2 - 6l_2)}{(2h_2 - 6l_2)^2} (e_{\varphi\varphi} + e_{\lambda\lambda})^2\right) \qquad (3)$$

and

$$H = - \frac{h_2}{h_2 - 3l_2} \frac{3}{2R} (e_{\varphi\varphi} + e_{\lambda\lambda}) \qquad (4)$$

Derivations of the formulae (1) - (4) are published in (Ekman, 1981), although (1) is given here in a slightly modified form.

As an illustration of formula (1) we show in Figure 1 a Gaussian tidal curvature map for the case $\delta_{\mathbb{C}} = \delta_{\odot} = \varepsilon$. It covers one half of the earth; on the other half the picture is similar but mirrored with respect to the equator.

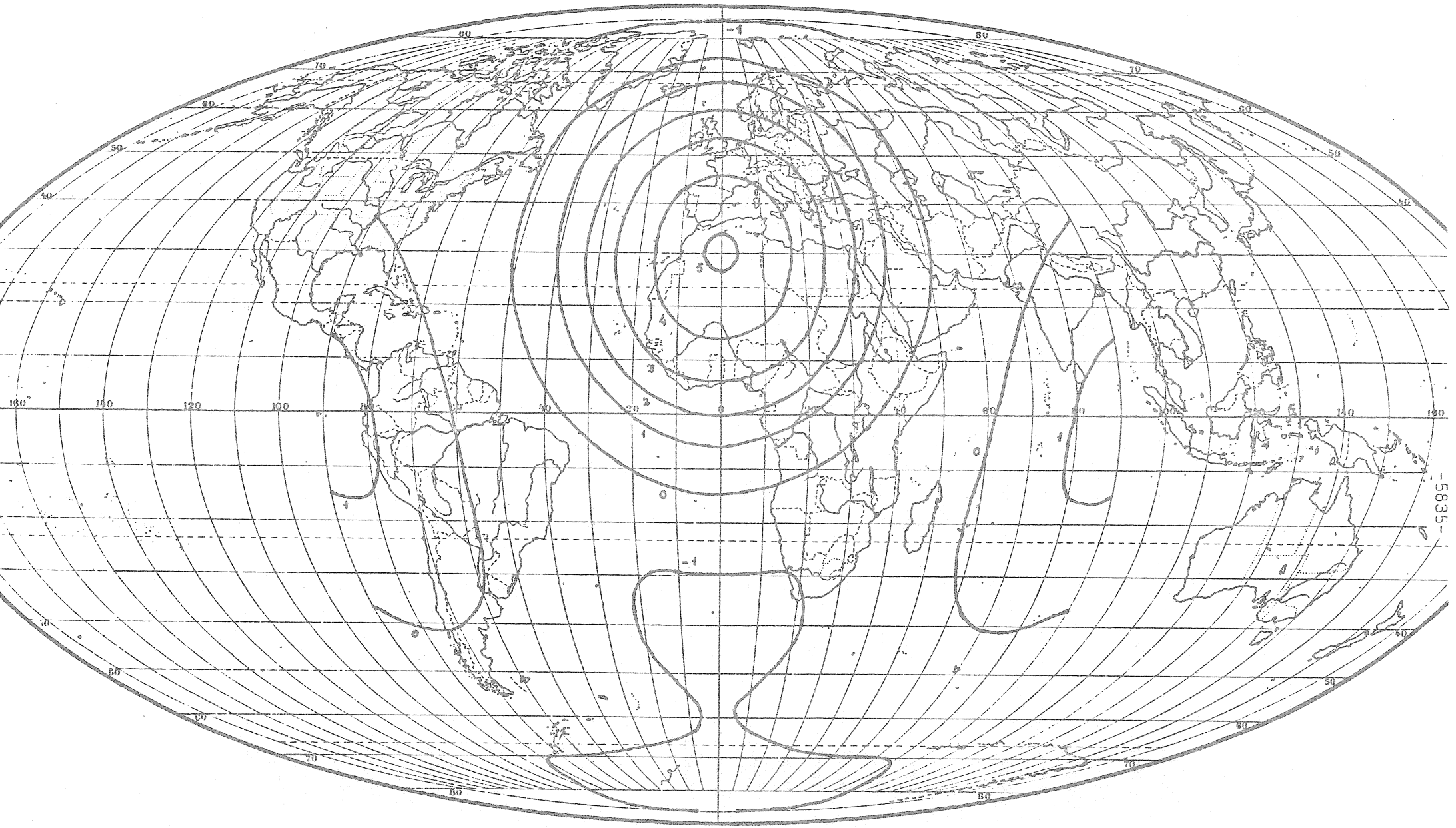

Figure 1: Gaussian tidal curvature map, $\delta_{\mathbb{C}} = \delta_{\odot} = \varepsilon = 23^{o}27'$, $t_{\mathbb{C}} = t_{\odot} = \lambda$. Unit of K: 10^{-34} mm^{-2}. (From Ekman, 1981)

2. Tidal triggering of earthquakes: Principles of investigation.

The existence of the phenomenon of tidal triggering of earthquakes was first indicated in (Heaton, 1975). Here the phases of the tidal stress tensor components were used to analyse earthquakes with known fault parameters, whereby a time correlation was found between maximum tidal stresses and certain types of earthquakes.

In the general case, however, fault parameters are not known, making the tidal stress (or strain) tensor unsuitable in more general treatments of earthquakes. In (Van Ruymbeke et al, 1981) the phase of the semi-diurnal tide M_2 itself (which is proportional to the cubic and the surface M_2 tidal strain) was analysed. Correlations between the M_2 tidal phases and the occurrence of earthquakes were found for certain regions, wherein different tectonic areas showed different phases.

We will now investigate the problem of tidal triggering of earthquakes as follows:

It is reasonable to assume tidal triggering of earthquakes to occur mainly where the tidal curvatures, especially the Gaussian curvature (cf. relation (3)), exhibit great variations during the course of a day. Let us then test the following hypothesis: The earthquakes here can be triggered when the combined semi-diurnal and diurnal tidal curvature is great enough and at the same time is increasing. In other words: Do significantly more earthquakes occur when the rotational tidal curvature is increasing than when it is decreasing, if the curvature is great enough?

In order to answer this question we have proceeded

in the following way:

1. The greatest tidal curvature variations occur in the latitude zones around $\varphi = \pm 30^{o}$; cf. Figure 1 and (Ekman, 1981). In order to avoid disturbing effects of ocean tides, restriction was made to continental areas. Accordingly the following zone was adopted for the analysis (see Figure 2):

$$15^{o} < \varphi < 45^{o}$$
$$0^{o} < \lambda < 105^{o}$$

This zone contains the great seismic belt along the border between the Eurasian plate on one hand and the African and Indian plates on the other hand.

2. Within this zone all shallow major earthquakes (depth $\leq$ 60 km, magnitude $\geq$ 6 for the Rothé catalogue and $\geq$ 5 for the ISC catalogue) during the years 1953 - 1978 were considered. These are all known by position

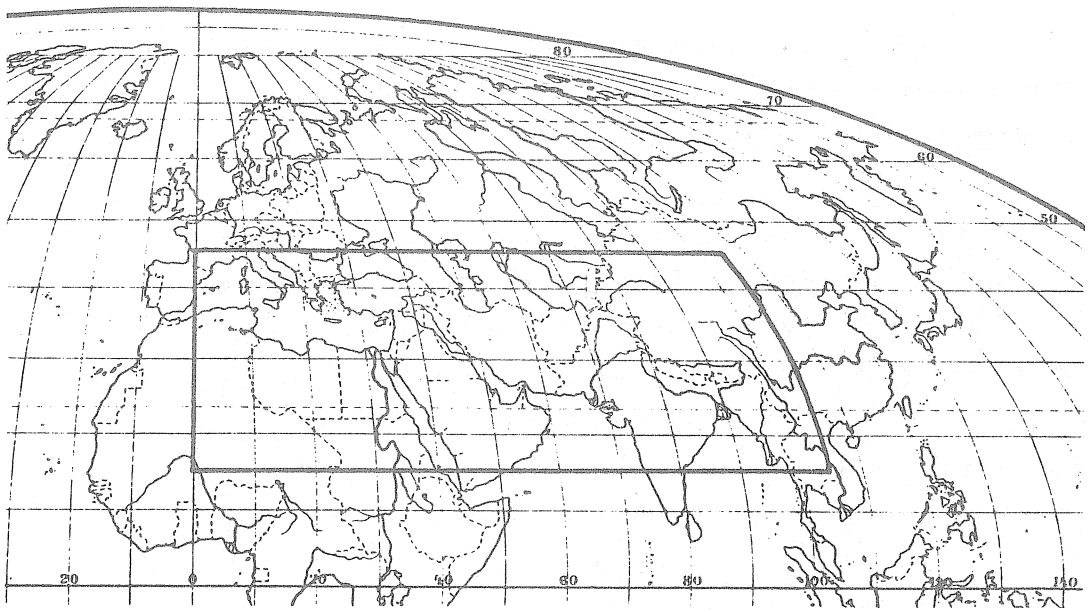

Figure 2: Area of investigation.

and time; they amounted to approximately 500. (In each of the few cases of several earthquakes within 6 hours at the same position the earthquakes were excluded except for the main earthquake if such a one existed, which it was considered to do if it was at least one magnitude greater than the others.)

3. Now the tidal curvatures for all the earthquakes were computed using the formulae (1) and (2). The celestial coordinates δ and t were, thereby, calculated according to (Heikkinen, 1978). Then those earthquakes which showed fairly great curvatures were selected. There turned out to be 39 earthquakes for which $|K| = K > 1.50$ and 65 earthquakes for which $1.50 > |K| > 0.75$.

4. For these earthquakes the time derivatives of the tidal curvatures were examined. The number of earthquakes with increasing tidal curvatures ($\dot{K}/K > 0$ or $\dot{H}/H > 0$) was counted as well as the number with decreasing tidal curvatures ($\dot{K}/K < 0$ or $\dot{H}/H < 0$).

5. Finally it was tested with the binomial distribution whether there was a significant difference or not between the mentioned numbers.

Both the Gaussian and mean tidal curvatures should be analysed. From their geometric interpretation it is evident that we can have e.g. $K < 0$ - hyperbolic curvature - at the same time as $H = 0$, or $K = 0$ at the same time as $H \neq 0$ - cylindric curvature. If both $K = 0$ and $H = 0$ we have a planar case (no curvature at all). When $K > 0$ - elliptic curvature - we always have $H \neq 0$. For $|K| > 1.50$ all K values are positive. This is the main reason for a close correlation between K and H for $|K| > 1.50$ (corresponding roughly to $|H| > 1.25$).

3. Tidal triggering of earthquakes: Result of the investigation.

The result of the analysis is summarized in Tables 1 and 2: For $K > 1.50$ or $|H| > 1.25$ we find - on the 95% level - significantly more earthquakes occurring when the tidal curvatures increase than when they decrease. We note that according to formula (2) the mean curvature is directly proportional to the height of the tide, so that $|H| = 1.25$ for $|u| = 17$ cm. For $|K| < 1.50$ or $|H| < 1.25$ we find no significant differences. In Table 3 we give a complete list of earthquakes with $|K| > 0.75$ showing their K values and if these are increasing or decreasing.

We may thus conclude: A major earthquake can be triggered by the combined semi-diurnal and diurnal earth tide in such a way that the earthquake is more likely to occur when the tidal curvature is increasing than when it is decreasing, provided the Gaussian tidal curvature exceeds about $1.5 \cdot 10^{-34}$ mm^{-2} or the mean tidal curvature exceeds about $\pm 1.2 \cdot 10^{-17}$ mm^{-1} (corresponding to the height $\mp$ 17 cm of the semi-diurnal + diurnal tide).

As an example we show in Figure 3 the Gaussian tidal curvature as function of time for the earthquake that showed the greatest K value ($K = 4.24$) of all investigated earthquakes. The curvature function is drawn for 18^h before and 6^h after the earthquake (Tibet, 1973 July 14th).

Table 1: Number of earthquakes during increasing ($\dot{K}/K > 0$) and decreasing ($\dot{K}/K < 0$) Gaussian tidal curvature, and level of significance. Unit of K: 10^{-34} mm^{-2}.

	$\dot{K}/K > 0$	$\dot{K}/K < 0$	α
$K > 1.50$	27	12	95%
$1.50 > \|K\| > 0.75$	36	29	-

Table 2: Number of earthquakes during increasing ($\dot{H}/H > 0$) and decreasing ($\dot{H}/H < 0$) mean tidal curvature, and level of significance. Unit of H: 10^{-17} mm^{-1}.

	$\dot{H}/H > 0$	$\dot{H}/H < 0$	α
$\|H\| > 1.25$	30	14	95%
$1.25 > \|H\| > 1.00$	21	22	-

Table 3: Position, time, Gaussian tidal curvature and its change for each earthquake of Table 1. Unit of K: 10^{-34} mm^{-2}.

φ	λ	Date	GMT	K	$\dot{K}/K$
35 10	86 24	1973-07-14	04 51 20	4.245	+
27 42	33 48	1972-06-28	09 49 36	3.917	+
36 24	27 18	1958-06-30	08 42 44	3.717	+
40 21	63 43	1977-07-14	05 49 08	3.261	+
27 40	101 02	1976-11-06	18 04 06	3.044	-
32 29	104 11	1976-08-23	03 30 06	3.038	+
25 00	93 48	1965-06-18	08 17 38	3.038	-
37 36	27 12	1955-07-16	07 07 10	3.005	+
39 42	68 00	1955-07-19	08 47 37	3.005	-
39 20	72 34	1978-11-01	19 48 24	2.996	-
38 14	22 39	1975-01-08	19 32 34	2.976	+
28 11	52 37	1964-08-20	05 39 46	2.760	+
41 49	32 23	1968-09-03	08 19 53	2.671	-
24 22	98 37	1976-05-31	05 08 30	2.659	+
29 54	70 00	1956-05-13	07 50 33	2.631	+
40 10	78 58	1972-01-15	20 21 47	2.616	-
30 36	84 12	1957-04-14	07 11 52	2.476	-
31 24	85 36	1953-12-03	14 54 05	2.420	+
36 30	01 30	1954-09-09	09 28 42	2.376	+
33 38	75 20	1967-02-20	15 18 39	2.317	+
29 37	80 47	1966-12-16	20 52 16	2.245	+
26 23	66 39	1974-10-04	22 24 33	2.229	-
38 06	38 31	1964-06-14	12 15 31	2.131	+
38 54	68 42	1961-08-23	04 12 36	2.120	+
31 37	99 59	1973-09-09	02 13 38	2.016	+
20 12	94 54	1965-06-01	04 32 45	1.877	+
34 29	25 14	1978-03-07	22 33 47	1.803	-
39 15	24 36	1967-03-04	17 58 09	1.797	+
28 25	94 17	1967-03-14	06 58 04	1.795	+
39 37	27 19	1971-02-23	19 41 23	1.752	+
23 52	94 05	1975-05-21	03 16 18	1.710	-
42 29	78 43	1970-06-05	04 53 07	1.687	+
32 12	29 36	1955-09-12	06 09 24	1.635	+
40 42	30 54	1957-05-26	06 33 34	1.614	+
21 20	93 41	1974-04-05	03 46 30	1.608	+
26 13	103 13	1966-02-05	15 12 33	1.590	+
38 20	22 34	1970-04-08	13 50 28	1.574	-
27 54	54 42	1961-06-11	05 10 26	1.545	+
40 06	77 48	1961-04-04	09 46 37	1.533	-

φ	λ	Date	GMT	K	K̊/K
24 07	102 29	1970-01-04	17 00 39	1.432	-
29 58	69 07	1975-03-22	15 32 15	1.427	+
29 53	67 24	1977-07-13	08 09 16	1.339	-
27 36	88 00	1965-01-12	13 32 24	1.286	+
38 14	08 11	1977-08-28	09 45 14	1.282	+
37 30	20 19	1969-07-08	08 09 13	1.277	-
42 54	104 24	1960-12-03	04 24 19	- 1.246	+
33 14	86 50	1973-08-16	08 02 50	1.240	-
27 20	55 00	1976-03-16	07 28 58	1.191	+
40 24	63 40	1978-06-04	19 30 23	- 1.188	-
38 26	66 47	1971-11-18	07 31 33	- 1.150	-
39 12	22 36	1957-11-27	03 08 04	1.124	-
28 00	99 24	1961-06-27	07 03 42	1.122	-
40 42	31 00	1957-05-27	11 01 27	1.110	-
39 20	73 46	1974-08-11	01 13 55	1.106	-
40 44	23 15	1978-05-23	23 34 11	- 1.105	-
42 07	24 02	1977-11-03	02 22 56	1.090	+
42 00	46 33	1978-05-26	13 43 38	1.086	-
43 15	17 05	1962-01-07	10 03 14	- 1.067	+
45 00	101 24	1957-12-04	13 20 08	1.062	+
16 36	95 53	1978-09-30	09 04 31	1.055	+
32 08	49 38	1978-12-14	07 05 22	- 1.028	+
33 07	48 00	1977-01-18	08 48 54	- 0.988	-
35 00	54 30	1953-02-12	08 15 31	- 0.986	-
31 35	51 03	1975-09-21	14 16 38	0.983	+
35 50	79 55	1975-06-04	02 24 33	0.969	+
37 18	50 12	1956-04-12	22 34 46	- 0.969	-
30 26	66 25	1975-10-03	17 31 36	0.961	+
27 25	91 52	1967-09-15	10 32 44	0.957	+
41 55	79 58	1978-03-12	08 29 18	0.951	+
28 35	85 31	1974-09-27	05 26 34	0.948	-
43 11	45 34	1976-07-28	20 17 44	- 0.947	+
25 20	62 24	1978-02-10	20 50 48	0.945	+
39 54	78 18	1953-07-09	19 02 08	- 0.937	-
36 36	28 24	1959-04-25	00 26 39	- 0.921	-
25 36	96 48	1958-01-06	11 24 11	0.920	+
39 30	39 30	1960-01-26	09 52 00	- 0.920	-
40 54	19 48	1959-09-01	11 37 40	0.907	-
30 15	69 53	1966-02-07	23 06 37	0.900	-
34 05	45 40	1967-01-11	11 20 46	- 0.894	-
25 06	96 12	1959-08-27	23 53 11	0.893	+
44 27	38 01	1978-09-03	00 21 17	- 0.892	-
39 22	72 42	1976-07-28	18 24 28	- 0.888	+
41 25	20 26	1967-11-30	07 23 50	- 0.887	+
27 41	56 38	1977-12-10	05 46 22	- 0.885	+
41 42	82 30	1963-12-18	06 40 06	- 0.881	+
34 54	33 48	1961-09-15	01 46 10	0.881	-
38 54	70 18	1958-01-07	06 05 09	- 0.869	+
40 47	23 14	1978-06-20	20 03 22	- 0.867	+
42 03	83 21	1976-01-10	12 51 21	0.862	+
24 16	98 43	1976-07-03	16 33 24	0.862	-

φ	λ	Date	GMT	K	K̊/K
41 58	85 52	1978-04-22	15 04 16	- 0.843	+
30 16	66 20	1975-10-03	05 14 24	0.832	+
36 30	69 12	1962-09-12	20 57 00	- 0.832	-
27 09	55 20	1977-05-19	22 58 32	- 0.821	-
39 15	28 26	1969-03-25	13 21 34	0.819	+
28 18	55 37	1971-04-12	19 03 25	- 0.818	+
37 31	20 35	1976-06-12	00 59 18	- 0.815	-
27 28	56 15	1977-01-05	05 44 41	- 0.799	+
21 36	92 42	1955-12-14	10 51 45	0.790	+
37 11	72 34	1974-04-06	20 19 33	- 0.788	+
35 12	67 30	1956-06-08	04 07 27	0.787	+
27 08	60 50	1973-04-26	14 30 05	0.773	+
38 31	40 46	1975-09-06	09 20 12	0.754	+
39 49	30 21	1956-02-20	20 31 37	0.754	-

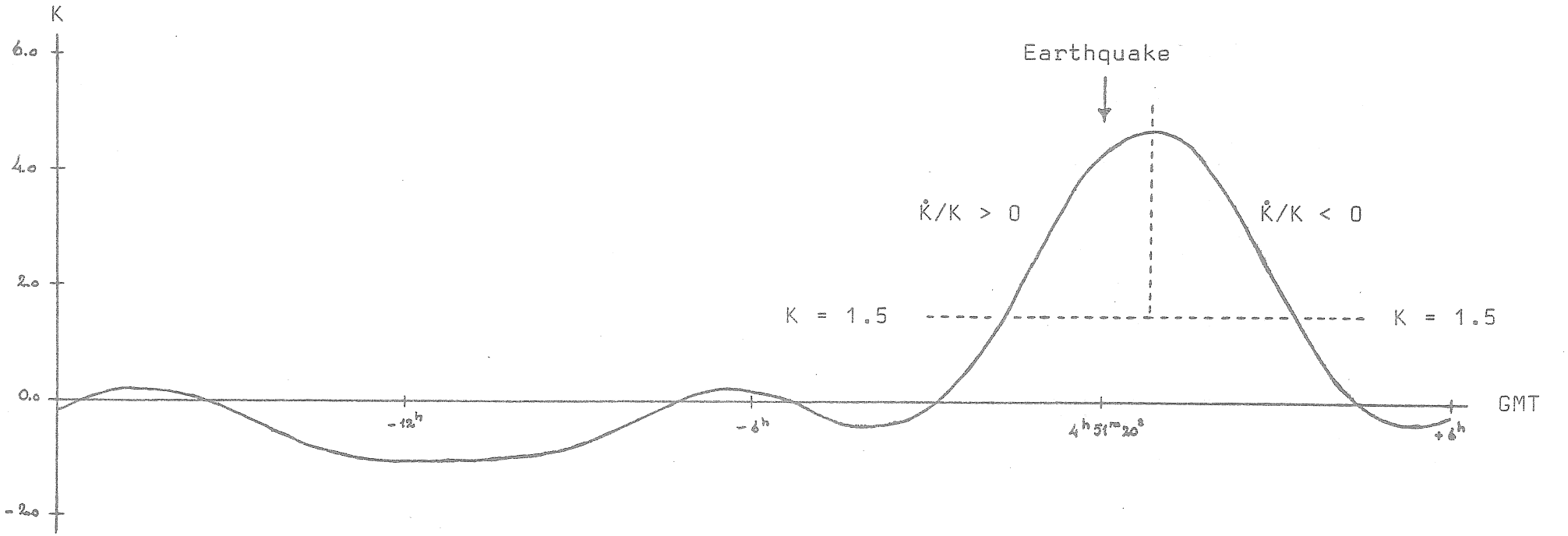

Figure 3: Gaussian tidal curvature as function of time for the earthquake of greatest curvature; $\varphi = 35^{o}10'$, $\lambda = 86^{o}24'$, 1973 July 14th, $4^{h}51^{m}20^{s}$ GMT. Unit of K: 10^{-34} mm^{-2}.

4. On elliptic, hyperbolic, cylindric and planar tidal curvatures.

We will finally use the curvature calculations for the earthquake of Figure 3 to show an example of the different stages of tidal curvature which the surface of the earth may go through during one day. The values of the Gaussian tidal curvature and the mean tidal curvature for each hour are given in Table 4. From these we find the following curvature stages:

I. $K \approx 0$, $H \neq 0$: Cylindric curvature.

II. $K < 0$ (H first $\neq 0$, then ≈ 0, then again $\neq 0$): Hyperbolic curvature.

III. $K \approx 0$, $H \neq 0$: Cylindric curvature again.

IV. $K \approx 0$, $H \approx 0$: Planar case.

V. $K > 0$ ($H \neq 0$): Elliptic curvature.

VI. $K \approx 0$, $H \approx 0$: Planar case again.

Table 4: Gaussian and mean tidal curvatures with curvature stages (I - VI) for $\varphi = 35^{o}10'$, $\lambda = 86^{o}24'$, 1973-07-13/14. Unit of K: 10^{-34} mm^{-2}, unit of H: 10^{-17} mm^{-1}.

GMT	K	H	
10 51 20	-0.119	0.803	
11 51 20	0.172	1.086	I
12 51 20	0.135	1.127	
13 51 20	-0.213	0.972	
14 51 20	-0.622	0.709	
15 51 20	-0.887	0.446	
16 51 20	-0.989	0.281	II
17 51 20	-1.001	0.272	
18 51 20	-0.925	0.422	
19 51 20	-0.687	0.680	
20 51 20	-0.284	0.951	
21 51 20	0.095	1.127	III
22 51 20	0.180	1.110	
23 51 20	-0.088	0.848	
0 51 20	-0.375	0.348	IV
1 51 20	-0.115	-0.320	
2 51 20	1.022	-1.038	
3 51 20	2.752	-1.666	
4 51 20	4.245	-2.073	
5 51 20	4.657	-2.173	V
6 51 20	3.740	-1.944	
7 51 20	2.027	-1.432	
8 51 20	0.449	-0.743	
9 51 20	-0.317	-0.016	VI
10 51 20	-0.255	0.608	

List of symbols.

$e_{\varphi\varphi}$ etc.	=	tidal strain tensor components
G	=	Newtonian gravitational constant
H	=	mean curvature
h_2	=	Love number
K	=	Gaussian curvature
l_2	=	Shida number
M	=	mass of moon or sun
R	=	mean radius of the earth
r	=	geocentric distance to moon or sun
t	=	hour angle of moon or sun
u	=	tidal height
α	=	level of significance
γ	=	normal gravity
δ	=	declination of moon or sun
ε	=	inclination of the ecliptic to the equator
λ	=	longitude
φ	=	latitude

Acknowledgements.

In the work with both the previous report (Ekman, 1981) and this one I have had great benefit of Professor Lars Sjöberg's encouragement and his ideas on various aspects of the subject. With Professor Erik Tengström I have also had discussions. My fiancée Britt Marie Björklund has made the necessary computer programming. Miss Ingegerd Ohlsson has typed the manuscripts with all my amendments and additions. I wish to express my thanks to them all.

References.

Ekman: Gaussian and Mean Curvatures of Tidal Surfaces of the Earth. University of Uppsala, Department of Geodesy, Report No. 11, Uppsala 1981.

Heaton: Tidal Triggering of Earthquakes. Geophysical Journal of the Royal Astronomical Society 43, London 1975.

Heikkinen: On the Tide-Generating Forces. Publications of the Finnish Geodetic Institute 85, Helsinki 1978.

Van Ruymbeke, Ducarme, De Becker: Parametrization of the Tidal Triggering of Earthquakes. Marées Terrestres - Bulletin d'Informations 86, Bruxelles 1981.

Earthquake Catalogues:

Rothé: The Seismicity of the Earth 1953-1965.

International Seismological Centre (ISC): Regional Catalogue of Earthquakes 1964-1978.